August, 2009

Thesis for Master degree

Protein tyrosine phosphatase 1B (PTP1B) inhibitors from the stem bark of *Erythrina abyssinica*

Chosun University Graduate School

College of Pharmacy

Nguyen Phi Hung

Protein tyrosine phosphatase 1B (PTP1B) inhibitors from the stem bark of *Erythrina abyssinica*

*Erythrina abyssinica*의 줄기 껍질로부터 protein tyrosine phosphatase 1B (PTP1B) 저해제의 분리

August, 25th, 2009

Chosun University Graduate School

College of Pharmacy

Nguyen Phi Hung

Protein tyrosine phosphatase 1B (PTP1B) inhibitors from the stem bark of *Erythrina abyssinica*

지도교수 오원근

이 논문을 천연물화학 석사학위신청 논문으로

제출함

2009 년 08 월

조선대학교 대학원

약학과

응구엔피홍

This thesis is examined and approved for Nguyen Phi Hung's master degree

Chairman Chosun Univ. Dr. Woo Eun-Rhan (印)

Member Chosun Univ. Dr. Kang Keon Wook (印)

Member Chosun Univ. Dr. Oh Won Keun (印)

2009 년 08 월

Chosun University Graduate School

*Erythrina abyssinica*의 줄기 껍질로부터 protein tyrosine phosphatase 1B (PTP1B) 저해제의 분리

*Erythrina abyssinica*의 줄기 껍질로부터 protein tyrosine phosphatase 1B (PTP1B) 저해제의 분리

*Erythrina abyssinica*의 줄기 껍질로부터 protein tyrosine phosphatase 1B (PTP1B) 저해제의 분리

*Erythrina abyssinica*의 줄기 껍질로부터 protein tyrosine phosphatase 1B (PTP1B) 저해제의 분리

*Erythrina abyssinica*의 줄기 껍질로부터 protein tyrosine phosphatase 1B (PTP1B) 저해제의 분리

CONTENTS

LIST OF SCHEMES

LIST OF TABLES

LIST OF FIGURES

LIST OF ABBREVIATIONS

$[\alpha]_D^{25}$: specific rotation measured by D line of sodium (589 nm) at temperature ^oC

COSY: correlated spectroscopy

CD: circular dichroism

DEPT: distortionless enhancement by polarization transfer

DMSO: dimethyl sulfoxide

HMBC: heteronuclear multiple bond correlation

HMQC: heteronuclear multiple quantum coherence

HPLC: high performance liquid chromatography

HR-EI-MS: high resolution electro impact mass spectroscopy

IC_{50}: 50% inhibition concentration

IR: infrared spectroscopy

m/z: mass to charge ratio

NMR: nuclear magnetic resonance

NOESY: nuclear overhauser effect spectroscopy

ppm: parts per min

RP: reverse phase

UV: ultraviolet absorption

PTP1B: Protein Tyrosine Phosphatase 1B

국문 초록

*Erythrina abyssinica*의 줄기 껍질로부터 protein tyrosine phosphatase 1B (PTP1B) 저해제의 분리

응구엔 피 훙
지도교수: 오 원 근
약학대학
조선대학교 대학원

인체에서 적절한 포도당 농도를 유지하는 기능에서의 손실과 관련되는 인슐린 내성은 제2형 당뇨병의 가장 중요한 인자로, 인슐린 신호전달과정에서의 문제와 관련된다. 그러므로 인슐린 신호전달과정에서의 많은 약물 목표점들이 인슐린 감수성을 개선하기 위한 과정을 이해하기 위하여 연구되어 왔다. 인슐린 감수성 개선 여러 약물 목표점 가운데에서, protein tyrosine phosphatase 1B (PTP1B)는 제 2형 당뇨병 치료에 효과적인 약물 목표점으로 최근 부상하고 있다. PTP1B 효소는 인슐린 수용체 인산화의 negative regulator로 PTP1B 효소를 저해하는 화합물이거나 PTP1B 유전자 발현을 저해하는 화합물은 제 2형 당뇨병의 치료제로서 혹은 비만 치료제로서의 유용할 것으로 제시되었다.

따라서 본 연구는 천연 식물로부터 protein tyrosine phosphatase 1B (PTP1B) 저해 활성 물질의 탐색을 통하여 PTP1B에 저해 활성을 나타내는 *Erythrina abyssinica*의 줄기 껍질로부터 silica gel (입자크기, 63–200 μm) 와

RP-18 (입자크기, 40-63 μm) 및 semi-preparative HPLC [C_{18} column (10 × 250 mm, 입자크기, 10 μm)] 등의 각종 크로마트그래피 방법을 사용하여 화합물을 분리하였고, 이러한 분리과정을 통하여 15개의 신규 화합물 (erythribyssins 1 - 15)를 얻었다. 분리한 화합물들의 구조는 각종 스펙트럼 방법 (1D, 2D-NMR, UV, IR, $[\alpha]_D$, CD 와 MS)과 보고된 문헌을 참고하여 동정 하였다.

분리된 화합물 중 화합물 1 - 4, 12 - 13 과 15은 새로운 prenylated pterocarpan 계열의 화합물로서 erythribyssin A - D (1 - 4), erythribyssin L - M (12 - 13)과 erythribyssin O (15)로 명명하였으며, 화합물 7, 9과 11는 flavanone 골격을 갖는 신규화합물로서 erythribyssin G (7), erythribyssin I (9)와 erythribyssin K (11)로 명명하였다. 화합물 6 과 8은 새로운 benzofuranoid 계열의 화합물로서 erythribyssin F (6)와 erythribyssin H (8)로 한 개의 특이한 화합물은 새로운 courmestan계열의 물질로서 erythribyssin N (14)로 명명 하였다.

분리한 신규 화합들 (1 - 15)를 in vitro PTP1B 효소 저해 활성을 측정하였을 때, 화합물 2 - 4, 6, 8, 9 와 11을 제외한 화합물들이 4.2 ± 0.4 μM 부터 26.7 ± 1.2 μM 범위에서 PTP1B 효소를 50% 저해함을 확인하였다. 플라보노이드 B링 부분에 3-hydroxy-2,2-dimethylpyran 구조를 갖는 화합물 3, 4 와 9는 prenyl 기가 존재하는 화합물 7이 22.6 ± 1.5 μM에서 저해작용을 갖는 것에 비하여 최종농도 50 μM 이상의 농도에서도 저해활성을 나타내지 않았다. 그러나, methoxy 기나 prenyl기가 존재하는 다른 화합물 1, 5, 10, 12 - 15는 prenyl 기가 없거나 플라보노이드의 수산기가 알데하이드나 카복실기로 치환딘 화합물 6, 8, 9 와 10이 저해활성을 나타내지 않는 것에 비하여 4.2 ± 0.4 μM 부터 26.7 ± 1.2 μM 범위에서 강한 저해활성을 보여 주었다. 이러한 결과는 화합물의 작용기에

methoxy나 prenyl기의 추가가 PTP1B 효소의 활성증가와 관련되며, 알데하이드나 카복실기의 치환은 PTP1B 효소의 활성저하와 관련됨을 보여주는 것이다.

비록 prenyl기가 치환된 플라보노이드의 구조와 활성간의 관계들이 완전히 규명 되지는 않았지만, flavonoids, isoflavonoids, pterocarpans, benzofurans, courmestran을 포함한 플라보노이드 화합물에서 prenyl 기의 존재가 PTB1B 저해작용에 있어서 중요함을 이 논문에서 제안한다. 따라서, *Erythrina abyssinica*로 분리된 화합물들은 비만과 2형 당뇨의 개선을 위한 치료제 개발에 유익하게 이용 될 수 있다고 제안한다.

Abstract

Protein tyrosine phosphatase 1B (PTP1B) inhibitors from the stem bark of *Erythrina abyssinica*

Nguyen Phi Hung

Advisor: Prof Oh Won Keun

Department of Pharmacy

Graduate School of Chosun University

Insulin resistance resulting in loss of proper glucose homeostasis is consider as the most important factor of type 2 diabetes and it is generally due to defects in insulin-mediated signal transduction. Therefore, a number of molecular targets in insulin signaling pathway are being investigated for improving insulin sensitivity. Among the various potential drug targets, protein tyrosine phosphatase 1B (PTP1B) has recently emerged as a promising one in the effective treatment of type 2 diabetes. As a PTP1B has been considered as a major negative regulator in the insulin signaling pathway, it has been suggested that compounds reducing PTP1B activity or the genetic expression levels of PTP1B may be useful in the treatment of type-2 diabetes and possibly obesity as well.

During this screening effort we found that EtOAc–soluble extract of the stem bark of *Erythrina abyssinica* Harms inhibited protein tyrosine phosphatase 1B (PTP1B) activity, fifteen new compounds (**1**–**15**) from the stem bark of *Erythrina abyssinica* were isolated by bioassay–guided isolation using silica gel (63–200 μm particle size), RP-18 (40–63 μm particle size) column chromatography, and semi-preparative HPLC [C_{18} column (10 × 250 mm, 10 μm particle size)]. Their structures were elucidated on the basis of

spectral (including 1D, 2D-NMR, IR, $[\alpha]_D$, UV, CD and MS data) and physicochemical analyses.

New compounds **1** – **4**, **12** – **13** and **15** were new prenylated pterocarpans named as erythribyssins A – D (**1** – **4**), erythribyssins L – M (**12** – **13**) and erythribyssin O (**15**). Compounds **7**, **9** and **11** were new compounds with flavanone skeleton named erythribyssin G (**7**), erythribyssin I (**9**) and erythribyssin K (**11**). As compounds **5** and **10** were new isoflavanones, these compounds were called as erythribyssin E (**5**) and erythribyssin J (**10**), respectively. Finally, compounds **6** and **8** were new benzofuranoids compounds, which are named erythribyssin F (**6**) and erythribyssin H (**8**), and erythribyssin N (**14**) is a new courmestan-type compound.

When compounds **1** – **15** were tested on *in vitro* PTP1B inhibitory assay, all the isolates with the exception of compounds **2** – **4**, **6, 8**, **9** and **11** inhibited strongly PTP1B activity with IC_{50} values ranging from 4.2 ± 0.4 to 26.7 ± 1.2 μM. Compound **3, 4** and **9**, which were fused as the 3-hydroxy-2,2-dimethylpyran moiety on the B ring, did not showed any inhibition at PTP1B enzyme activity over the final concentration of 50 μM with compared to that of compound **7** (22.6 ± 1.5 μM) which the prenyl group was present. However, other compounds **1, 5, 10, 12 - 15** which were attached by either mehoxyl groups or prenyl groups showed a stronger activity with IC_{50} value ranging from 4.2 ± 0.4 to 26.7 ± 1.2 μM than compounds **6, 8, 9** and **11** (IC_{50} > 50 μM), which the prenyl groups are absent or OH group was substituted to CHO or COOH functional groups. These results indicated that the addition of prenyl group or methoxyl substituent to functional group of compounds may be responsible for increasing PTP1B enzyme activity, and substitution of hydroxyl group to the CHO or COOH groups may decrease the inhibitory activity on this enzyme.

Although structure-activity relationships of flavonoids bearing prenyl groups were not

thoroughly investigated, these results indicated that substitution of prenyl groups on flavonoids may be important for *in vitro* PTP1B inhibitory activity. Flavonoids, isoflavonoids, pterocarpans and benzofurans, as well as courmestans with prenyl groups could be consider as promising classes of PTP1B inhibitors. Thus, its constituents from *Erythrina abyssinica* might be used beneficially in the treatment of diabetes as well as obesity.

I. INTRODUCTION

1. Diabetes

Diabetes mellitus is characterized by high levels of glucose in the bloodstream, resulting from impairment in insulin release and its action. Normally, insulin is produced by the pancreas to move glucose from the blood stream into muscle and other cells for the production of ATP. In diabetes patients, however, either the pancreas can not produces enough insulin for regulating blood glucose levels, or the insulin produced fails to act appropriately on the cells. Consequently, the glucose level increases in the blood. Diabetes may be divided into three main types (**Table 1**). First, in type 1 diabetes, the immune system attacks the insulin-producing β cells in the pancreas, and then the pancreas produces little or no insulin. It occurs mainly in children and young adults. Second, in type 2 diabetes, the insulin does not produce expected results - a phenomenon known as insulin resistance. Most of its patients are over age 40 and overweight. Third, gestational diabetes occurs during pregnancy. Although it usually disappears after delivery, the mother will more likely develop type-2 diabetes later.

Among three types of diabetes, type-2 diabetes, known as non-insulin-dependent diabetes mellitus (NIDDM), accounts for > 90% of all diabetes cases. This disease afflicts over 140 million people in the worldwide and the patients of type-2 diabetes continue to grow each year, potentially will be reached over 200 million cases in 2010.[1]

In type 2 diabetes, hyperglycemia is one of the characteristic pathogenesis, and it is clear that control of hyperglycemia can attenuate the development of chronic complications such as retinopathy and nephropathy.[2] Therefore, therapy for type 2 diabetes relies mainly on several approaches to reduce the hyperglycemia itself: sulphonylureas (and related insulin secretagogues), which increase insulin release from

pancreatic islets; metformin, which acts to reduce hepatic glucose production; peroxisome proliferator-activated receptor-γ (PPARγ) agonists (thiazolidinediones), which enhance insulin action; α-glucosidase inhibitors, with gut glucose absorption.[3]

These therapeutic drugs have a number of limitations, such as adverse effects and high rates of secondary failure; for example, a problem to have the sulphonylureas is that many patients who respond initially become refractory to treatment over time. Moreover, these drugs play an insufficient role in a fundamental defect, insulin resistance.[4] Thus, newer and more effective approaches are desperately needed.

Insulin resistance resulting in loss of proper glucose homeostasis is consider as the most important factor of type 2 diabetes and it is generally due to defects in insulin-mediated signal transduction.[5] Therefore, a number of molecular targets in insulin signaling pathway are being investigated for improving insulin sensitivity (**Table 2**).[4] Among the various potential drug targets, protein tyrosine phosphatase 1B (PTP1B) has recently emerged as a promising one in the effective treatment of type 2 diabetes.[6]

2. Protein tyrosine phosphatases

Most intracellular signaling takes place via formation of phosphate ester on protein, continuously phosphorylation, hydrolysis these protein-associated phosphate esters, and finally by dephosphorylation of insulin receptor protein. These reactions are catalyzed by protein kinases and protein phosphatases, respectively.[7]

Protein kinases can be divided into two groups: serine-threonine kinases and tyrosine kinases, and they share similarties in amino acid sequence as well as three-dimensional structure.[8, 9] Phosphatases can be classified as nonspecific phosphatases and phosphoprotein (serine/threonine) phosphatases (PPases) and protein tyrosine phosphatases (PTPases). Nonspecific phosphatases do not share amino acid sequence

similarities with on another, while PPases share amino acid sequence similarities with on another and they are distinct in amino acid sequence from both nonspecific phosphatases and PTPases.[10] PTPases are known to include 90-100 members in mammalian and contain a common -250 amino acid catalytic domain and/or PTP signature motif, (I/V) HCX5R (S/T).[11] Particularly, dual specificity PTPases, a sort of PTPases, share the greatest sequence similarity with the product of vaccinia virus open reading frame H1 (VH1), and these enzyme can dephosphorylate phosphoserine and phosphothreonine in addition to phosphotyrosine as substrates.[13]

PTPases play a critical role in the regulations of a variety of cellular processes, such as growth, proliferation and differentiation, metabolism, immuns, such as growth, proliferation and differentioation, metabolism, immune response, cell-cell adhesion, and cell-matrix contacts.[14, 15] Blocking PTPases with nonspecific inhibitors results in the massive stimulation of kinase-catalyzed phosphorylation cascades, and consequently, interest in PTPases as drug target in signaling is rapidly increasing.[16] Especially, several PTPases attenuate insulin-stimulated signal transduction pathway by dephosphorylating the insulin receptor (IR); therefore inhibition of the phosphatases is expected to prolong insulin signaling and thereby facilitate glucose uptake, and presumably, result in a lowering of blood glucose.[17] These phosphatases include PTP1B, LAR (Leukocyte antigen-related), PTPα and SH-PTP2 (Src homology 2-containing PTP2), and among them, PTP1B is known as a major negative regulator of insulin receptor signaling.[18] Accordingly, PTP1B is consider as an attractive target for the treatment of type 2 diabetes and related metabolic syndromes.[19, 20]

3. PTP1B in human diabetes and obesity

Insulin is the most potent anabolic hormone secreted from pancreatic β-cell in

response to increase of glucose concentrations in the blood. Insulin increases glucose uptake in muscle and adipose tissue, and inhibits hepatic glucose production, thus serving as the primary regulator of blood glucose concentration.[21] Also, insulin stimulates cell growth and differentiation, and it promotes the storage of substrates in fat, liver and muscle by stimulating lipogenesis, glycogen and protein synthesis, and by inhibiting lipolysis, glycogenesis, and protein breakdown.[20] Although the exact molecular mechanism of type 2 diabetes has not been fully elucidated, a variety of evidences suggest that the disease is a result of a defect in the insulin signaling pathway.[22]

Insulin's actions are initiated by the binding of insulin to its receptor (**Fig. 1**).[23] This activates the tyrosine kinase of the β-subunit of the receptor which undergoes autophosphorylation on tyrosine residues. Insulin receptor substrates 1, 2 and 3 (IRS-1, IRS-2 and IRS-3) are downstream targets of the insulin receptor (IR) tyrosine kinase.[23] These substrates recruit the enzyme phosphatidylinositol 3-kinase (PI3K) to the cell membrane. Other signal transduction proteins also interact with IRS molecules. PI3K activates PtdIns (3, 4) P2 / PtdIns (3, 4, 5) P3-dependent kinase (PDK1), which activates protein kinase B (PKB).[24] PKB deactivates glycogen synthase kinase 3 (GSK-3)[25] mediating the effects of insulin on metabolism. Insulin signaling leads to translocation of glucose transporters, like GLUT-4, from the cytoplasm into plasma membrane thus allowing glucose to enter the cell. Also, to promote the mitogenic effect of insulin, the adapter protein Shc upon phosphorylation by IR forms a complex with Grb2 and the guanine nucleotide exchange factor SOS, which is required for Ras activation in response to insulin. Activation of the Ras/MAP kinase pathway is essential for the mitogenic effects of insulin, but is not required for insulin-stimulated glucose transport.

The insulin action is attenuated by PTPs, which dephosphorylate the IR and IRS, and

several PTPs have been suggested as negative regulators of insulin signaling pathway.[26] Among these, PTP1B has emerged as a key player that negatively regulates insulin signaling by dephosphorylating the IR as well as IRS proteins.[27, 28]

It is suggested that PTP1B has been associated with the insulin resistance of obesity and type-2 diabetes mellitus. If loss of PTP1B activity increases insulin action and, at the same time, prevents obesity and diabetes, PTP1B would be an ideal target for the drug development against these disorders. These dramatic effects of PTP1B were demonstrated in PTP1B knockout mice.[29. 30]

4. PTP1B inhibitors

Early studies with the nonspecific PTPase inhibitor, vanadate, were focused at PTPase in insulin signaling.[31] Vanadate has long been considered in the treatment of diabetes due to its insulin-mimetic effect; however, vanadate has severe toxic effects in both animal and man.[32, 33]

Over the last several years, a significant amount of effort has gone into generating PTP1B-specific inhibitors for the treatment of type-2 diabetes, and a number of recent publications have described the design of various PTP1B inhibitors. Although there have been described many reports on the designing and development of synthetic PTP1B inhibitors,[19] there are few studies for PTP1B inhibitors derived from natural resources such as plant or microbial resources (**Fig. 2**). For example, there are PK-682 (3-hexadecanoyl-5hydrowymethyl-tetronic acid) (C) from *Streptomyces*,[34] flavonoids (E, H) from *Broussonetia papyrifra*,[35] metabolite (D, G) from *fungus*[36] and phenols (A, B) from *psoraled corylifolia*.[37] In addition, the bioactive compounds from cinnamoncan stimulate autophosphorylation of insulin receptor and can inhibit PTP1, a rat homolog of PTP1B.[38] Also, as Et-3, 4-dephostatin (F) is one of PTP1B inhibitors derived from

Streptomyces, Et-3, 4-dephostation has been shown to strongly inhibit PTP1B activity *in vitro*, and to potentiate insulin-related signal transduction in cultured mouse adipocytes.[39] Considering the track record of success in the development of a number of useful therapeutics, it seems reasonable to search for PTP1B inhibitors from natural resources.

Table 1. Classification of diabetes

	Type 1 (IDDM)	Type 2 (NIDDM)
Distribution	< 10%	> 90%
Cause	Autoimmune disease	Insulin resistance (obese)
		Insulin secretion defect (nonobese)
Age	< 30 (mainly 11 - 14)	> 45
Clinical	Fast progress	Slow progress
	Hypoinsulinemia	Hyperinsulinemia (obese)
	Ketonemia	Normal insulin level (non-obese)
Treatment	Injection of insulin	Die, Glucose-lowing agent, linsulin

Table 2. Potential drug targets in insulin signaling pathway

Target	Potential mechanism (s)
Insulin	Apparent direct activation of the receptor
PTP1B	Mediates dephosphorylation of the insulin receptor (and its tyrosyl-phosphorylated substrates)
SHIP2	Dephosphorylation of phosphoinositides (for example, products of PI(3)K
GSK3	Phosphorylation of glycogen synthase leading to inhibition of glycogen synthesis; negative regulation of other insunlin signaling events
IKK	Serine-threonine phosphorylation of insulin signaling intermediates (forexample, IRS proteins)
PKCθ	Negative regulation of insulin signaling; potential serine-threonine phosphorylation of IRS proteins

SHIP2: SH2 domain-containing inositol 5-phosphatase type 2

GSK3: glycogen synthase kinase 3

IKK: IkB kinase

PKCθ: protein kinase C-θ

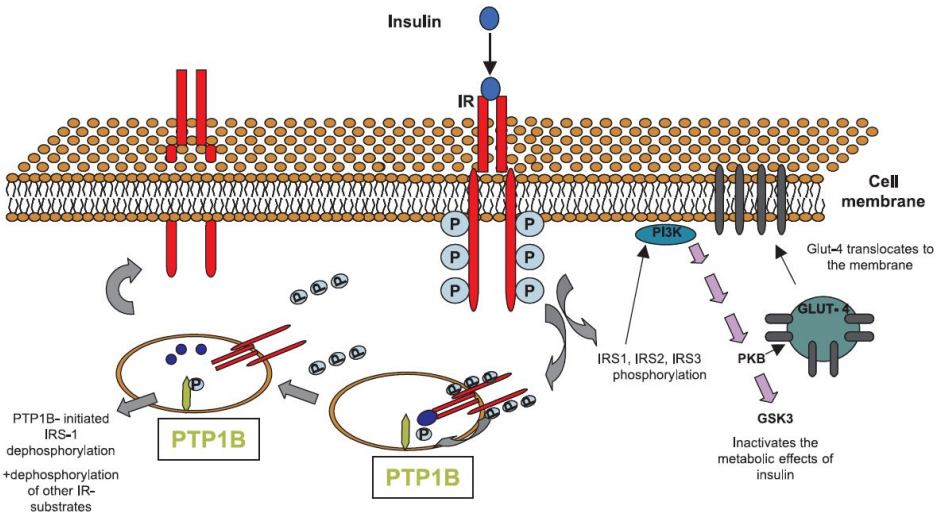

Fig. 1. The role of PTP1B in the regulation of insulin signalling.

Insulin binds to the insulin receptor (IR). This activates the tyrosine kinase of the β-subunit of the receptor which autophosphorylates. Insulin receptor substrates (IRS-1, IRS-2 and IRS-3) are downstream targets of the IR tyrosine kinase. These substrates recruit the enzyme phosphatidylinositol 3-kinase (PI3K) to the cell membrane. Other signal transduction proteins also interact with IRS molecules. PI3K activates PtdIns (3, 4) P2/PtdIns (3, 4, and 5) P3-dependent kinase (PDK1), which activates protein kinase B (PKB). PKB deactivates glycogen synthase kinase 3 (GSK-3) mediating the effects of insulin on metabolism. Insulin signalling leads to translocation of glucose transporters, like GLUT-4, from the cytoplasm into plasma membrane thus allowing glucose to enter the cell. The activated IR complex is moved to the endoplasma by the process which is dependent on tyrosine autophosphorylation. In the endosomal compartment insulin dissociates from its receptor which dephosphorylates leading to translocation and recycling of the receptor to the plasma membrane. PTP1B plays a role in the negative regulation of insulin signalling. The phosphorylated and activated IR phosphorylates also tyrosine residues of PTP1B which increases its catalytic activity. It interacts with the IR and removes tyrosine phosphates induced by autophosphorylation in response to insulin binding. PTP1B is able to dephosphorylate also IRSs thus attenuating the insulin action.[23]

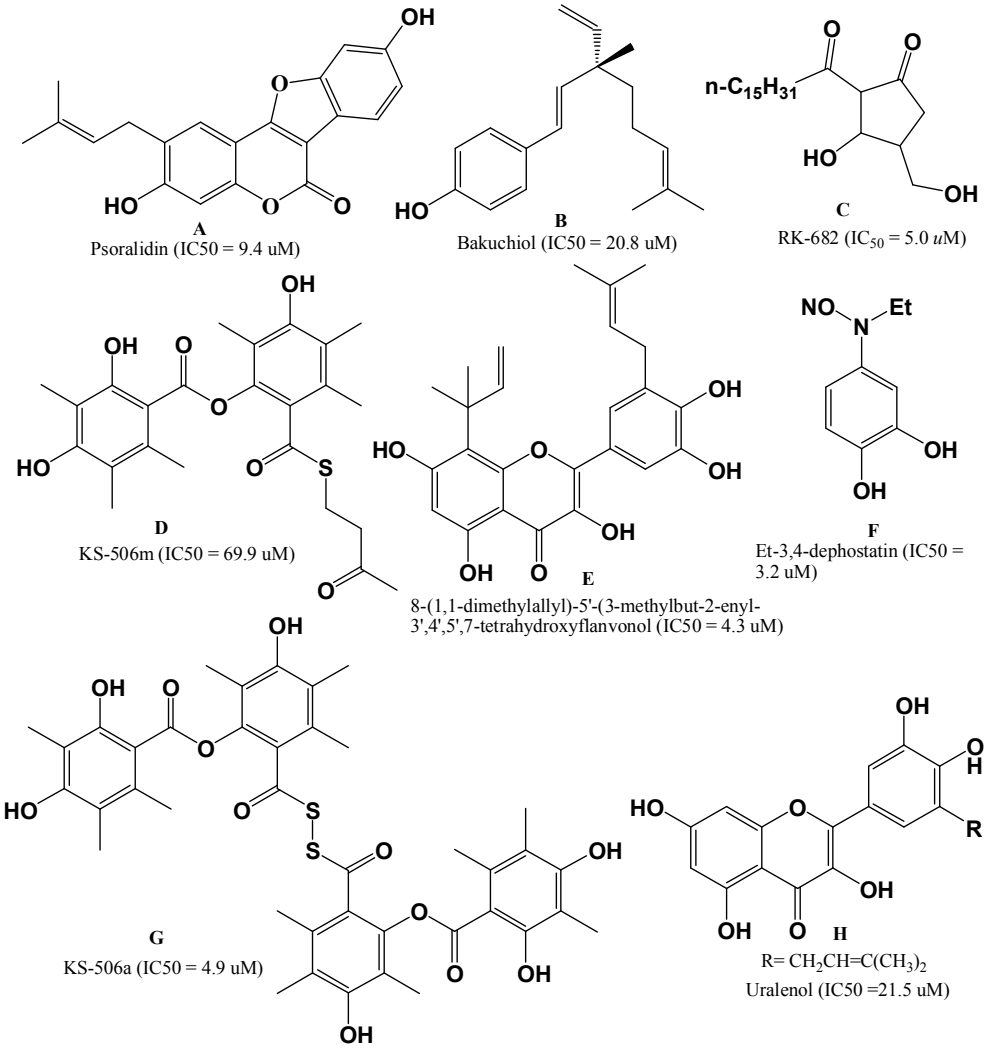

Fig. 2. PTP1B inhibitor derived from natural resources.

5. *Erythrina abyssinica*

The genus *Erythrina* of the Leguminosae family comprises over 110 species of trees and shrubs that are widely distributed in tropical and subtropical regions (Angola, Burundi, Ethiopia, Kenya, Malawi, Mozambique, Rwanda, Sudan, Tanzania, Uganda, Zaire, Zambia, Zimbabwe), and representative species have been used in indigenous medicine.[40] Alkaloids, pterocarpans, and other flavonoids have been reported as constituents of this genus and have been found to possess a wide range of biological activities that include anti-HIV, antioxidant, antimicrobial, and anti-inflammatory activities.[41 - 46]

Among these, *E. abyssinica* (Other names: *Erythrina eggelingii*, *Erythrina huillensis*, *Erythrina platyphyllos*, *Erythrina suberifera*, *Erythrina tomentosa*, *Erythrina webberi*) is the most widely used to treat microbial infection and malaria in traditional medicinal practice. As major biologically constituents, flavonoids and isoflavonoids have been reported to be responsible for the traditional antimicrobial uses of this plant.[35, 46]

The previous studies have demonstrated that a pterocarpan, erycristagallin, isolated from *E. abyssinica*, reduced phospholipase A2-induced paw edema in mice and inhibited 12-*O*-tetradecanoylphorbol 13-acetate-induced ear edema, possibly through inhibition of

5-lipoxygenase.[42]

Despite a number of studies on the chemical constituents and biological activities of the genus *Erythrina*, there have been few phytochemical investigations on *E. abyssinica* previously. In this study, the methanol extract and hexane, EtOAc and H_2O-soluble fractions of the stem bark of *Erythrina abyssinica* were tested for protein tyrosine phosphatase-1B (PTP1B). Bioassay-guided fractionation of the EtOAc soluble extract of the root bark of this plant has led to the isolation of a series of isoprenylated flavonoids and pterocarpans, including fifteen new compounds (**1**–**15**), as the active principles. In this thesis, we describe the isolation and structure elucidation of these compounds, as well as the evaluation of their inhibitory effects on this PTP1B enzyme.

II. MATERIALS AND METHODS

1. Materials

1.1. Plant material

The stem bark of *E. abyssinica* was collected in June 2005 in Mukono, Uganda. The sample was botanically authenticated by Prof. John Silike-Muruumu, and its voucher specimen (No. 0001) has been deposited at the Department of Botany, Makerere University, Uganda.

1.2. Chemicals, reagents and chromatography

Column chromatography was conducted on silica gel (63 - 200 μm particle size) and RP-18 (40 - 63 μm particle size) from Merck. TLC was carried out with silica gel 60 F_{254} plates from Merck. HPLC was carried out using a Gilson System 321 pump equipped with a model UV/VIS-155 UV detectors and an Optima Pak C_{18} column (10 × 250 mm, 10 μm particle size, RS Tech Korea). Baker analyzed HPLC solvents MeCN was purchased from Mallinckrodt Baker, Inc. USA; Deuterated solvent for NMR analysis Me_2CO-d_6 , D_2O, Methanol-d_4 were purchased form CIL (Cambridge Isotope Lab., USA).

1.3. General experimental procedures

The optical rotations were determined on an Autopol IV A7040–12 automatic polarimeter using a 100 mm glass microcell. The ultraviolet (UV) spectra were obtained in MeOH using an Optizen 3220UV spectrophotometer. The CD spectra were recorded in MeOH on a JASCO J-715 spectrometer. ^{1}H nuclear magnetic resonance (NMR, 300 *MHz*) and ^{13}C NMR (75 *MHz*) spectra were recorded on an YH300-OXFORD NMR

spectrometer. The ^{1}H NMR (500 *MHz*) and ^{13}C NMR (125 *MHz*) spectra were measured on a Unity INOVA 500 FT–NMR spectrometer with TMS as the internal standard at Korea Basic Science Institute (KBSI, Gwangju Center, Korea). Electron ionization (EI)-mass spectroscopy (MS) and high-resolution ESI-MS spectra were recorded on a Micromass ESI–Tof II (Micromass, Wythenshawe, UK) mass spectrometer. Column chromatography was carried out using silica gel 60 (40–63 and 63–200 μm particle size) and RP-18 (40–63 μm particle size) from Merck. Precoated TLC silica gel 60 F_{254} plates from Merck were used for thin-layer chromatography. The spots were visualized using UV light or 10% sulfuric acid. The HPLC runs were carried out using a Gilson System LC-321 pump with a UV/vis–155 UV detectors, and an Optima Pak C18 column (10 × 250 mm, 10 μm particle size, RS Tech, Korea) for semi-preparative runs.

2. Methods

2.1. Isolation of compounds from *E. abyssinica*

The dried stem bark of *Erythrina abyssinica* (5 kg), collected in Uganda, was extracted with MeOH at room temperature. The EtOAc-soluble fraction (106 g) was found to be most active (70% inhibition at 30 μg/mL) among the solvent fractions. This fraction was fractionated by silica gel column chromatography (20 × 80 cm; 63–200 μm particle size) using a gradient of *n*-Hexane: Acetone (from 20:1 to 0:1), to yield five combined fractions according to their TLC profiles. Fraction 1 was purified by semi-preparative Gilson HPLC systems [using RS Tech Optima Pak C18 column (10 × 250 mm, 10 μm particle size); mobile phase Acetonitrile in water (MeCN: H_2O = 85:15) for 35 min; flow rate 2mL/min; UV-detection at 205 and 254 nm] resulted in the isolation of compounds **6** (3.9 mg; t_R = 25.5 min), compounds **13** (2.4 mg; t_R = 29.8 min), respectively. Fraction 2 was purified by semi-preparative Gilson HPLC systems [using

RS Tech Optima Pak C18 column (10 × 250 mm, 10 μm particle size); mobile phase Acetonitrile in water (MeCN: H_2O = 70:30) for 40 min; flow rate 2mL/min; UV-detection at 205 and 254 nm] resulted in the isolation of compounds **1** (9.2 mg; t_R = 15.5 min), compounds **14** (3.5 mg; t_R = 25.5 min) and compound **15** (3.8 mg; t_R = 38.9 min), respectively. Fraction 3 was purified using a Gilson HPLC system [RS Tech Optima Pak C18 column (10 × 250 mm, 10 μm particle size); eluted with 55% Acetonitrile in H_2O + 0.1 % formic acid for 60 min; flow rate 2 mL/min; UV-detection at 205 and 254 nm] resulting in the isolation of compounds **2** (3.7 mg; t_R = 26.5 min), compounds **5** (17.9 mg; t_R = 48.5 min), and compound **12** (2.5 mg; t_R = 58.5 min), respectively. Fraction 4 was also purified by HPLC using an isocratic solvent system of 40% MeCN in H_2O for 55 min, [RS Tech Optima Pak C18 column (10 × 250 mm, 10 μm particle size), flow rate 2 mL/min; UV-detection at 205 and 254 nm], led to the isolation of compounds **3** (9.8 mg, t_R = 33.2 min), compound **4** (8.0 mg, t_R = 27.5 min), compound **7** (10.1 mg, t_R = 39.5 min), compound **11** (6.4 mg, t_R = 45.5 min), respectively. Fraction 5 was also purified by HPLC using an isocratic solvent system of 28% MeCN in H_2O for 60 min, [RS Tech Optima Pak C18 column (10 × 250 mm, 10 μm particle size), flow rate 2 mL/min; UV-detection at 205 and 254 nm], led to the isolation of compounds **8** (2.0 mg, t_R = 27.5 min), compound **9** (10.2 mg, t_R = 33.2 min), compound **10** (12.1 mg, t_R = 45.5 min), respectively (**Scheme 1**).

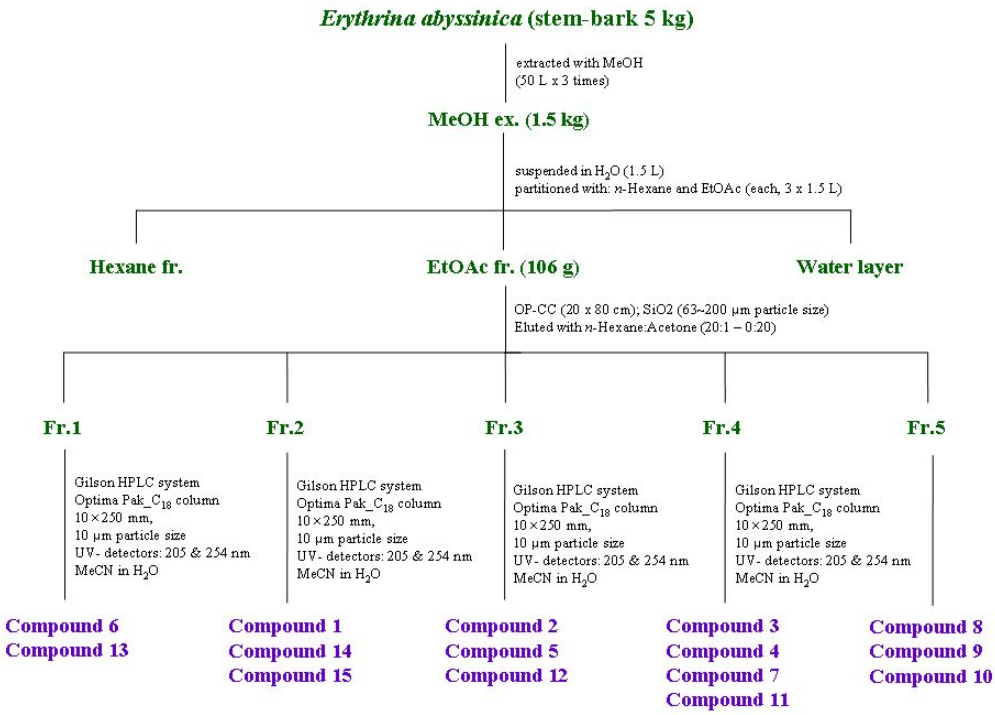

Scheme 1. Isolation of compounds (**1-15**) from the EtOAc fraction of the stem bark of *E. abyssinica*

Compound 1 (Erythribyssin A): Appearance: Yellow amorphous powder; $[\alpha]_D^{25}$: –205° (c = 0.03, MeOH); IR (KBr) ν_{max} cm^{-1}: 3406, 2927, 1468, 1193, 1119, 1061, 1041; UV (c 0.025, MeOH) λ_{max} nm (log ε): 209 (4.79), 233 (4.23), 282 (3.81); CD (*c* 0.1, MeOH) $[\theta]_{230}$ –18.7, $[\theta]_{295}$ +0.98; ^{1}H (500 *MHz*) and ^{13}C (125 *MHz*, Acetone-d_6) NMR data, see **Table 3**; HRESIMS *m/z* 368.1628 $[M]^+$ (calcd for $C_{22}H_{24}O_5$, 368.1624).

Compound 2 (Erythribyssin B): Appearance: Yellowish amorphous powder; $[\alpha]_D^{25}$: –110° (c = 0.02, MeOH); IR (KBr) ν_{max} cm^{-1}: 3418, 2924, 1650, 1622, 1418, 1160**,** 1041; UV (c 0.025, MeOH) λ_{max} nm (log ε): 208 (4.80), 228 (4.46), 277 (4.32), 363 (3.71); ^{1}H

(500 *MHz*) and ^{13}C (125 *MHz*, Acetone-d_6) NMR data, see **Table 4**; HREIMS *m/z* 284.0688 $[M]^+$ (calcd for $C_{16}H_{12}O_5$, 284.0685

Compound 3 (Erythribyssin C): Yellow amorphous powder; $[\alpha]_D^{25}$: –16.7° (c = 0.02, MeOH); IR (KBr) v_{max} cm^{-1}: 3406, 2927, 1606, 1468, 1374, 1279, 1142, 1062; UV (c 0.025, MeOH) λ_{max} nm (log ε): 209 (4.77), 2.30 (4.14), 282 (3.83); CD (*c* 0.55 MeOH): $[\theta]_{206}$ +27.11, $[\theta]_{224}$ +8.88, $[\theta]_{253}$ +3.73, $[\theta]_{290}$ –25.69, $[\theta]_{327}$ +5.48; ^1H (500 *MHz*) and ^{13}C (125 *MHz*, Acetone-d_6) NMR data, see **Table 5**; HREIMS *m/z* 340.1313 $[M]^+$ (calcd for $C_{20}H_{20}O_5$ 340.1311).

Compound 4 (Erythribyssin D): Yellow amorphous powder; $[\alpha]_D^{25}$: –54.9° (c = 0.02, MeOH); IR (KBr) v_{max} cm^{-1}: 3406, 2927, 1606, 1468, 1374, 1279, 1142, 1062; UV (c 0.025, MeOH) λ_{max} nm (log ε): 209 (4.77), 2.30 (4.14), 282 (3.83); CD (*c* 0.55 MeOH): $[\theta]_{206}$ +27.11, $[\theta]_{224}$ +8.88, $[\theta]_{253}$ +3.73, $[\theta]_{290}$ –25.69, $[\theta]_{327}$ +5.48; ^1H (500 *MHz*) and ^{13}C (125 *MHz*, Acetone-d_6) NMR data, see **Table 6** HREIMS *m/z* 363.1216 $[M + Na]^+$ (calcd for $C_{20}H_{20}O_5Na$ 363.1208).

Compound 5 (Erythribyssin E): Appearance: white amorphous powder; IR (KBr): v_{max} 3331, 2962, 1670, 1593, 1242, 1033 cm^{-1}; UV (c 0.025, MeOH) λ_{max} nm: 206, 216, 234, 276, 310 nm; ^1H (500 *MHz*) and ^{13}C (125 *MHz*, Acetone-d_6) NMR data, see **Table 7**; HREIMS m/z 368.1628 $[M]^+$, (calcd $C_{22}H_{24}O_5$ 368.4230).

Compound 6 (Erythribyssin F): Appearance: Brown powder; IR (KBr): v_{max} 3415, 2904, 1709, 1621, 1496, 1033 cm^{-1}; UV (c 0.025, MeOH) λ_{max} nm: 229, 245 nm; ^1H

(500 *MHz*) and ^{13}C (125 *MHz*, Acetone-d_6) NMR data, see **Table 8**; HREIMS m/z 445.1636 $[M + Na]^+$, (calcd $C_{25}H_{26}O_6Na$ 445.1626).

Compound 7 (Erythribyssin G): Appearance: White amorphous powder; IR (KBr): v_{max} 3419, 2926, 1664, 1606, 1468, 1278, 1142 cm^{-1}; UV (c 0.025, MeOH) λ_{max} nm: 208, 232, 276, 313 and 370 nm; CD (*c* 0.55 MeOH): $[\theta]_{206}$ +27.11, $[\theta]_{224}$ +8.88, $[\theta]_{253}$ +3.73, $[\theta]_{290}$ −25.69, $[\theta]_{327}$ +5.48; ^1H (500 *MHz*) and ^{13}C (125 *MHz*, Acetone-d_6) NMR data, see **Table 9**; HREIMS m/z 431.1859 $[M + Na]^+$, (calcd $C_{25}H_{28}O_5Na$ 431.1834).

Compound 8 (Erythribyssin H): Appearance: Brown yellow powder; $[\alpha]_D^{25}$: −0.7° (c = 0.01, MeOH); IR (KBr): v_{max} 3419, 2926, 1664, 1606, 1468 cm^{-1}; UV (c 0.025, MeOH) λ_{max} nm: 206, 232, 288, 316 nm; ^1H (500 *MHz*) and ^{13}C (125 *MHz*, Acetone-d_6) NMR data, see **Table 10**; HREIMS m/z 288.0952 $[M]^+$, (calcd $C_{16}H_{16}O_5$ 288.0998).

Compound 9 (Erythribyssin I): Appearance: White amorphous powder; $[\alpha]_D^{25}$: −10.8° (c = 0.02, MeOH); IR (KBr): v_{max} 3419, 2926, 1664, 1606, 1468, 1278, 1142 cm^{-1}; UV (c 0.025, MeOH) λ_{max} nm: 206, 216, 234, 276, 310 nm; CD (*c* 0.41 MeOH): $[\theta]_{230}$ +22.25, $[\theta]_{249}$ +9.88, $[\theta]_{287}$ −55.66, $[\theta]_{328}$ +15.18; ^1H (500 *MHz*) and ^{13}C (125 *MHz*, Acetone-d_6) NMR data, see **Table 11**; HREIMS m/z 340.1311 $[M]^+$, (calcd $C_{20}H_{20}O_5$ 340.1331).

Compound 10 (Erythribyssin J): Appearance: White amorphous powder; $[\alpha]_D^{25}$: −10.8° (c = 0.02, MeOH); IR (KBr): v_{max} 3331, 2916, 1670, 1593, 1061-1033 cm^{-1}; UV (c 0.025, MeOH) λ_{max} nm: 211, 230, 279, 310 nm; CD (*c* 0.41 MeOH): $[\theta]_{230}$ +22.25, $[\theta]_{249}$

+9.88, $[\theta]_{287}$ −55.66, $[\theta]_{328}$ +15.18; ^{1}H (500 *MHz*) and ^{13}C (125 *MHz*, Acetone-d_6) NMR data, see **Table 12**; HREIMS m/z 370.1458 $[M]^+$, (calcd $C_{21}H_{22}O_6$ 370.1416).

Compound 11 (Erythribyssin K): Appearance: Brown powder; IR (KBr): ν_{max} 3038, 1825, 1618, 1497, 609 cm^{-1}; UV (c 0.025, MeOH) λ_{max} nm: 208, 214, 231, 276, 309 nm; CD (*c* 0.55 MeOH): $[\theta]_{211}$ +7.44, $[\theta]_{232}$ +8.52, $[\theta]_{286}$ −26.47, $[\theta]_{327}$ +2.99; ^{1}H (500 *MHz*) and ^{13}C (125 *MHz*, Acetone-d_6) NMR data, see **Table 13**; HREIMS m/z 284.0586 $[M]^+$, (calcd $C_{16}H_{12}O_5$ 284.0685).

Compound 12 (Erythribyssin L): Appearance: White amorphous powder; $[\alpha]^{25}_{D}$: −54.9^{o} (c = 0.02, MeOH); IR (KBr): ν_{max} 3425, 2973, 2926, 1599, 1450 cm^{-1}; UV (c 0.03, MeOH) λ_{max} nm: 210, 214, 232, 286, 320 nm; ^{1}H (500 *MHz*) and ^{13}C (125 *MHz*, Acetone-d_6) NMR data, see **Table 14**; HREIMS m/z 408.1937 $[M]^+$, (calcd $C_{25}H_{28}O_5$ 408.1948).

Compound 13 (Erythribyssin M): Appearance: Brown powder; $[\alpha]^{25}_{D}$: −16.7^{o} (c = 0.01, MeOH); IR (KBr): ν_{max} 3408, 2928, 1657, 1625, 1161-1033 cm^{-1}; UV (c 0.02, MeOH) λ_{max} nm: 208, 228, 277, 363 nm; ^{1}H (500 *MHz*) and ^{13}C (125 *MHz*, Acetone-d_6) NMR data, see **Table 15**; HREIMS m/z 368.1624 $[M]^+$, (calcd $C_{22}H_{24}O_5$ 368.1620).

Compound 14 (Erythribyssin N): Appearance: Brown powder; IR (KBr): ν_{max} 3447, 2923, 1716, 1628, 1423, 1264 cm^{-1}; UV (c 0.02, MeOH) λ_{max} nm: 210, 214, 242, 299, 336, 352 nm; ^{1}H (500 *MHz*) and ^{13}C (125 *MHz*, Acetone-d_6) NMR data, see **Table 16**; HREIMS m/z 350.1154 $[M]^+$, (calcd $C_{21}H_{18}O_5$ 350.1126).

Compound 15 (Erythribyssin O): Appearance: Yellow amorphous powder; IR (KBr): v_{max} 3038, 1825, 1618, 1497, 609 cm^{-1}; UV (c 0.025, MeOH) λ_{max} nm: 208, 214, 231, 276, 309 nm; ^{1}H (500 *MHz*) and ^{13}C (125 *MHz*, Acetone-d_6) NMR data, see **Table 17**; HREIMS m/z 350.1154 $[M]^+$, (calcd $C_{21}H_{18}O_5$ 350.1146).

2.2. *In vitro* PTP1B assay

PTP1B (human, recombinant) was purchased from BIOMOL International LP (USA) and the enzyme activity was measured using *p*-nitrophenyl phosphate (*p*-NPP) as a substrate. To each 96-well (final volume: 200 lL) were added 2 mM p-NPP and PTP1B (0.05–0.1 μg) in a buffer containing 50 mM citrate (pH 6.0), 0.1 M NaCl, 1 mM EDTA, and 1 mM dithiothreitol (DTT) with or without test compounds. Following incubation at 37°C for 30 min, the reaction was terminated with 10M NaOH. The amount of produced *p*-nitrophenol was estimated by measuring the absorbance at 405 nm. The nonenzymatic hydrolysis of 2mM *p*-NPP was corrected by measuring the increase in absorbance at 405 nm obtained in the absence of PTP1B enzyme.

III. RESULTS AND DISCUSSION

1. Structure determination of new compounds isolated from *E. abyssinica*

1.1 Structure determination of compound 1

Compound **1** was obtained as yellow amorphous powder with the molecular formula $C_{22}H_{24}O_5$, as determined by the HR-EI mass spectrum ($[M]^+$, *m/z* 368.1628). The IR spectrum of compound **1** suggested the presence of OH functional groups at 3406 cm^{-1}, 2927 (C–C), 1468 and 1193–1119, and C–O stretching vibrations at 1061–1041 cm^{-1}. The UV spectral data, ^1H and ^{13}C NMR spectra of compound **1** showed signals assignable to a methylene, a methine and one aliphatic quaternary carbon with an oxygen function [δ_H 4.07 (1H, d, J = 11.5 Hz), 4.32 (1H, d, J = 11.5 Hz), and 5.59 (1H, s)]; [δ_C 69.2 (C-6), 80.9 (C-6a), 82.6 (C-11a)]. This suggests that compound **1** is a pterocarpan derivative with an oxygenated functional group attached to C-6a.[47-48] Two methoxy groups were observed from the signals in the ^1H– and ^{13}C–NMR spectra (acetone-d_6, Table 1) [δ_H 3.12 (3H, s), δ_C 50.9 (6a-OCH_3)]; and [δ_H 3.81 (3H, s), δ_C 56.4 (9-OCH_3)]. One prenyl group [δ_H 1.56, 168 (each 3H, s), 3.19 (2H, d, J = 7.5 Hz), 5.13, (1H, t-like, J = 7.5 Hz); δ_C 17.9, 25.9, 23.1, 123.1, and 131.7], two *ortho*-coupled aromatic protons [δ_H 7.20 (1H, d, J = 8.0 Hz) and 6.59 (1H, d, J = 8.0 Hz)], and one ABX–type aromatic spin system at [δ_H 7.33 (1H, d, J = 8.5 Hz), 6.26 (1H, d, J = 2.5 Hz), and 6.59 (1H, dd, J = 2.5, 8.5 Hz)] were also observed. These assignments resembled those of erythrabyssin I,[47] except for the signal for the 6a-methoxy moiety. Placement of this methoxyl group at C-6a was further confirmed by the HMBC correlation of the signal from δ_H 3.12 (3H, s) to C-6a (δ_C 80.9) (Table 3). The attached positions of the prenyl moiety and the other methoxyl group of compound **1** were also determined by HMBC experiments with δ_H 3.81 (3H, s) and C-9 (160.8); H_2-1′ and C-9, 10; H_2-6 and

C-4a, 6a, 11a, 6b; H-11a and C-1, 4a, 11b, 6b, 10a; H-1 and C-11a, 3, 4a; H-4 and C-3, 4a, 11b; H-7 and C-6a, 6b, 9, 10a; H-8 and C-6b, 10 and C-9 (Table 3). Compound **1** contains two chiral centers at C-6a and C-11a, which were considered to possess either *R*,*R* or *S*,*S* configurations from the stereochemical environment around the C-6a and C-11a.[49] However, it is generally accepted that the absolute configuration of a pterocarpan compound may be presumed from the sign of its optical rotation.[49] Levorotatory pterocarpans have 6a*R* and 11a*R* configurations, while the dextrorotatory ones have 6a*S* and 11a*S* configurations.[50] In the case of compound **1**, the specific optical rotation value was – 205º (c = 0.03, MeOH). Therefore, the absolute configuration at C-6a and C-11a was assigned to *S* from its negative optical rotation value.[47, 50, 51] The circular dichroism (CD) spectrum of compound **1** revealed a positive Cotton effect [MeOH, λ_{max} = 295 nm ($\Delta\varepsilon$ = +0.98)], indicating an absolute configuration of 6a*S* and 11a*S*.[51] Based on the above data, Compound **1** was identified as (6a*S*,11a*S*)-3-hydroxy-6a,9-dimethoxy-10-(3′,3′-dimethylallyl)pterocarpan, a new natural product named erythribyssin A.

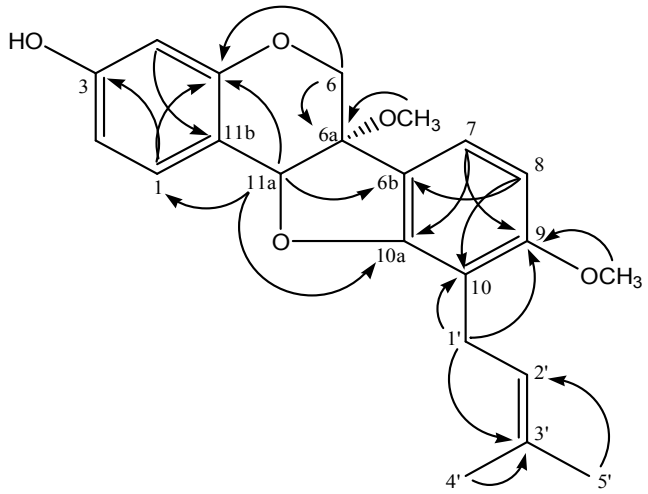

Key HMBC correlations of erythribyssin A (**1**) (H → C)

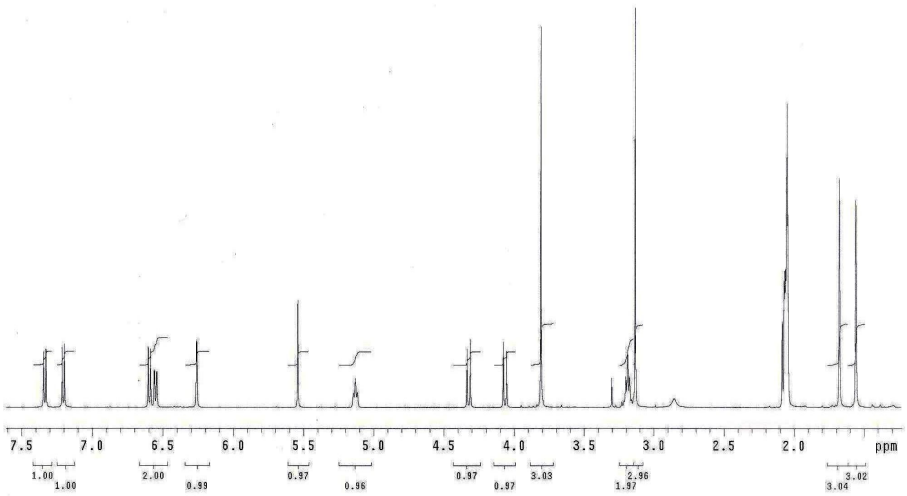

Fig. 3. ^{1}H-NMR spectrum of compound **1** (500 MHz, acetone-d_6)

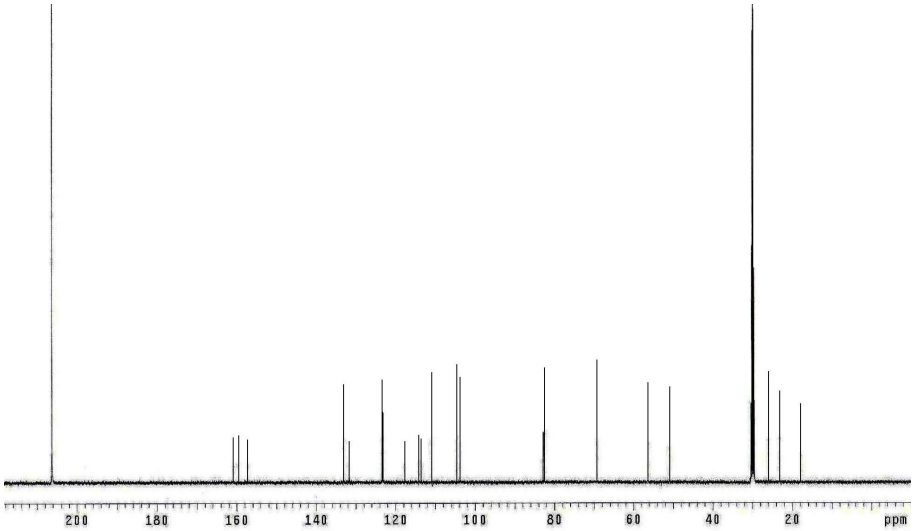

Fig. 4. ^{13}C-NMR spectrum of compound **1** (125 MHz, acetone-d_6)

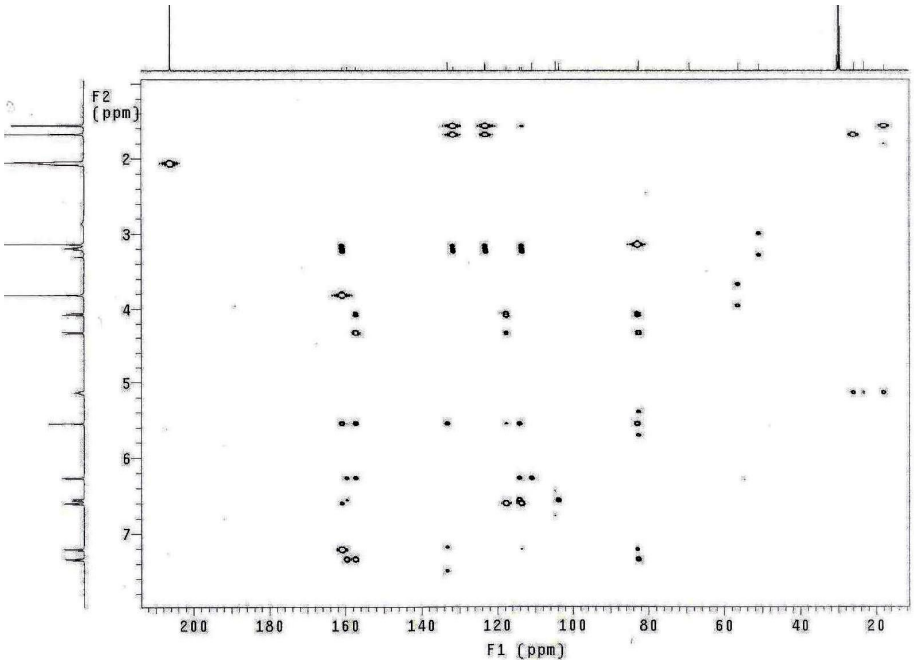

Fig. 5. HMBC spectrum of compound **1** (500 MHz, acetone-d_6)

Table 3. ^{1}H and ^{13}C NMR spectral data of compound **1** (acetone-d_6, 500*MHz*)

position	δ_H mult. (*J* in Hz)	δ_C	HMBC (H → C)
1	7.33 (d, *J* = 8.5)	133.1	C-3, C,-4a, C-11a
2	6.59 (dd, *J* = 2.5, 8.5)	110.9	C-3, C-4, C-11b
3		160.0	
4	6.26 (d, *J* = 2.5)	103.7	C-2, C-3, C-4a, C-11b
4a		157.2	
6	4.23 (d, *J* = 11.5) 4.07 (d, *J* = 11.5)	69.2	C-4a, C-6a, C-6b, C-11a
6a		80.9	
6b		117.6	
7	7.20 (d, *J* = 8.0)	123.4	C-6a, C-9, C-10a
8	6.59 (d, *J* = 8.0)	104.6	C-6b, C-9, C-10
9		160.8	
10		113.5	
10a		160.9	
11a	5.54 (s)	82.6	C-1, C-11b, C-4a, C-6a, C-6b, C-10a
11b		114.1	
1'	3.19 (d, *J* = 8.0)	23.1	C-9, C-10, C-2', C-3'
2'	5.13 (d, *J* = 8.0)	123.1	C-1', C-4', C-5', C-3'
3'		131.7	
4'	1.56 (s)		C-2', C-3', C-5'
5'	1.68 (s)	25.9	C-2', C-3', C-4'
6a-OCH_3	3.12 (s)	17.9	C-6a
9-OCH_3	3.81 (s)	50.9	C-9

1.2 Structure determination of compound 2

Compound **2** was isolated as a yellowish amorphous powder and showed absorption maxima at 208 nm (log ε = 4.80), 228 nm (log ε = 4.46), 277 nm (log ε = 4.32) and 363 nm (log ε = 3.71) in the UV spectrum. The IR spectrum of compound **2** showed absorption bands at 3418 (OH), 2924 (C–C), 1650 (CHO), and 1418, 1160**,** 1041 cm^{-1} ascribable to aromatic ring. The molecular formula for compound **2**, $C_{16}H_{12}O_5$, was determined from the molecular ion peaks (*m/z* 284.0688) observed by high-resolution EI-MS measurement. The ^{1}H-NMR spectrum of compound **2** showed four signals at δ_H 4.32 (1H, dd), 3.72 (1H, dd), and 3.71 (1H, m), and 5.80 (1H, d), which were reminiscent of a pterocarpan skeleton.[50, 52] The presence of 1,2,4-trisubstituted benzene [δ_H 7.38 (1H, d), 6.59 (1H, dd), and 6.38 (1H, d)] and *ortho*-coupled aromatic protons [δ_H 7.55 (1H, d, J = 8.0 Hz) and 6.41 (1H, d, J = 8.0 Hz)] on rings A and D in the ^{1}H- and ^{13}C-NMR spectra was assigned. The ^{13}C NMR spectrum showed 16 carbons, of which 15 were assigned to the pterocarpan skeleton. The remaining one carbon signal at δ_C 193.5 and the corresponding proton signal δ_H 10.14 (1H, s) was characteristic of an aldehyde group. The assignment of the aldehyde group at C-10 was supported by the HMBC experiment, which indicated a correlation from the aldehyde proton to the aromatic quaternary carbon at C-10 (δ_C 108.3) (See Table 4). The absolute stereochemistry at C-6a and C-11a was found to be *R* from the negative optical rotation value [– 110° (c = 0.02, MeOH)].[50, 53] From the above data, compound **2** was determined to be **[**3,9-dihydroxy-(6a-*R* and 11a-*R*)-10-formyl]pterocarpan named as erythribyssin B.

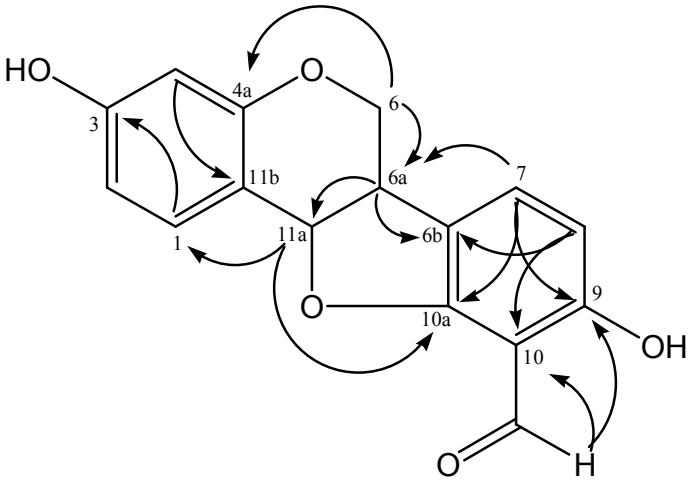

Key HMBC correlations of erythribyssin B (**2**) (H → C)

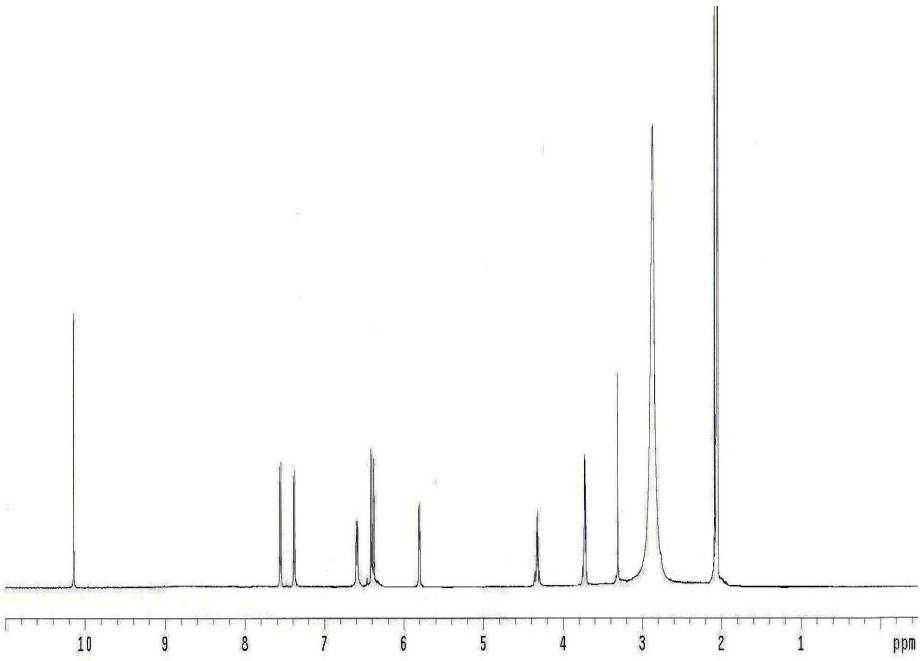

Fig. 6 ^{1}H-NMR spectrum of compound **2** (500 MHz, acetone-d_6)

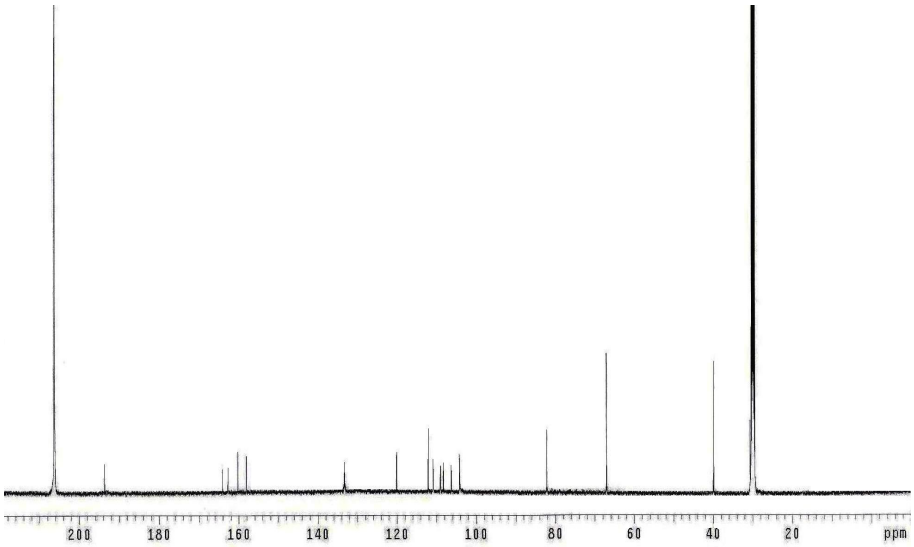

Fig. 7. ^{13}C-NMR spectrum of compound **2** (125 MHz, acetone-d_6)

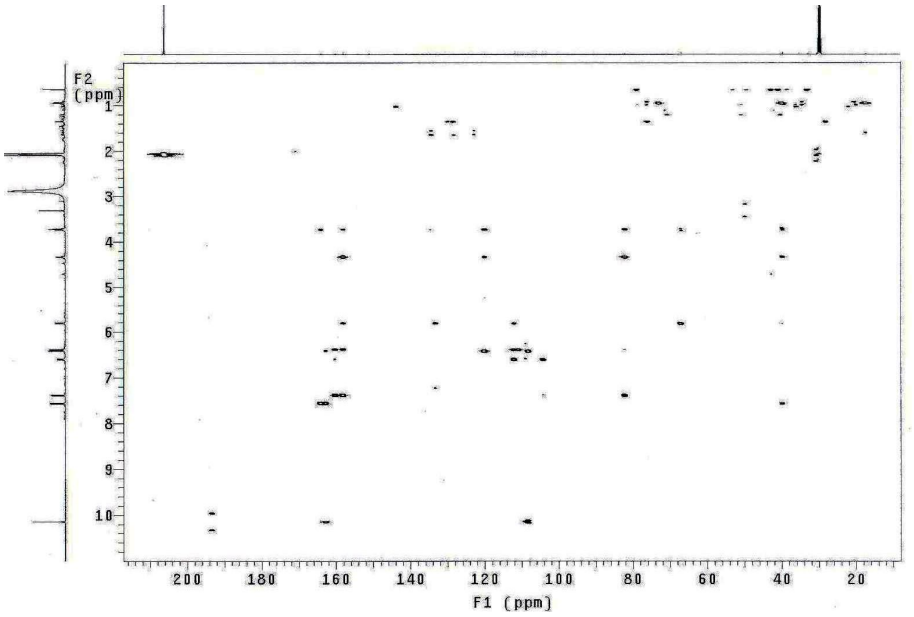

Fig. 8. HMBC spectrum of compound **2** (500 MHz, acetone-d_6)

Table 4. ^{1}H and ^{13}C NMR spectral data of compound **2** (500 MHz, acetone-d_6)

position	δ_H mult. (J in Hz)	δ_C	HMBC (H → C)
1	7.38 (d, J = 8.0)	133.3	C-3, C-4a, C-11a
2	6.59 (dd, J = 2.0, 8.0)	112.1	C-4, C-11b
3		160.2	
4	6.38 (d, J = 2.0)	104.2	C-2, C-3, C-4a, C-11b
4a		158.1	
6	4.32 (m) 3.72 (m)	67.1	C-4a, C-6a, C-11a, C-6b
6a	3.72 (m)	42.8	C-6, C-7, C-10a
6b		106.3	
7	7.55 (d, J = 8.0)	120.1	C-6a, C-9, C-10a
8	6.41 (d, J = 8.0)	109.0	C-6b, C-7, C-9, C-10
9		162.7	
10		108.3	
10a		164.1	
11a	5.80 (d, J = 7.5)	82.2	C-1, C-6, C-6a, C-6b, C-10a
11b		110.9	
10-CHO	10.14 (s)	193.5	C-9, C-10

1.3 Structure determination of compound 3

Compound **3** was obtained as a white amorphous powder with absorption bands at 3406 (OH), 2927(C–C), 1606, 1468, 1374, 1279, 1142, and 1062 cm^{-1} in the IR spectrum. The HREI-MS of compound **3** showed a molecular ion peak at *m/z* 340.1313 $[M]^+$ (calcd $C_{20}H_{20}O_5$ 340.1311). The ^1H NMR spectrum of compound **3** showed characteristic signals of a pterocarpan skeleton as shown in Table 5.[47-48, 51-53] A comparison of the ^1H NMR spectrum of compound **3** with those of compounds **1** and **2** showed the same substitution patterns except for some peaks assignable to the 3-hydroxy-2,2-dimethyldihydropyran moiety at δ_H 3.75 (1H, dd, J = 6.0, 7.5 Hz), 2.90 (1H, dd, J = 6.0, 16.5 Hz), 2.46 (1H, dd, J = 7.5, 16.5 Hz), 1.33 (3H, s), and 1.20 (3H, s).[52] The dihydropyran ring fused to the C-9 and C-10 position was assigned from the HMBC spectrum, which showed correlations from the aliphatic protons at C-1′ [δ_H 2.90 (1H, dd, J = 6.0, 16.5 Hz), and 2.46 (1H, dd, J = 7.5, 16.5 Hz)] to the carbons at C-10 (δ_C 105.2) and C-9 (δ_C 155.1), and from the oxygenated aliphatic proton δ_H 3.75 (1H, dd, J = 6.0, 7.5 Hz) to a carbon at C-10 (δ_C 105.2). Compound **3** showed the same HMBC correlations for the ring arrangement (ring A and D) found in compound **2**, and a negative optical rotation value [– 16.7° (c = 0.02, MeOH)], confirmed the absolute stereochemistry of C-6a and C-11a of compound **3** to be (6a*R*:11a*R*).[52] The configuration at C-2′ was determined as 2′-β-hydroxy based on the chemical shift and the coupling constant of the 2′-H. Therefore, the structure of compound **3** was represented as formula **3** (6a*R* and 11a*R*), and called erythribyssin C.

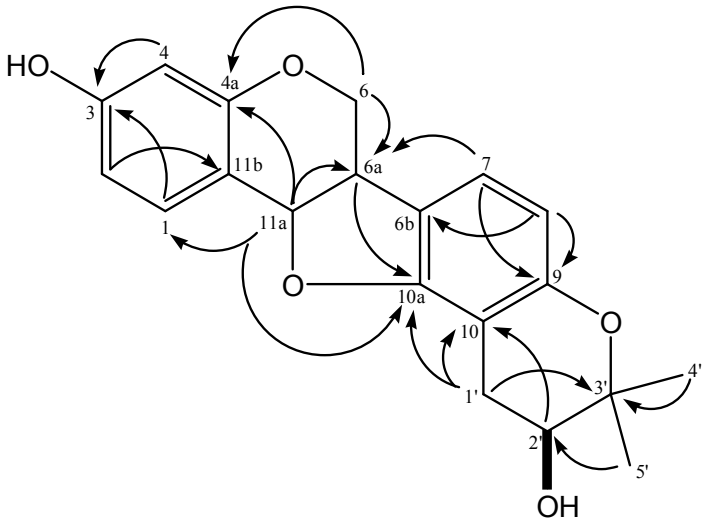

Key HMBC correlations of erythribyssin C (**3**) (H → C)

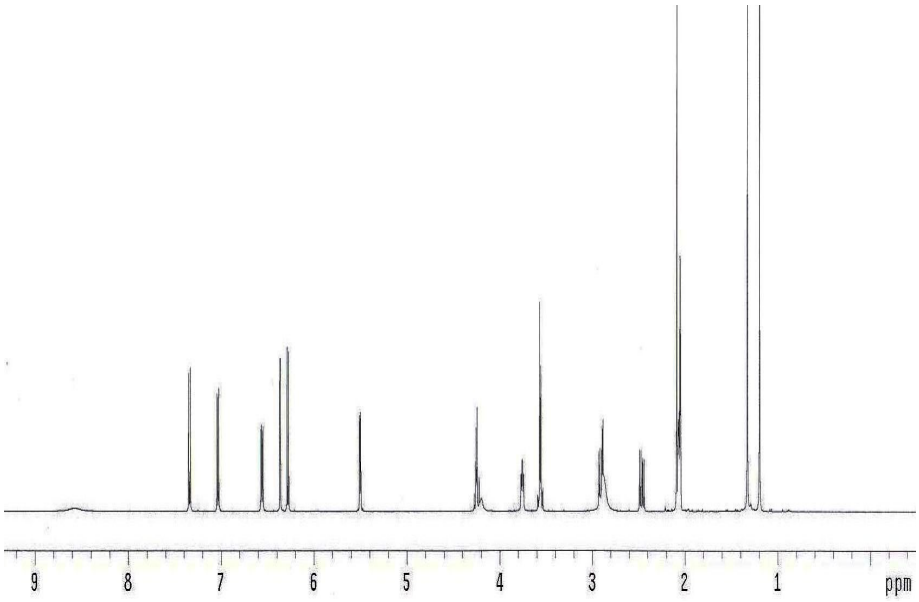

Fig. 9 ^{1}H-NMR spectrum of compound **3** (500 MHz, acetone-d_6)

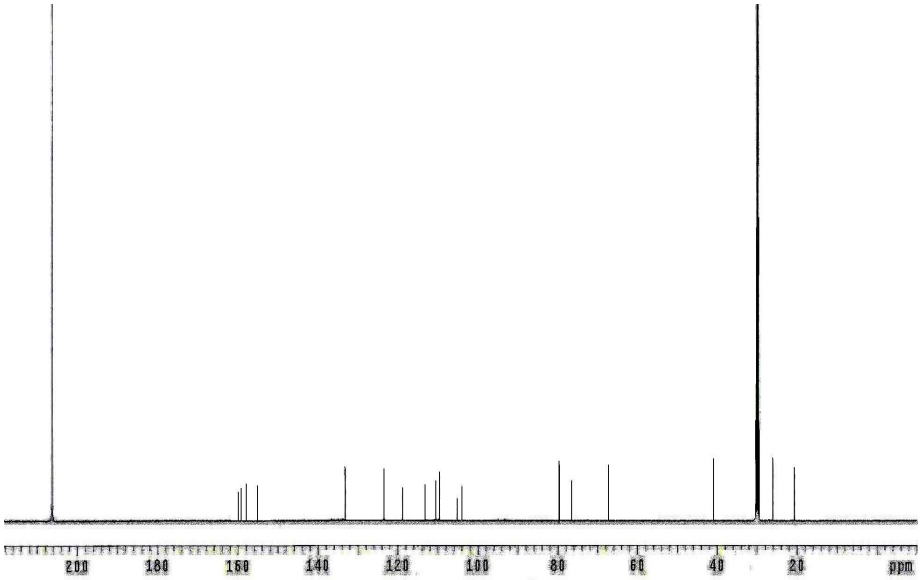

Fig. 10. ^{13}C-NMR spectrum of compound **3** (125 MHz, acetone-d_6)

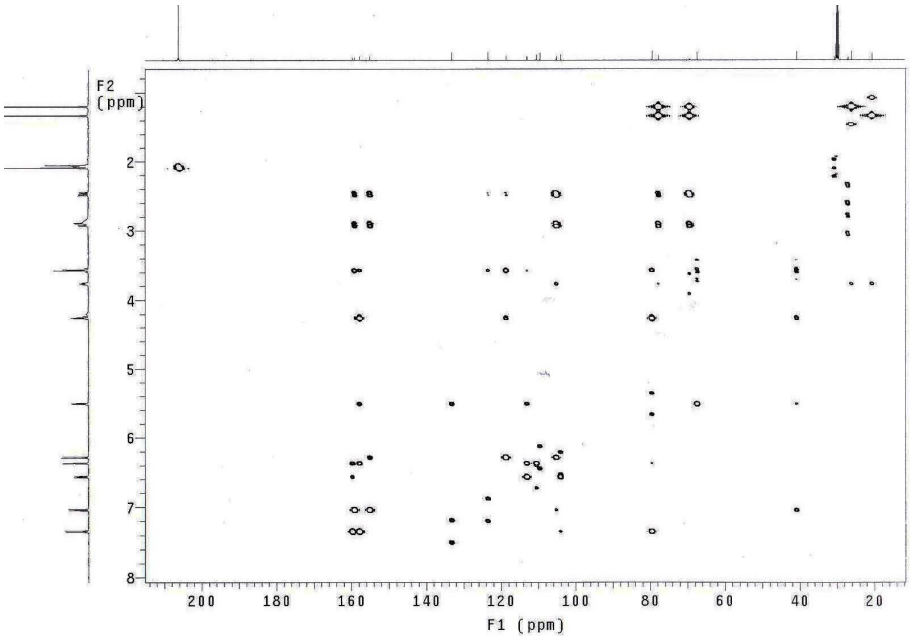

Fig. 11. HMBC spectrum of compound **3** (500 MHz, acetone-d_6)

Table 5. ^{1}H and ^{13}C NMR spectral data of compound **3** (500 MHz, acetone-d_6)

position	δ_H mult. (J in Hz)	δ_C	HMBC (H → C)
1	7.34 (d, J = 8.0)	133.2	C-3, C-4a, C-11a
2	6.56 (dd, J = 2.5, 8.0)	110.5	C-3, C-4, C-11b
3		159.7	
4	6.36 (d, J = 2.5)	104.0	C-2, C-3, C-4a, C-11b
4a		157.8	
6	4.25-ax (dd, J = 10.5, 16.5) 3.65-eq (dd, J = 2.0, 16.5)	67.4	C-4a, C-6a, C-11a, C-6b
6a	3.55 (m)	40.8	C-6, C-7, C-10a, C-11a, C-11b
6b		118.7	
7	7.03 (d, J = 8.0)	123.5	C-6a, C-9, C-10a
8	6.28 (d, J = 8.0)	109.6	C-6b, C-7, C-9, C-10
9		155.1	
10		105.2	
10a		159.2	
11a	5.50 (d, J = 6.0)	79.5	C-1, C-6, C-6a, C-6b, C-10a, C-4a
11b		113.1	
1'	2.90 (dd, J = 6.0, 16.5) 2.46 (dd, J = 7.5, 16.5)	27.1	C-9, C-10, C-10a, C-2', C-3'
2'	3.75 (dd, J = 6.5, 7.5)	69.5	C-1', C-10, C-3', C-4', C-5'
3'		77.8	
4'	1.33 (s)	20.6	C-2', C-3', C-5'
5'	1.20 (s)	26.1	C-2', C-3', C-4'

1.4 Structure determination of compound 4

Compound **4** was also obtained as a white amorphous powder with absorption bands at 3406 (OH), 2927(C–C), 1606, 1468, 1374, 1279, 1142, and 1062 cm^{-1} in the IR spectrum. The HR-EI-MS of compound **4** showed a molecular ion peak at *m/z* 363.1216 $[M + Na]^+$ (calcd $C_{20}H_{20}O_5Na$ 363.1208). The ^1H and ^{13}C NMR spectra of compound **4** showed absolutely same with those of compound **3.** From the 1D and 2D NMR data (Table 5 and Table 6) and HR-EI-MS of **3** and **4** indicated that **3** and **4** had an identical structure. The dihydropyran ring fused to the C-9 and C-10 position was also assigned from the HMBC spectrum. However, two signals were observed in HPLC experiment, the retention time of compound **3** was shorter than compound **4**. Comparison of the IR, UV ^1H and ^{13}C NMR between **4** and **3** suggested that compound **4** was an isomer of **3**. A negative optical rotation value [– 54.9° (c = 0.02, MeOH)] was produced from $[\alpha]_D$ experiment confirmed the absolute stereochemistry of C-6a and C-11a of compound **4** to be (6a*R*:11a*R*).[52] Based on the characteristic of the proton at C-2′ δ_H 3.75 (1H, dd, *J* = 5.0, 7.0), that the configuration at C-2′ was deduced as α-hydoxy. Therefore, the structure of compound **4** was also represented as shown and called erythribyssin D.

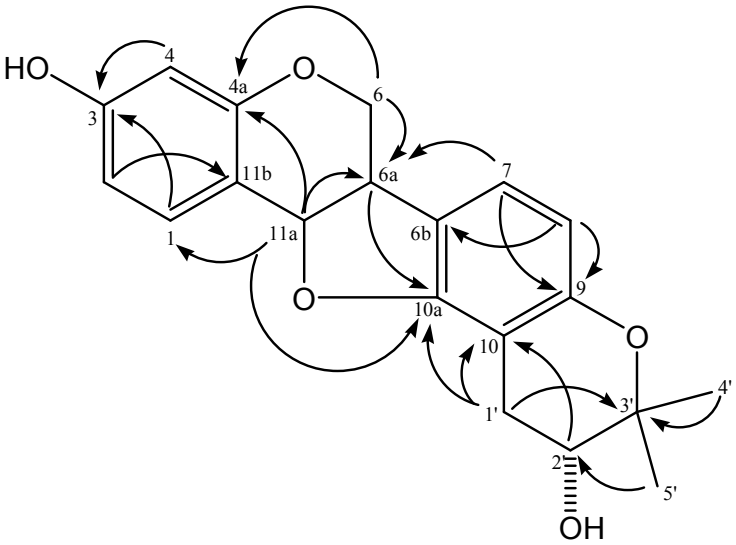

Key HMBC correlations of erythribyssin D (**4**) (H → C)

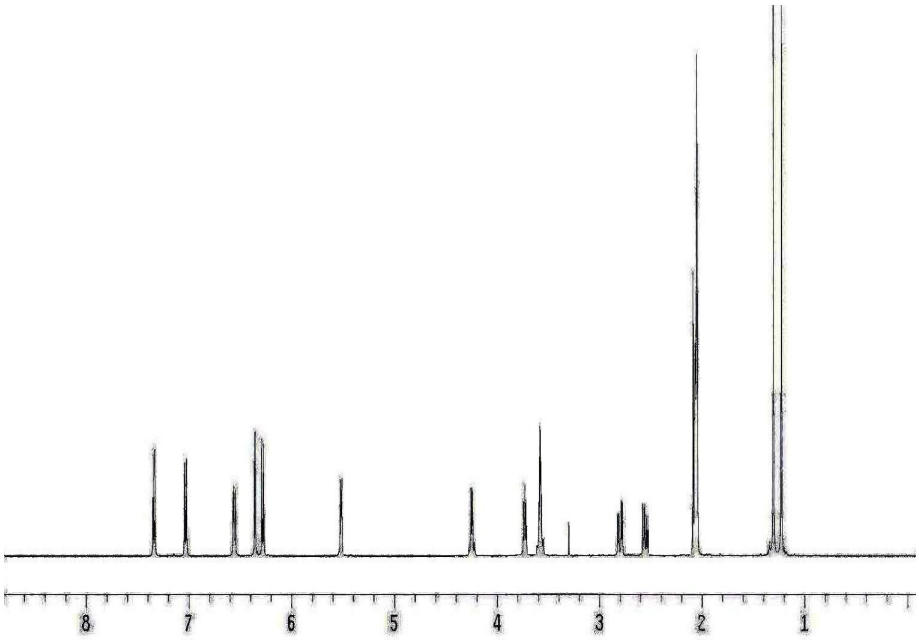

Fig. 12 ^{1}H-NMR spectrum of compound **4** (500 MHz, acetone-d_6)

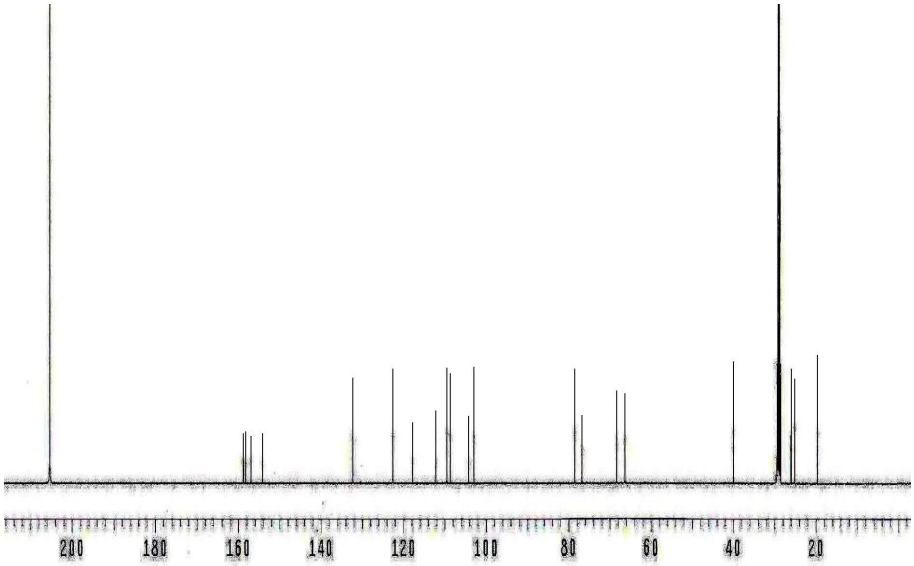

Fig. 13. ^{13}C-NMR spectrum of compound **4** (125 MHz, acetone-d_6)

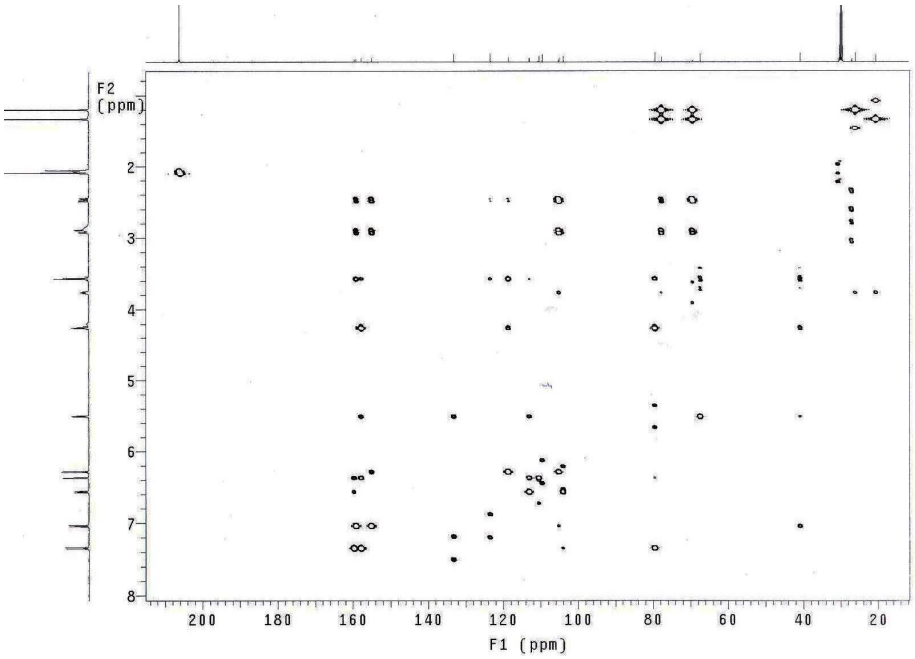

Fig. 14. HMBC spectrum of compound **4** (500 MHz, acetone-d_6)

Table 6. ^{1}H and ^{13}C NMR spectral data of compound **4** (500 MHz, acetone-d_6)

position	δ_H mult. (J in Hz)	δ_C	HMBC (H → C)
1	7.34 (d, J = 8.0)	133.2	C-3, C-4a, C-11a
2	6.56 (dd, J = 2.5, 8.0)	110.5	C-3, C-4, C-11b
3		159.7	
4	6.36 (d, J = 2.5)	104.0	C-2, C-3, C-4a, C-11b
4a		157.8	
6	4.25-ax (dd, J = 10.5, 16.5) 3.65-eq (dd, J = 2.0, 16.5)	67.4	C-4a, C-6a, C-11a, C-6b
6a	3.55 (m)	40.8	C-6, C-7, C-10a, C-11a, C-11b
6b		118.7	
7	7.03 (d, J = 8.0)	123.5	C-6a, C-9, C-10a
8	6.28 (d, J = 8.0)	109.6	C-6b, C-7, C-9, C-10
9		155.1	
10		105.2	
10a		159.2	
11a	5.50 (d, J = 6.0)	79.5	C-1, C-6, C-6a, C-6b, C-10a, C-4a
11b		113.1	
1'	2.90 (dd, J = 6.0, 16.5) 2.46 (dd, J = 7.5, 16.5)	27.1	C-9, C-10, C-10a, C-2', C-3'
2'	3.75 (dd, J = 5.0, 7.0)	69.5	C-1', C-10, C-3', C-4', C-5'
3'		77.8	
4'	1.33 (s)	20.6	C-2', C-3', C-5'
5'	1.20 (s)	26.1	C-2', C-3', C-4'

1.5 Structure determination of compound 5

Compound **5** was obtained as a yellowish amorphous powder, its molecular formula $C_{22}H_{24}O_5$, was established from the HR-EI-MS spectrum. Its UV spectrum (c 0.025, MeOH) 206, 216, 234, 276, 310 nm and the ^{1}H as well as the ^{13}C spectra showed **5** to be an isoflavanone [δ_H 4.12 (1H, dd, J = 5.0, 11.0 Hz, H-3), 4.42 (1H, dd, J = 5.0, 11.0 Hz, H-2$_{eq}$), and 4.55 (1H, t, J = 11.0 Hz, H-2$_{ax}$)], together with [δ_C 48.1 (C-3), 71.7 (C-4), and a conjugated carbonyl carbon δ_C 191.3 (C-4)] having a γ,γ-dimethylallyl [δ_H 1.61, 1.63 (each 3H, 4′, 5′-Me), 3.16 (2H, br d, J = 7.0 Hz, H-1′) and 5.19 (1H, m, H-2′); δ_C 17.7, 25.8 (4′, 5′-Me), 28.3 (C-1′), 123.8 (C-2′), 132.2 (C-3′)], and two methoxyl groups [δ_H 3.79 (3H, s), δ_C 55.9 (4′-OCH$_3$); δ_H 3.84 (3H, s), δ_C 56.2 (2′-OCH$_3$)]. The ^{1}H NMR spectrum also showed the presence of two sharp one proton singlets at δ_H 6.66 (1H, s) and δ_H 6.84 (1H, s) assignable to two *para*-coupled aromatic protons in one ring, and a typical ABX spin system at δ_H 7.75 (1H, d, J = 8.5 Hz), 6.58 (1H, dd, J = 8.5 and 2.5 Hz), and 6.39 (1H, d, J = 2.5 Hz), establishing an *ortho*-, *ortho*/*meta*-, and *meta*-coupling system due, respectively, to proton H-5, H-6 and H-8 in ring A. Comparison of the ^{1}H and ^{13}C NMR data of **5** with those of sigmoidin I and prostratol C[54] show quiet similarity, except only for one additional methoxyl group [δ_H 3.84 (3H, s), (δ_C 56.2)] in **5**. The position of these two methoxyl groups were assigned by an HMBC experiment, correlations between the methoxyl signal from δ_H 3.79 (3H, s) to C-4′ (δ_C 157.7) and from δ_H 3.84 (3H, s) to C-2′ (δ_C 158.4) (See Table 7) supported for the observations. The attachment of the prenyl group to C-5′ was also confirmed by correlations between H-1′ (δ_H 3.16 (2H, d, J = 7.0 Hz) to C-4′ (δ_C 157.7), C-5′ (δ_C 116.5) and C-6′ (δ_C 129.9) in the HMBC experiment. On the basic of the above spectroscopic studies, compound **5** was thus assigned as 7-hydroxy-2′,4′-dimethoxy-5′-(3methylbut-2-enyl) isoflavanone, and named erythribyssin E.

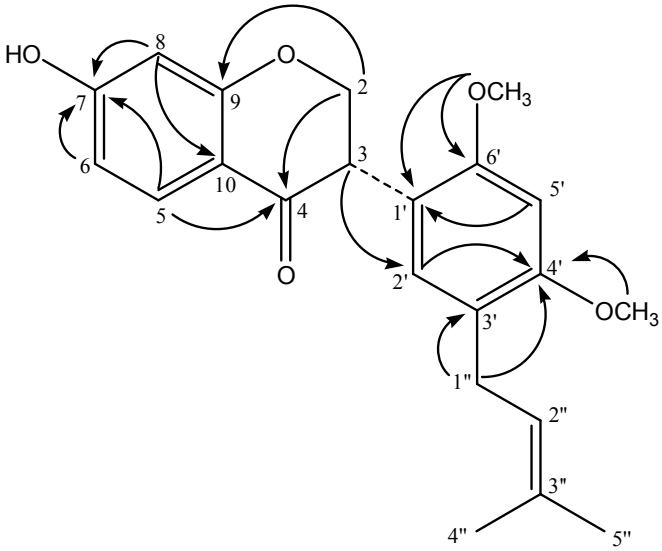

Key HMBC correlations of erythribyssin E (**5**) (H → C)

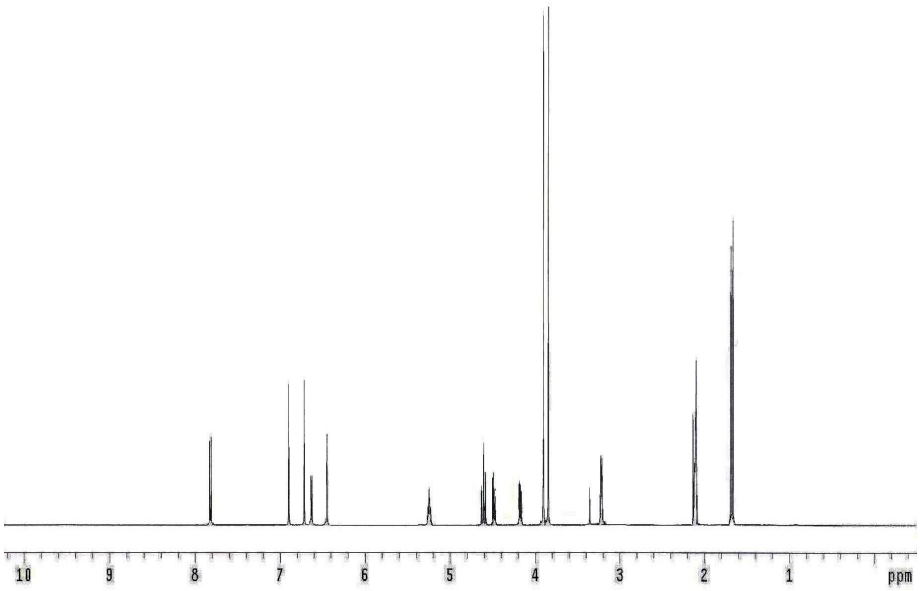

Fig. 15 ^{1}H-NMR spectrum of compound **5** (500 MHz, acetone-d_6)

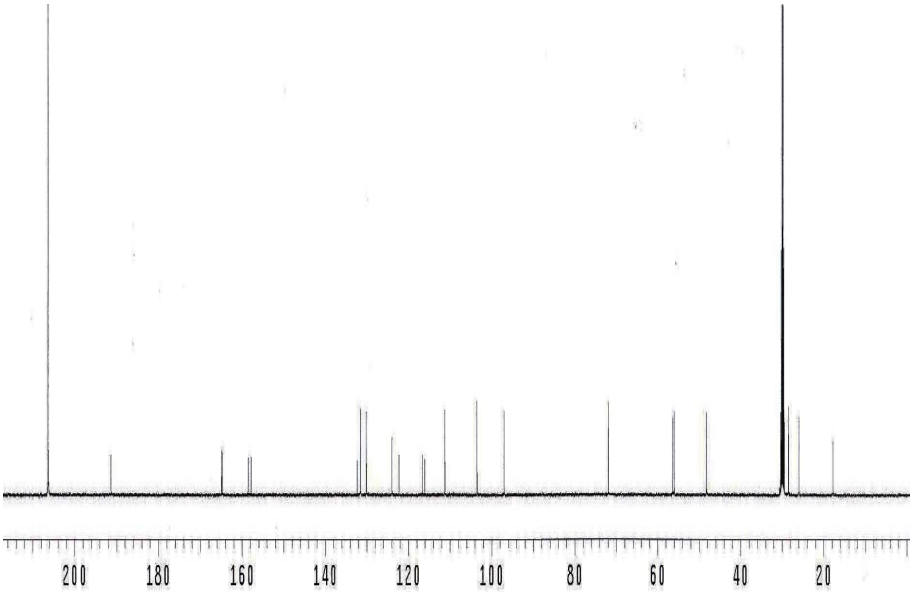

Fig. 16. ^{13}C-NMR spectrum of compound **5** (125 MHz, acetone-d_6)

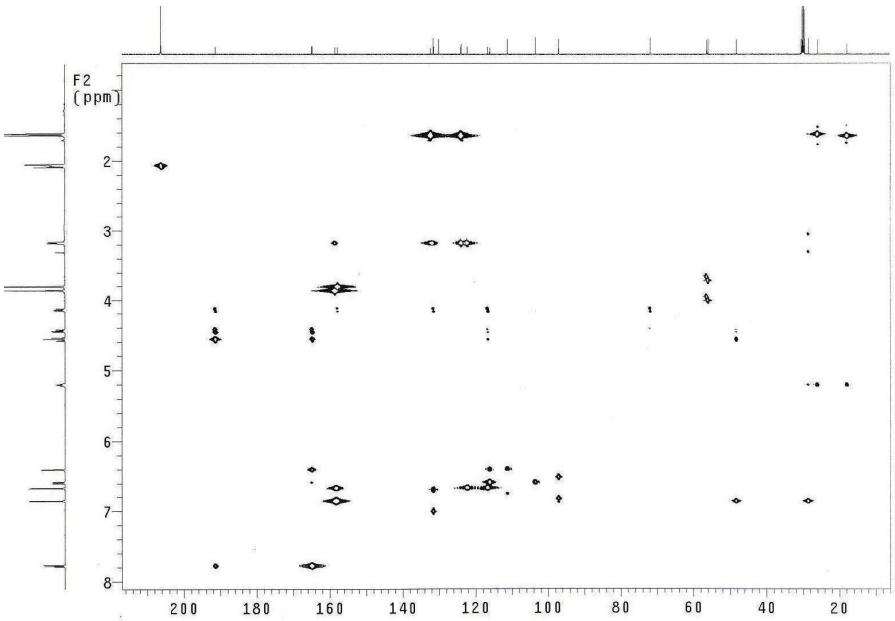

Fig. 17. HMBC spectrum of compound **5** (500 MHz, acetone-d_6)

Table 7. ^{1}H and ^{13}C NMR spectral data of compound **5** (500 MHz, acetone-d_6)

position	δ_H mult. (J in Hz)	δ_C	HMBC (H → C)
1			
	4.55-ax (t-like, J = 10.5,	71.7	C-3, C-4, C-9, C-1'
2	11.0)		
	4.42-eq (dd, J = 5.1, 11.0)		
3	4.12 (dd, J = 5.1, 10.5)	48.1	C-10, C-2', C-6'
4		191.3	
5	7.75 (d, J = 8.5)	131.4	C-4, C-7, C-9
6	6.58 (dd, J = 2.5, 8.5)	111.1	C-7, C-8, C-10
7		164.9	
8	6.39 (d, J = 2.5)	96.8	C-6, C-7, C-9, C-10
9		164.7	
10		115.9	
1'		122.1	
2'	6.84 (s)	129.9	C-3, C-4', C-6', C-1"
3'		116.5	
4'		157.8	
5'	6.66 (s)	103.4	C-1', C-3'
6'		158.5	
1"	3.16 (d, J = 7.5)	28.3	C-2', C-3', C-4', C-2", C-3"
2"	5.19 (m)	123.8	C-3', C-4", C-5"
3"		132.2	
4"	1.61 (s)	25.8	C-2", C-3", C-5"
5"	1.63 (s)	17.8	C-2", C-3", C-4"
4'-OCH_3	3.79 (s)	55.9	C-1', C-6'
6'-OCH_3	3.84 (s)	56.2	C-4'

1.6 Structure determination of compound 6

Compound **6** was isolated as a brown powder with a molecular formula $C_{25}H_{26}O_6$, as determined by the HR-EI mass spectrum with a molecular ion peak at *m/z* 445.1636 ($[M+Na]^+$; cacl. 445.1627). The IR spectrum of compound **6** suggested the presence of OH functional groups at 3415 cm^{-1}, 2914 (C–C), 1709 (C=O), 1620, 1496 and 1159–1033 cm^{-1}. The UV spectrum of **6** was characteristic of 2-arylbenzofurans, with maxima at 329, and 345 nm. Comparison of the ^1H and ^{13}C NMR spectra of **6** (Table 8) with those of eryvarin Q,[55] indicated that they had an identical structure. The major differences between **6** and eryvarin Q were that a quaternary carbon [δ_C 188.3 (3-CHO)] in eryvarin Q was shifted to up field in **6** (δ_C 168.9), and the aldehyde proton (δ_H 10.17, s) was disappeared in **6**. Comparison of the HR-EI mass spectrum of **6** with that of eryvarin Q showed that compound **6** has more over one oxygen atom in its molecular formula ($C_{25}H_{26}O_6$; *m/z* 445.1636 $[M+Na]^+$) than that of eryvaryn Q ($C_{25}H_{26}O_5$; *m/z* 429.1776 $[M+Na]^+$). The arrangement of the rings and the attachment of two prenyl groups were established by the HMBC experiment (Table 8). All of these data indicated that the aldehyde group (3-CHO) in eryvarin Q was replaced by a carboxylic group (3-COOH) in compound **6**. Base on the above data analyses and the spectroscopic studies, compound **6** was therefore established to be 6-hydroxy-2-(2′,4′-dihydroxy-5′-(3-methylbut-2-enyl)phenyl)-7-(3-methylbut-2-enyl)benzofuran-3-carboxylic acid, named erythribyssin F.

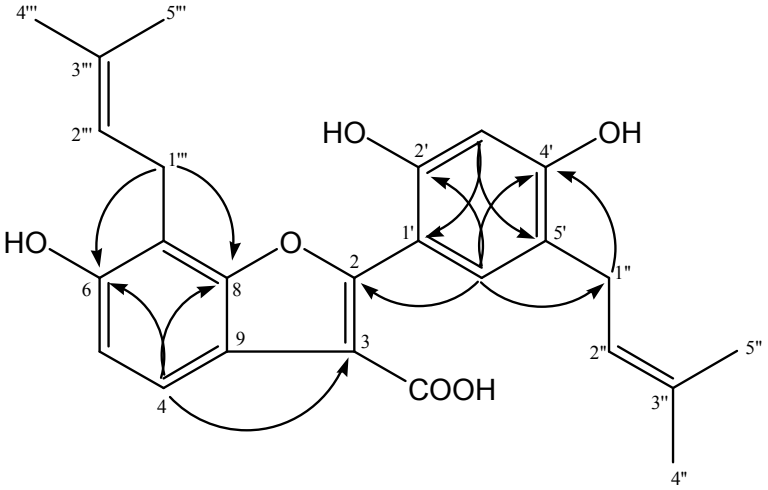

Key HMBC correlations of erythribyssin F (**6**) (H → C)

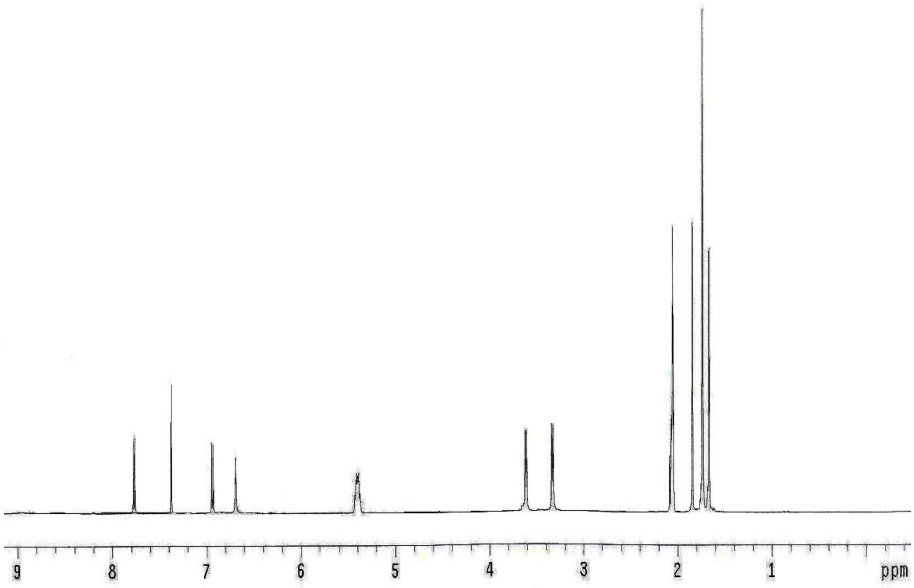

Fig. 18. ^{1}H-NMR spectrum of compound **6** (500 MHz, acetone-d_6)

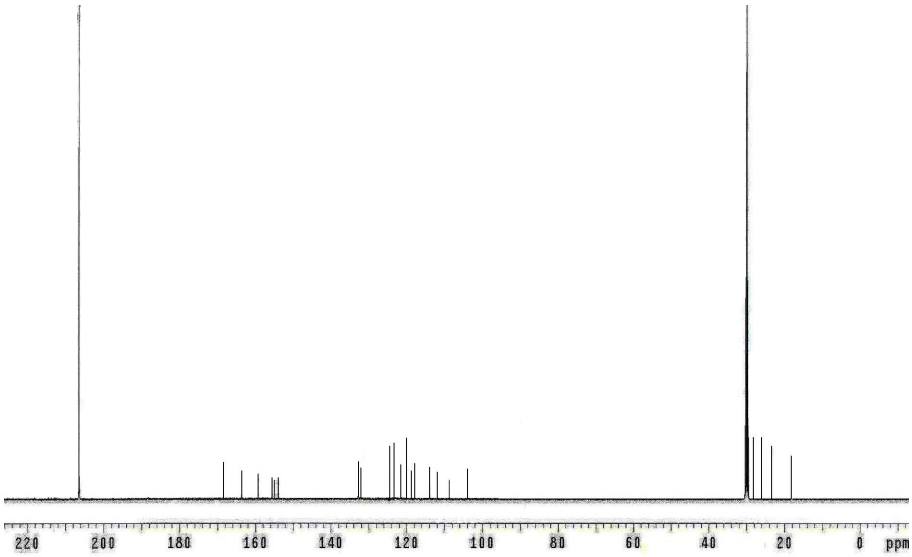

Fig. 19 ^{13}C-NMR spectrum of compound **6** (125 MHz, acetone-d_6)

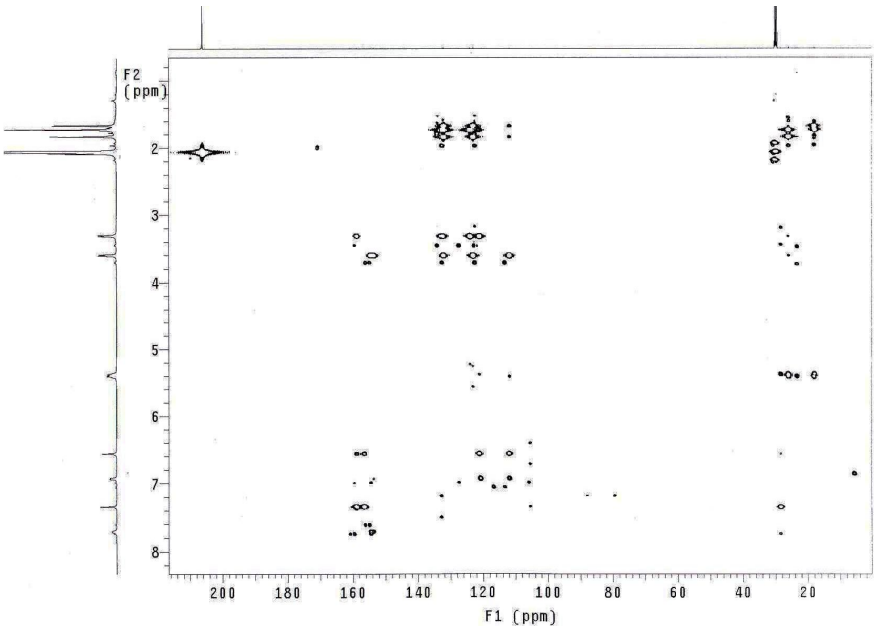

Fig. 20. HMBC spectrum of compound **6** (500 MHz, acetone-d_6)

Table 8. ^{1}H and ^{13}C NMR spectral data of compound **6** (500 MHz, acetone-d_6)

position	δ_H mult. (J in Hz)	δ_C	HMBC (H → C)
1			
2		159.1	
3		111.1	
4	7.70 (d, J = 7.5)	120.4	C-3, C-6, C-8
5	6.92 (d, J = 7.5)	113.6	C-6, C-7, C-9
6		153.6	
7		111.9	
8		154.6	
9		120.7	
1'		112.0	
2'		156.5	
3'	6.56 (s)	105.5	C-1', C-4', C-5'
4'		158.9	
5'		121.1	
6'	7.34 (s)	132.8	C-2, C-2', C-4', C-1"
1"	3.31 (d, J = 7.0)	28.4	C-4', C-5', C-6', C-2", C-3"
2"	5.36 (m)	124.0	C-5', C-4", C-5"
3"		132.5	
4"	1.72 (s)	17.9	C-2", C-3", C-5"
5"	1.72 (s)	26.0	C-2", C-3", C-4"
1'''	3.59 (d, J = 7.0)	23.3	C-6, C-7, C-8, C-2", C-3"
2'''	5.39 (m)	123.1	C-7, C-3''', C-4''', C-5'''
3'''		132.2	
4'''	1.66 (s)	25.9	C-2''', C-3''', C-5'''
5'''	1.83 (s)	18.1	C-2''', C-3''', C-4'''
3-COOH		168.9	

1.7 Structure determination of compound 7

Compound **7** was obtained as a yellowish powder, $[\alpha]_D^{25}$: –16.7° (c = 0.02, MeOH). The molecular formula of **7** was determined as $C_{25}H_{28}O_5$ from a molecular ion peak at *m/z* 408.1933 $[M]^+$ (calcd for 4038.1937) in the HR-EI-MS. Its UV spectrum showed absorption bands at λ_{max} 208, 232, 276, 313 and 370 nm. The ^{1}H NMR displayed an AMX-type spin system at δ_H 5.25 (1H, dd, *J* = 3.0, 13.0 Hz, H-2), 2.93 (1H, dd, *J* = 13.0, 17.0 Hz, H-3_{ax}), and 2.51 (1H, dd, *J* = 3.0, 17.0 Hz, H-3_{eq}) and another ABX-type aromatic spin system at δ_H 7.60 (1H, d, *J* = 8.5 Hz, H-5), 6.44 (1H, dd, *J* = 2.0, 8.5 Hz, H-6), and 6.28 (1H, d, *J* = 2.0 Hz, H-8), together with an AX spin system δ_H 7.10 (1H, d, *J* = 1.5 Hz, H-2′), and 7.15 (1H, d, *J* = 1.5 Hz, H-6′), but showed no proton resonance for a hydroxyl group at C-5, this evidenced for non-substitution at C-5. The ^{13}C NMR showed an oxygenated carbon resonance at δ_C 80.8 (C-2), a methylene resonance at δ_C 44.6 (C-3), and a carbonyl resonance at δ_C 190.5 (C-4). All of these observations were indicative of a flavanone skeleton for **7**. In addition, the ^{1}H and ^{13}C NMR patterns of **7** exhibited the presence of a 3-hydroxy-2,2-dimethyldihydropyran moiety at δ_H 3.68 (1H, dd, *J* = 8.0, 13.0 Hz), 2.91 (1H, dd, *J* = 13.0, 17.0 Hz), 2.62 (1H, dd, *J* = 8.0, 17.0 Hz), 1.38 (3H, s), and 1.12 (3H, s). The dihydropyran ring fused to the C-3′ and C-4′ position was assigned from the HMBC experiment, which showed correlations from the aliphatic protons at C-1′ δ_H 2.91 and 2.46 to the carbons at C-3′ (δ_C 121.0) and C-4′ (δ_C 152.0), and from the oxygenated aliphatic proton δ_H 3.68 to a carbon at C-3′ (δ_C 121.0). Accordingly, the ^{1}H and ^{13}C NMR data of **7** were closely similar to those of abyssinoflavone XXII, which was also isolated from the *E. abyssinica* species in a previous study.[56] However, the ^{1}H and ^{13}C NMR patterns displayed an additional prenyl moiety (Table 9) and the position of the prenyl group was determined to be at C-5′ by correlations from H-1‴ (δ_H 3.28) to C-4′ (δ_C 152.0) and C-5′ (δ_H 130.2) and from H-6′

(δ_H 7.15) to C-5′, C-1‴ in the HMBC spectrum (See Table 9). The configuration at C-2 was inferred to be 2*S*, as indicated by CD data. Hence, compound **7** was identified as a new flavanone, erythibyssin G.

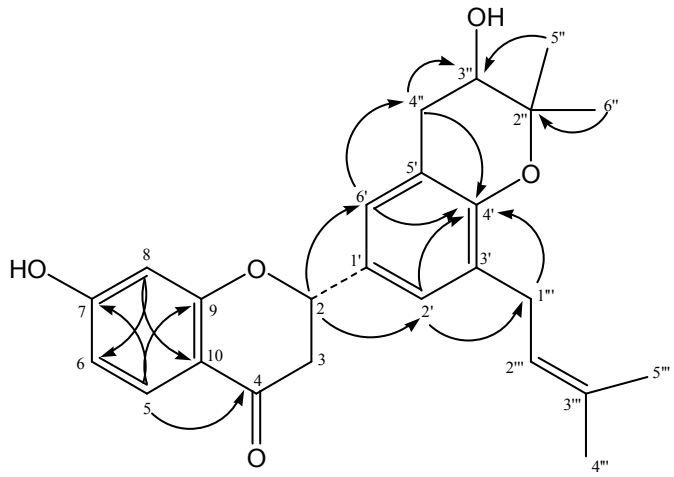

Key HMBC correlations of erythribyssin G (**7**) (H → C)

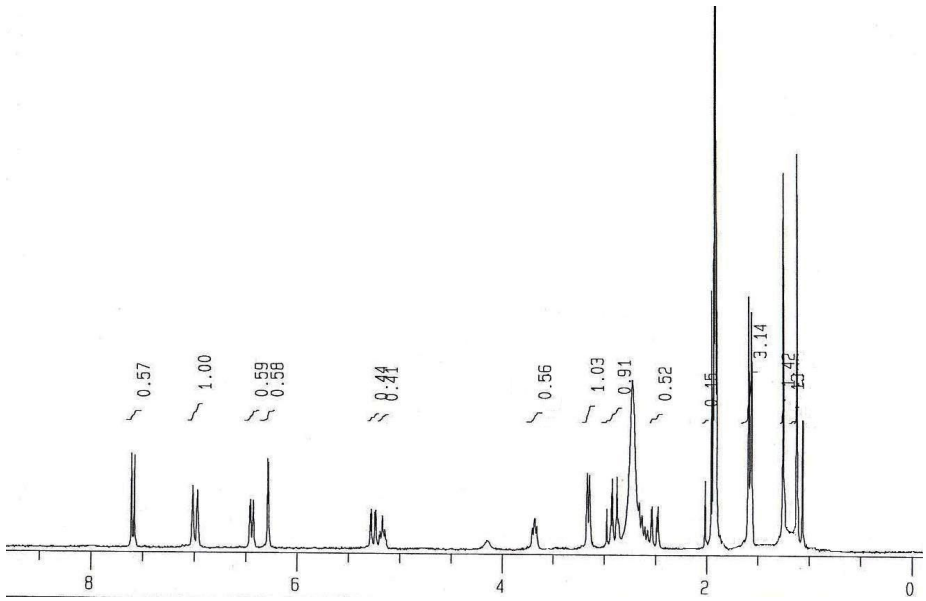

Fig. 21 ^{1}H-NMR spectrum of compound **7** (500 MHz, acetone-d_6)

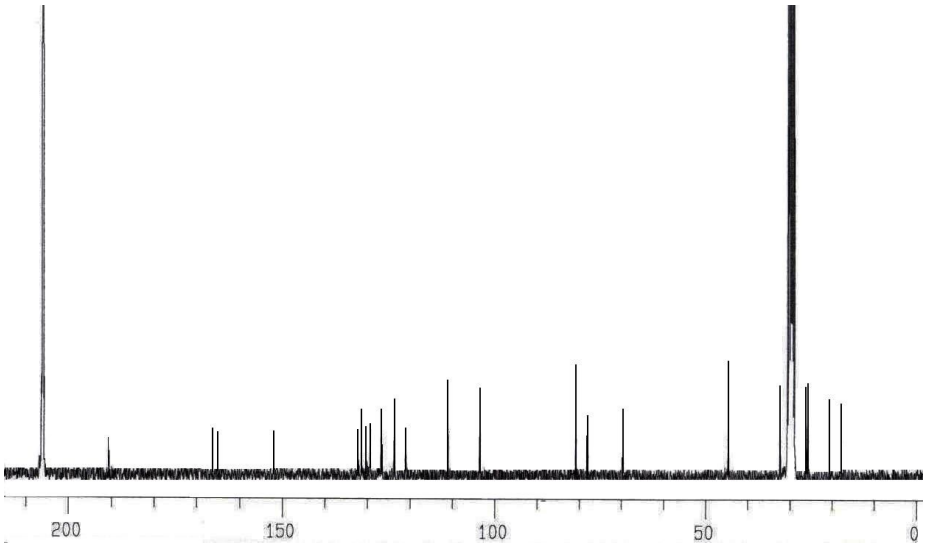

Fig. 22. ^{13}C-NMR spectrum of compound **7** (125 MHz, acetone-d_6)

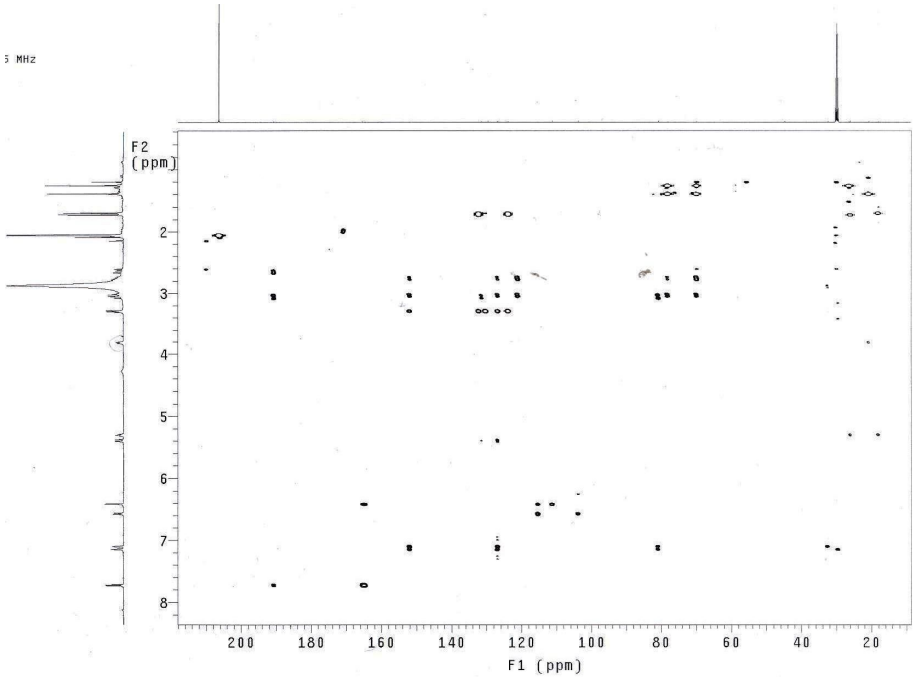

Fig. 23. HMBC spectrum of compound **7** (500 MHz, acetone-d_6)

Table 9. ^{1}H and ^{13}C NMR spectral data of compound **7** (300 MHz, acetone-d_6)

position	δ_H mult. (J in Hz)	δ_C	HMBC (H → C)
1			
2	5.25 (dd, J = 3.0, 13.2)	80.8	C-4, C-2', C-6'
3	2.93-ax (dd, J = 13.2, 16.8) 2.51-eq (dd, J = 3.0, 16.8)	44.6	C-1', C-10
4		190.5	
5	7.60 (d, J = 8.7)	129.4	C-4, C-7, C-9
6	6.44 (dd, J = 2.1, 8.7)	111.1	C-8, C-10
7		165.1	
8	6.28 (d, J = 2.1)	103.6	C-6, C-9, C-10
9		164.5	
10		115.5	
1'		132.0	
2'	6.97 (s)	126.6	C-2, C-4', C-6'
3'		121.0	
4'		152.0	
5'		120.2	
6'	7.01 (s)	126.7	C-2, C-2', C-4', C-5', C-1'''
1''	2.91-ax (dd, J = 13.2, 16.8) 2.62-eq (dd, J = 8.1, 16.8)	32.3	C-2', C-4', C-2'', C-3''
2''	3.68 (dd, J = 13.2, 7.8)	69.7	C-3'
3''		78.0	
4''	1.12 (s)	20.7	C-2'', C-3'', C-5''
5''	1.38 (s)	26.2	C-2'', C-3'', C-4''
1'''	3.28 (d, J = 6.9)	29.5	C-4', C-5', C-6', C-2''',
2'''	5.17 (m)	123.7	
3'''		133.0	
4'''	1.69 (s)	25.8	C-2''', C-3''', C-5'''
5'''	1.71 (s)	17.9	C-2''', C-3''', C-4'''

HMBC spectrum was measured in acetone-d_6, at 500 MHz

1.8 Structure determination of compound 8

Compound **8** was purified as a yellowish amorphous powder with absorption bands at 3419 cm^{-1} (OH), $[\alpha]_D^{25}$: –0.7° (c = 0.01, MeOH). The molecular formula of **7** was determined as $C_{16}H_{16}O_5$ from a molecular ion peak at *m/z* 288.0998 $[M]^+$ (calcd for 288.0952) in the HR-EI-MS. Its UV spectrum showed absorption bands at λ_{max} 206, 232, 288 and 316 nm. The ^{1}H NMR displayed an AMX-type spin system at δ_H 4.21 (1H, dd, *J* = 4.0, 6.0 Hz, H-3), 4.80 (1H, dd, *J* = 6.0, 10.0 Hz, H-2_{ax}), and 4.82 (1H, dd, *J* = 4.0, 10.0 Hz, H-2_{eq}), these observation seem to be the characteristic of a isoflavanone skeleton. The ^{13}C NMR, however, did not show the signal assignable to the carbonyl carbon at C-4 for the flavanone skeleton,[56] but to the O-atom carrying a CH_2 group at C-2 (δ_C 79.9), and the methine carbon at C-3 (δ_C 41.5). The ^{1}H and ^{13}C NMR also showed an ABX-type aromatic spin system at δ_H 6.87 (1H, d, *J* = 8.0 Hz, H-4), 6.36 (1H, dd, *J* = 2.5, 8.0 Hz, H-5), and 6.31 (1H, d, *J* = 2.0 Hz, H-7), as well as two singlet H-atoms δ_H 6.58 (1H, s) and 6.57 (1H, s), and two MeO groups δ_H 3.64 (3H, s, 3′-OMe), 3.78 (3H, s, 6′-OMe) on a 4-hydroxy-3,6-dimethoxyphenyl substituent (B ring). The attachments of the two methoxyl group to C-3′ and C-6′ on B ring and of the B ring to the benzofuran ring at C-3 were established by the HMBC experiment (Table 10), revealing correlations between δ_H 3.64 (3′-OMe)/C-3′, 3.78 (6′-OMe)/C-6′ and δ_H 6.58 (H-2′)/C-3, δ_H 4.21 (H-3)/C-1′ and C-2′, and H-2/C-1′. Thus, compound **8** was characterized as 2,3-dihydro-3-(4-hydroxy-2,5-dimethoxyphenyl)benzofuran-6-ol, a new natural 2,3-dihydrobenzofuran derivative named erythribyssin H.

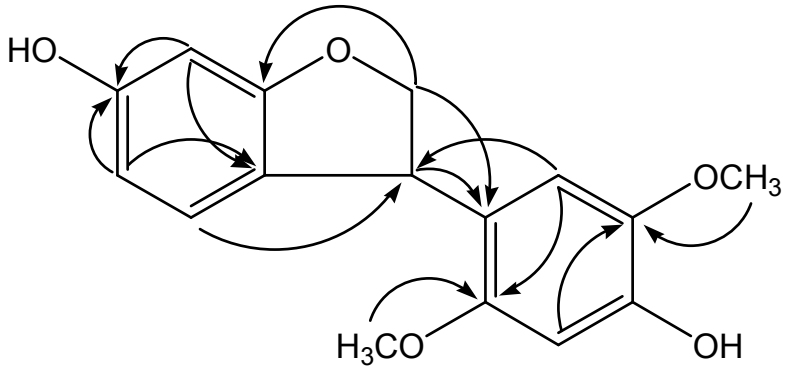

Key HMBC correlations of erythribyssin H (**8**) (H → C)

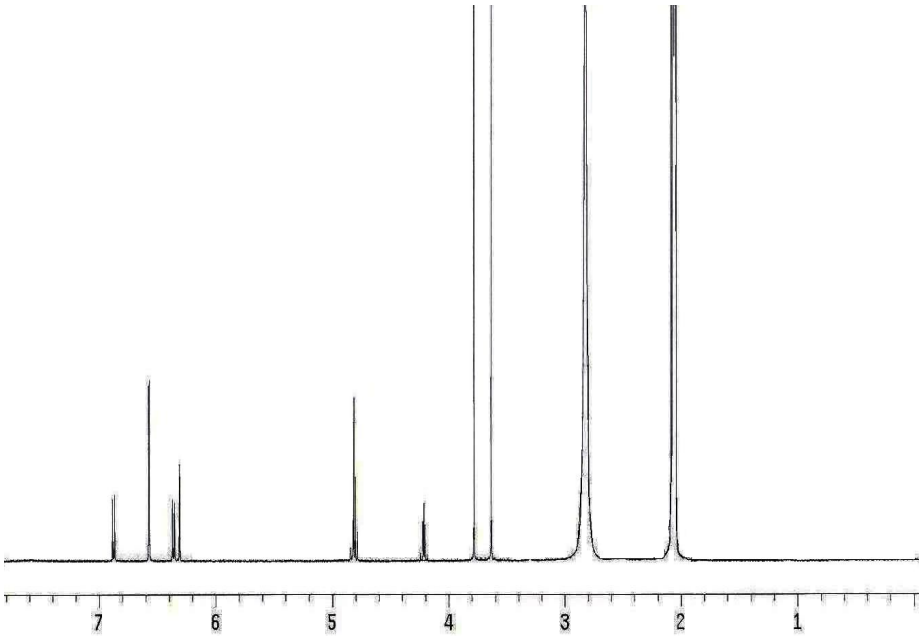

Fig. 24. ^{1}H-NMR spectrum of compound **8** (500 MHz, acetone-d_6)

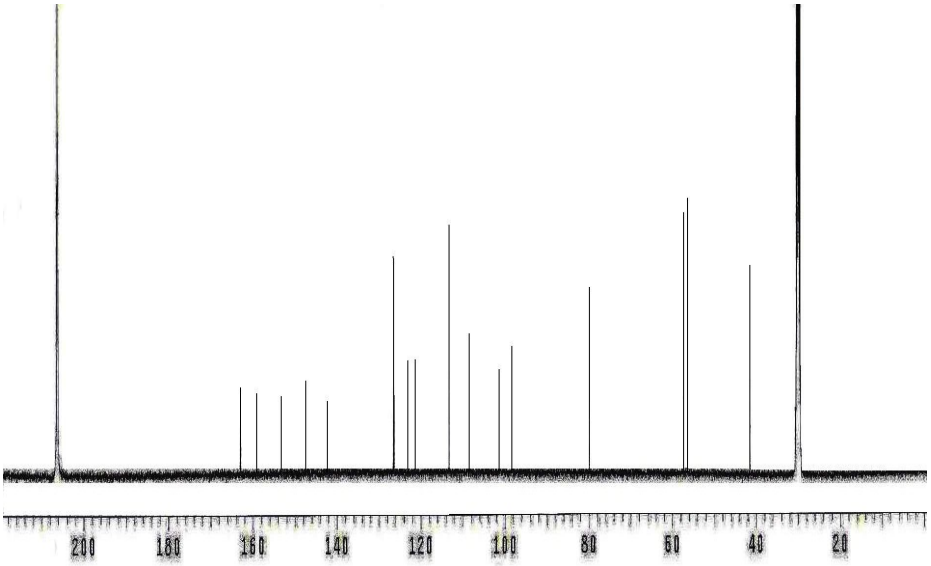

Fig. 25. ^{13}C-NMR spectrum of compound **8** (125 MHz, acetone-d_6)

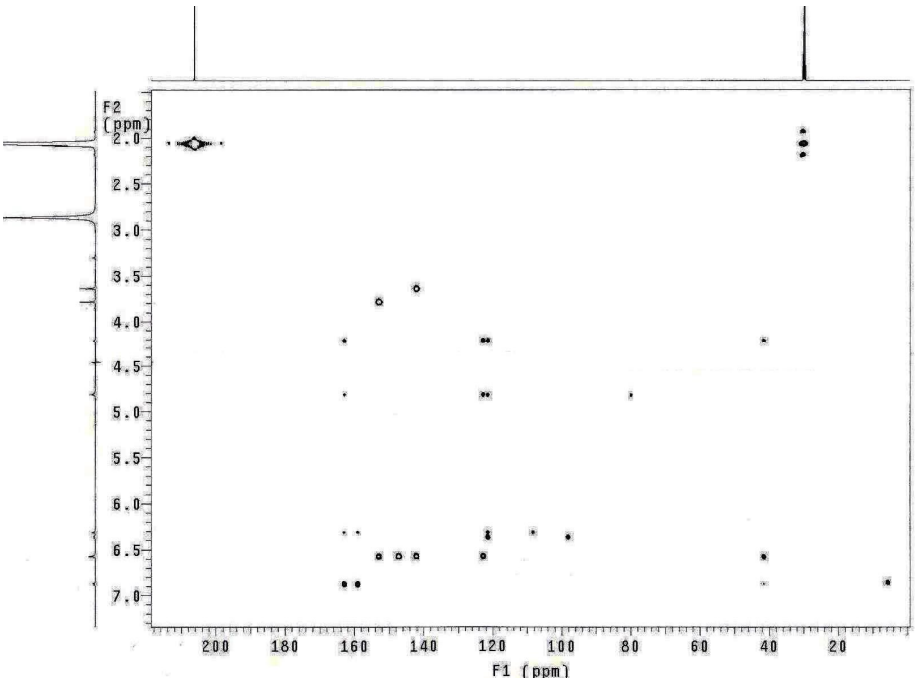

Fig. 26. HMBC spectrum of compound **8** (500 MHz, acetone-d_6)

Table 10. ^{1}H and ^{13}C NMR spectral data of compound **8** (500 MHz, acetone-d_6)

position	δ_H mult. (J in Hz)	δ_C	HMBC (H → C)
1			
2	4.82-eq (dd, J = 4.0, 10.0) 4.80-ax (dd, J = 6.0, 10.0)	79.9	C-8, C-9, C-1'
3	4.21 (dd, J = 4.0, 6.0)	41.5	C-8, C-9, C-1'
4	6.87 (d, J = 8.0)	126.4	C-3, C-6, C-8
5	6.36 (dd, J = 2.5, 8.0)	108.3	C-6, C-7, C-9
6		159.0	
7	6.31 (d, J = 2.5)	98.2	C-5, C-6, C-8, C-9
8		162.9	
9		121.5	
1'		122.8	
2'	6.58 (s)	113.3	C-3, C-1', C-3', C-4', C-6'
3'		142.1	
4'		147.3	
5'	6.56 (s)	101.0	C-1', C-3', C-4', C-6'
6'		152.9	C-2, C-2', C-4', C-1"
3'-OCH_3	3.64 (s)	57.3	C-3'
6'-OCH_3	3.78 (s)	56.5	C-6'

1.9 Structure determination of compound 9

Compound **9** was obtained as a brown-yellow amorphous powder. $[\alpha]_D^{25}$: –10.8° (c = 0.02, MeOH). The molecular formula of **9** was determined as $C_{20}H_{20}O_5$ from a molecular ion peak at *m/z* 340.1311 $[M]^+$ (calcd for 340.1331) in the HR-EI-MS. Its UV spectrum showed absorption bands at λ_{max} 206-216, 234, 276, and 310 nm. The ^{1}H NMR displayed an AMX-type spin system at δ_H 5.42 (1H, dd, *J* = 3.0, 13.0 Hz, H-2), 3.05 (1H, dd, *J* = 13.0, 17.0 Hz, H-3_{ax}), and 2.65 (1H, dd, *J* = 3.0, 17.0 Hz, H-3_{eq}) and one ABX-type aromatic spin system at δ_H 7.72 (1H, d, *J* = 8.5 Hz, H-5), 6.57 (1H, dd, *J* = 2.0, 8.5 Hz, H-6), and 6.42 (1H, d, *J* = 2.0 Hz, H-8), and one another ABX aromatic spin system at δ_H 6.77 (1H, d, *J* = 8.0 Hz, H-5′), 7.26 (1H, dd, *J* = 1.5, 8.0 Hz, H-6′), and 7.25 (1H, d, *J* = 1.5 Hz, H-2′), but showed no proton resonance for a hydroxyl group at C-5, indicating that this position was not substituted.[56] The ^{13}C NMR showed an oxygenated carbon resonance at δ_C 80.7 (C-2), a methylene resonance at δ_C 44.7 (C-3), and a carbonyl resonance at δ_C 190.6 (C-4). All of these observations were indicative of a flavanone skeleton for **9**. In addition, the ^{1}H and ^{13}C NMR patterns of **9** exhibited the presence of a 3-hydroxy-2,2-dimethyldihydropyran moiety at δ 3.81 (1H, dd, *J* = 5.0, 8.0 Hz), 3.02 (1H, dd, *J* = 5.0, 17.0 Hz), 2.76 (1H, dd, *J* = 8.0, 17.0 Hz), 1.35 (3H, s), and 1.25 (3H, s). The dihydropyran ring fused to the C-3′ and C-4′ position was assigned from the HMBC spectrum, which showed correlations from the aliphatic protons at C-1′ (δ_H 2.91 and 2.46) to the carbons at C-3′ (δ_C 121.0) and C-4′ (δ_C 152.0), and from the oxygenated aliphatic proton (δ_H 3.68) to the carbon at C-3′ (δ_C 121.0). All of the spectroscopic (UV, CD, ^{1}H and ^{13}C NMR) patterns for compound 9 were similar to those of compound **7**. However, there was no NMR resonance for the prenyl group (Table 9 and 11), whereas NMR resonance for an additional aromatic proton was observed. The ring arrangements were assigned by the HMBC experiment and the

configuration at C-2 was inferred to be 2*S*, as indicated by CD spectrum, which showed two maxima of positive and negative Cotton effects at 328 and 290 nm, respectively. Hence, compound **9** was identified as a new compound, 2(*S*)-7-hydroxy-[2″-hydroxy-3″,3″-dimethylpyrano)]flavanone, named erythibyssin I.

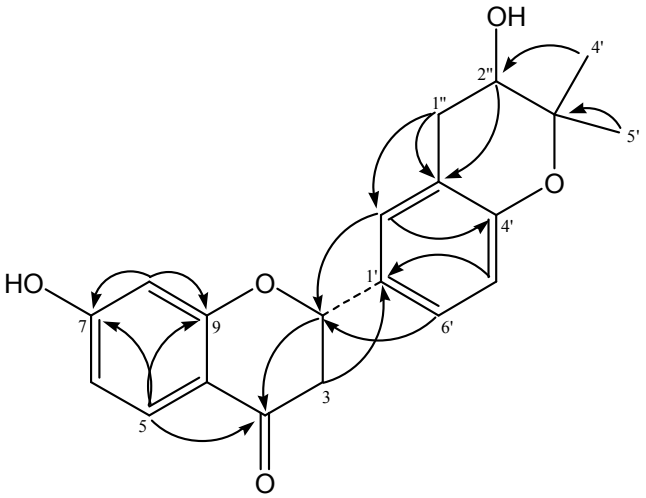

Key HMBC correlations of erythribyssin I (**9**) (H → C)

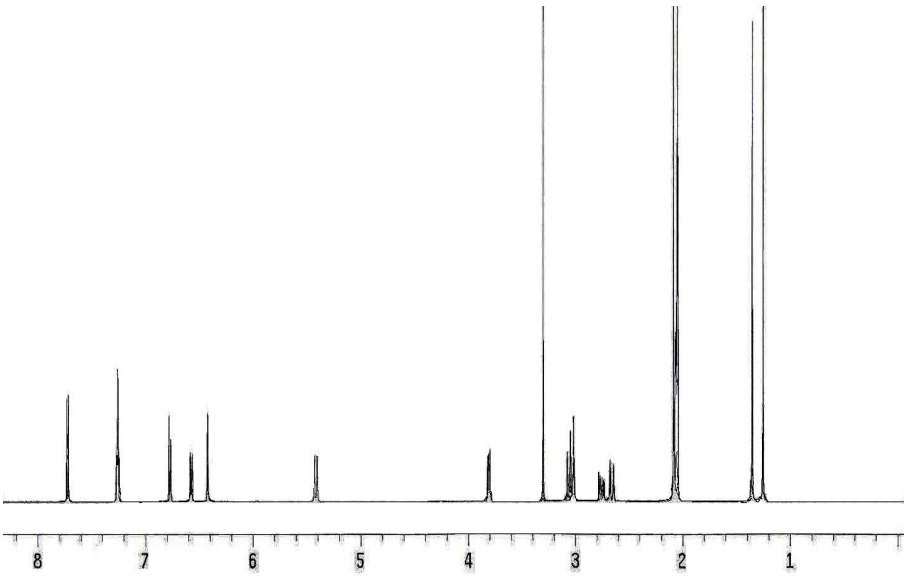

Fig. 27. ^{1}H-NMR spectrum of compound **9** (500 MHz, acetone-d_6)

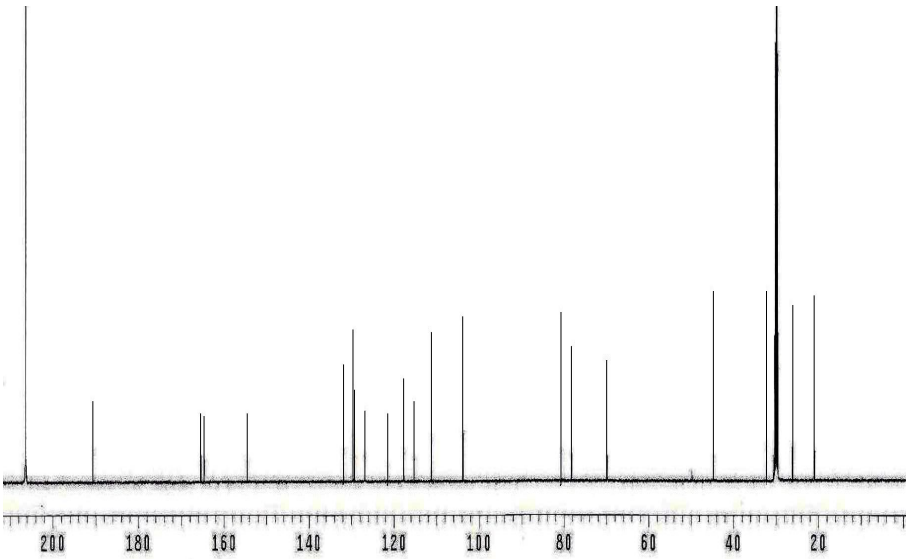

Fig. 28. ^{13}C-NMR spectrum of compound **9** (125 MHz, acetone-d_6)

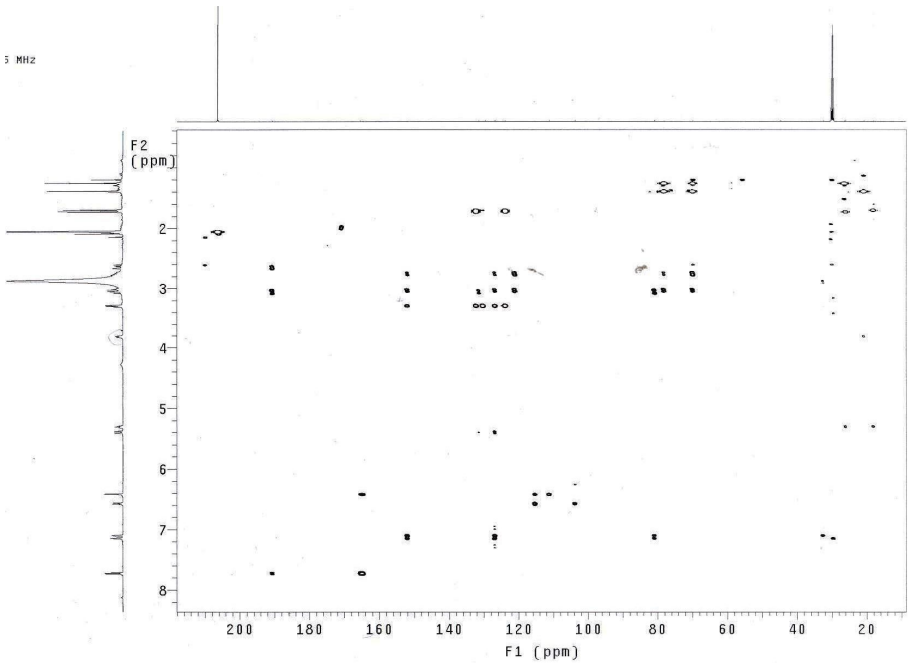

Fig. 29. HMBC spectrum of compound **9** (500 MHz, acetone-d_6)

Table 11. ^{1}H and ^{13}C NMR spectral data of compound **9** (500 MHz, acetone-d_6)

position	δ_H mult. (J in Hz)	δ_C	HMBC (H → C)
1			
2	5.42 (dd, J = 3.0, 13.0)	80.7	C-4, C-2', C-6'
3	3.05-ax (dd, J = 13.0, 17.0) 2.65-eq (dd, J = 3.0, 17.0)	44.7	C-2, C-4, C-1', C-10
4		190.5	
5	7.68 (d, J = 9.0)	129.6	C-4, C-7, C-9
6	6.57 (dd, J = 2.0, 8.5)	111.3	C-7, C-8, C-10
7		165.3	
8	6.42 (d, J = 2.0)	103.7	C-6, C-7, C-9, C-10
9		164.6	
10		115.2	
1'		131.8	
2'	7.26 (br, d, J = 8.0)	126.8	C-2, C-4', C-6'
3'	6.77 (d, J = 8.5)	117.6	C-1', C-4', C-5'
4'		154.5	
5'		121.4	
6'	7.25 (br, s)	129.3	C-2, C-2', C-4', C-1'''
1''	3.02-ax (dd, J = 5.0, 17.0) 2.76-eq (dd, J = 8.0, 17.0)	32.2	C-4', C-5', C-6', C-2'', C-3''
2''	3.81 (dd, J = 5.0, 8.0)	69.7	C-5', C-4'', C-5''
3''		78.2	
4''	1.21 (s)	26.1	C-2'', C-3'', C-5''
5''	1.31 (s)	20.7	C-2'', C-3'', C-4''

1.10 Structure determination of compound 10

Compound **10** was obtained as yellow powder with the molecular formula $C_{20}H_{20}O_5$, as determined by the HR-EI mass spectrum ($[M]^+$, *m/z* 340.1311). The IR spectrum of compound **10** suggested the presence of OH functional groups at 3331 cm^{-1}, 2916 (C–C), 1670 and 1593, and C–O stretching vibrations at 1061–1033 cm^{-1}. The ^1H NMR spectra of compound **10** showed signals assignable to the AB system at C-2 position [δ_H 4.85 (1H, d, J = 11.5 Hz) and 4.32 (1H, d, J = 11.5 Hz)], indicating that position 3 was substituted.[57] This was further evidenced by ^{13}C NMR spectrum [δ_C 74.6 (C-2) and 75.1 (C-3)] and confirmed by the HSQC, and HMBC experiment (See also Table 12). All of these evidences support for the presence of a hydroxyl group at C-3.[57] Comparison of the spectroscopic (IR, UV, CD, ^1H and ^{13}C NMR) spectra of **10** with those of (3*S*)-3,7,2′3′-tetrahydroxy-4′-methoxy-5′-prenylisoflavanone[57] indicated that compound **10** is similar with authentic compound excepts only for an additional aromatic proton at δ_H 6.41 (1H, s, H-3′) in the ^1H NMR spectrum. Comparison of the HR-EI mass spectrum between **10** ($C_{21}H_{22}O_6$ *m/z* 370) and (3*S*)-3,7,2′3′-tetrahydroxy-4′-methoxy-5′-prenylisoflavanone ($C_{21}H_{22}O_7$ *m/z* 386)[57] suggested that **10** was lost an oxygen atom in the molecular. This indicated that the 3′-OH group in the authentic compound was replaced by an H-atom in **10**. Indeed, the correlations between H-3′ (δ_H 6.41) to the C-4′ (δ_C 159.3) and the 4′-OMe (δ_H 3.75) to the C-4′ and C-3′ (δ_C 100.6) in the HMBC spectrum were further evidenced for this observation. The attachment of the prenyl group to the C-5′ (δ_C 121.0), and the arrangement of the rings for this compound were assigned by HMBC experiment (See Table 12). A negative Cotton Effects at 331 nm in its CD spectrum indicates the absolute configuration at C-3 to be *S*. Thus, compound **10** was elucidated as (3*S*)-3,7,2′-trihydroxy-4′-methoxy-5′-prenyl-isoflavanone, a new natural product and called erythribyssin J.

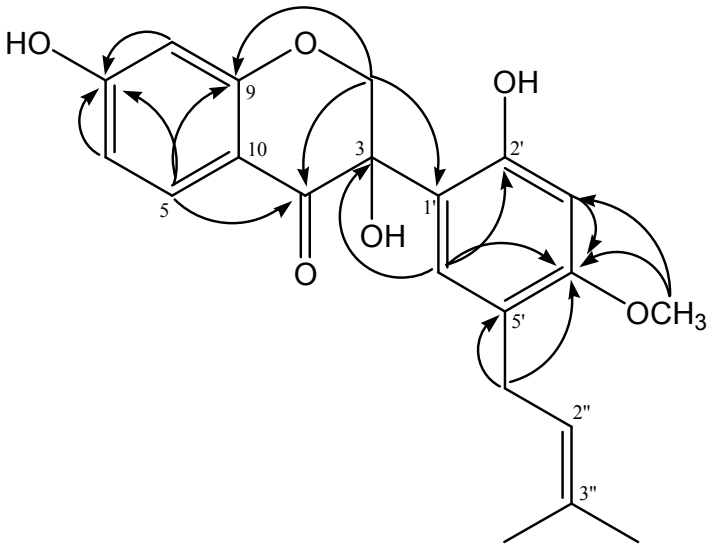

Key HMBC correlations of erythribyssin J (**10**) (H → C)

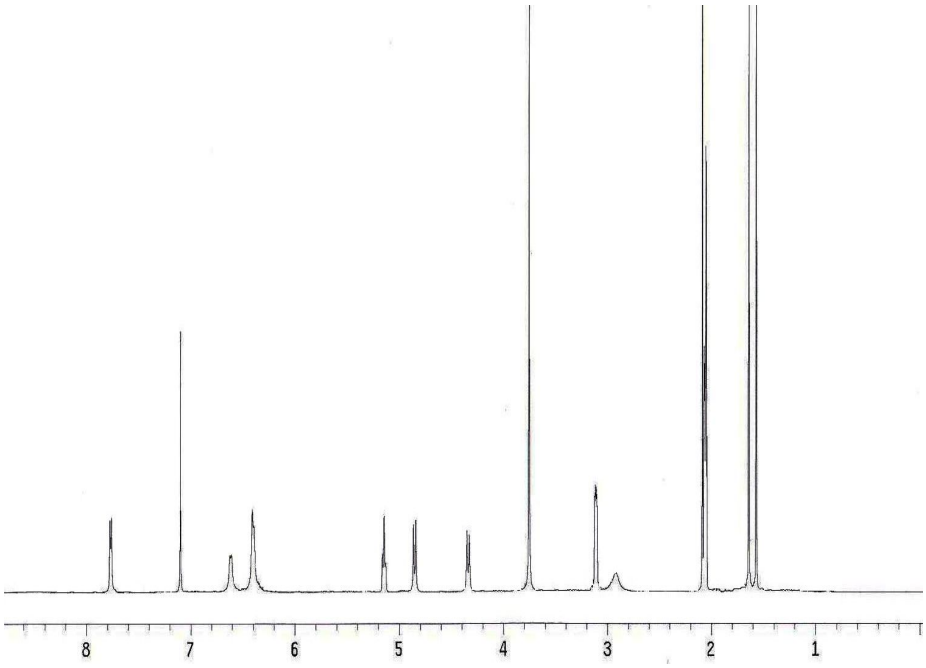

Fig. 30. ^{1}H-NMR spectrum of compound **10** (500 MHz, acetone-d_6)

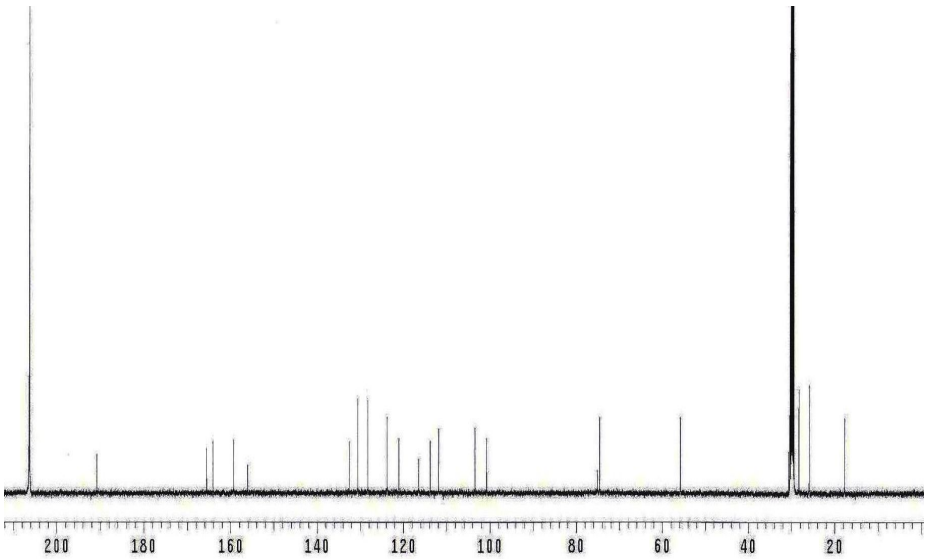

Fig. 31. ^{13}C-NMR spectrum of compound **10** (125 MHz, acetone-d_6)

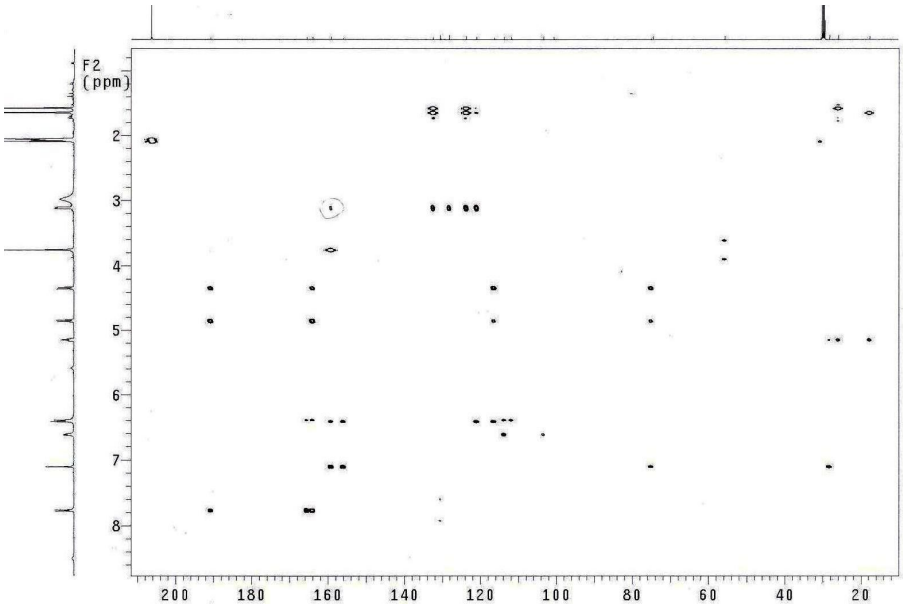

Fig. 32. HMBC spectrum of compound **10** (500 MHz, acetone-d_6)

Table 12. ^{1}H and ^{13}C NMR spectral data of compound **10** (500 MHz, acetone-d_6)

position	δ_H mult. (J in Hz)	δ_C	HMBC (H → C)
1			
2	4.85 (d, J = 11.5) 4.34 (d, J = 11.5)	74.6	C-3, C-4, C-9, C-1'
3		75.1	
4		190.8	
5	6.76 (d, J = 7.5)	130.6	C-4, C-7, C-9
6	6.61 (br, d, J = 7.5)	111.9	C-8, C-10
7		165.6	
8	6.40 (br, s)	103.3	C-6, C-9, C-10
9		164.1	
10		113.8	
1'		116.5	
2'		159.3	
3'	6.41 (s)	100.6	C-1', C-4', C-5'
4'		156.1	
5'		121.0	
6'	7.10 (s)	128.2	C-3, C-2', C-4', C-1'''
1''	3.11 (d, J = 7.5)	28.3	C-4', C-5', C-6', C-2'', C-3''
2''	5.15 (t-like, J = 7.5)	123.8	C-4'', C-5''
3''		132.5	
4''	1.57 (s)	17.7	C-2'', C-3'', C-5''
5''	1.64 (s)	25.9	C-2'', C-3'', C-4''

1.11 Structure determination of compound 11

Compound **11** was obtained as yellowish amorphous powder with the molecular formula $C_{16}H_{12}O_5$, as determined by the HR-EI mass spectrum ($[M]^+$, *m/z* 284.0685). $[\alpha]_D^{25}$: –11.0° (c = 0.44, MeOH). The IR spectrum of compound **11** suggested the presence of OH functional group at 3038, 1825, 1618 (C=O), 1497, 609 cm^{-1}.Its UV spectrum showed absorption maxima at 208, 214, 231, 276, 309 nm. The ^{1}H-NMR spectrum of compound **11** showed an AMX-type spin system at δ_H 5.60 (1H, dd, *J* = 2.5, 13.0 Hz, H-2), 3.09 (1H, dd, *J* = 13.0, 17.0 Hz, H-3_{ax}), and 2.77 (1H, dd, *J* = 3.0, 17.0 Hz, H-3_{eq}), and two ABX-type aromatic spin systems. The first one belong to the ring A with δ_H 7.75 (1H, d, *J* = 8.5 Hz, H-5), 6.60 (1H, dd, *J* = 2.0, 8.5 Hz, H-6), and 6.46 (1H, d, *J* = 2.0 Hz, H-8), the second one belong to ring B with δ_H 8.00 (1H, d, *J* = 1.5 Hz, H-6′), 7.83 (1H, dd, *J* = 1.5, 8.5 Hz, H-2′) and 7.07 (1H, d, *J* = 8.5 Hz, H-3′), but showed no proton resonance for a hydroxyl group at C-5, this evidenced for non-substitution at C-5. The ^{1}H and ^{13}C NMR displayed an aldehyde group at δ_C 190.1, δ_H 10.10 (1H, s). All of these observations were indicative of a flavanone skeleton for **11**. The proton at δ_H 7.07 was upfield than two remained protons in the second ABX system of the ring B, this observation suggested that this proton was neighbored by an oxygen atom. Analysis of an HMBC experiment showed the correlations from the formyl proton δ_H 10.10 to the carbon at C-5′ (δ_C 121.8) and C-4′ (δ_C 164.3), and from the upfield proton δ_H 7.07 to a carbon at C-4′ (δ_C 164.3). The configuration at C-2 was inferred to be 2*S*, as indicated by CD data. Hence, compound **11** was identified as 7,4′-dihydroxy-5′-formyl-flavanone, and named erythibyssin G, a new flavanone bearing an fomyl functional group.

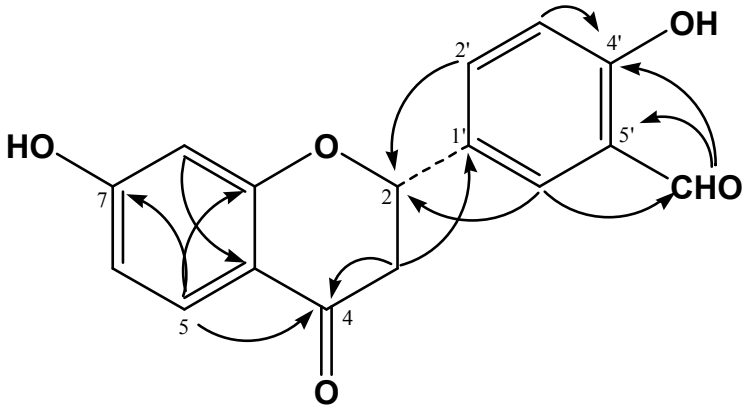

Key HMBC correlations of erythribyssin K (**11**) (H → C)

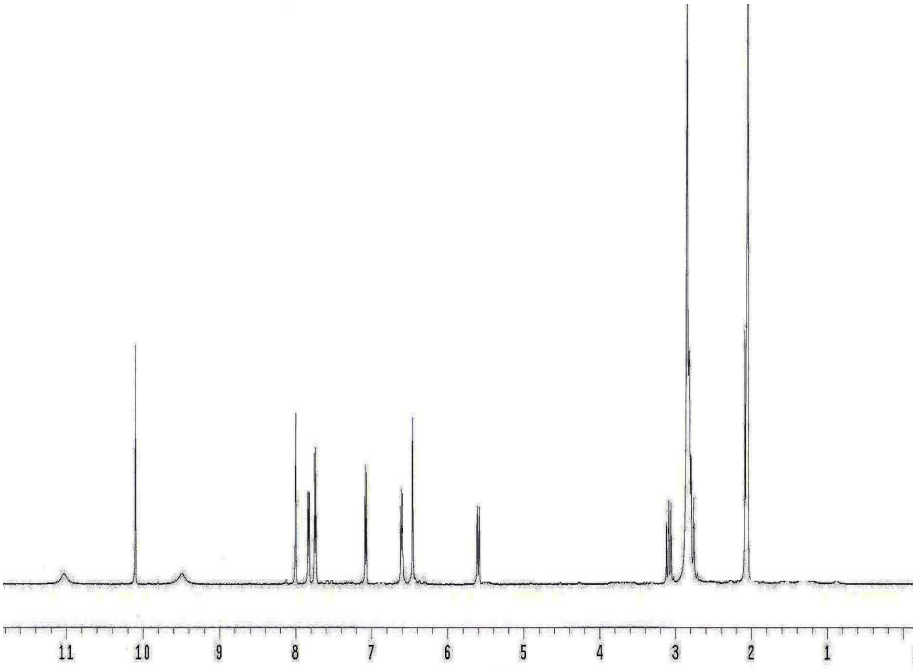

Fig. 33. ^{1}H-NMR spectrum of compound **11** (500 MHz, acetone-d_6)

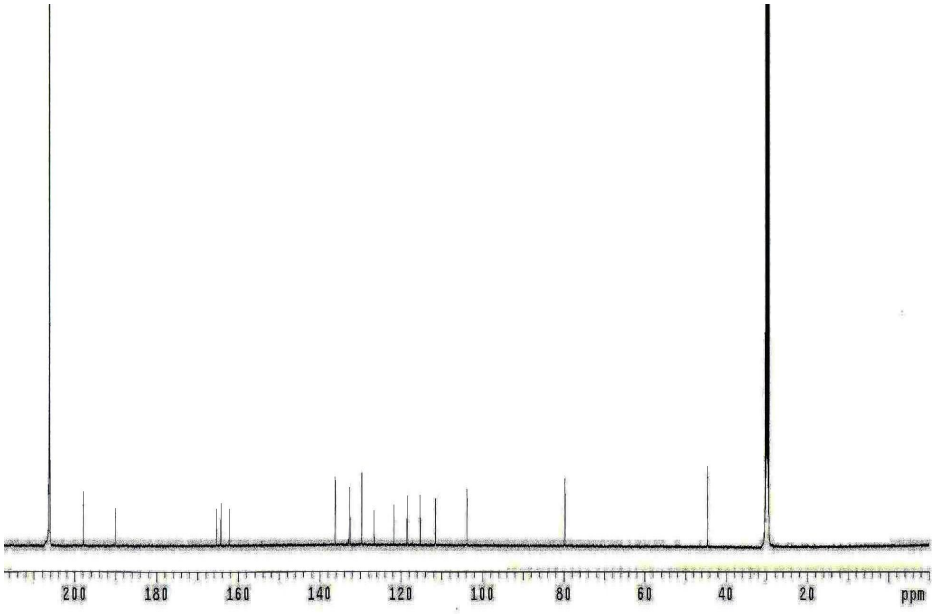

Fig. 34. ^{13}C-NMR spectrum of compound **11** (125 MHz, acetone-d_6)

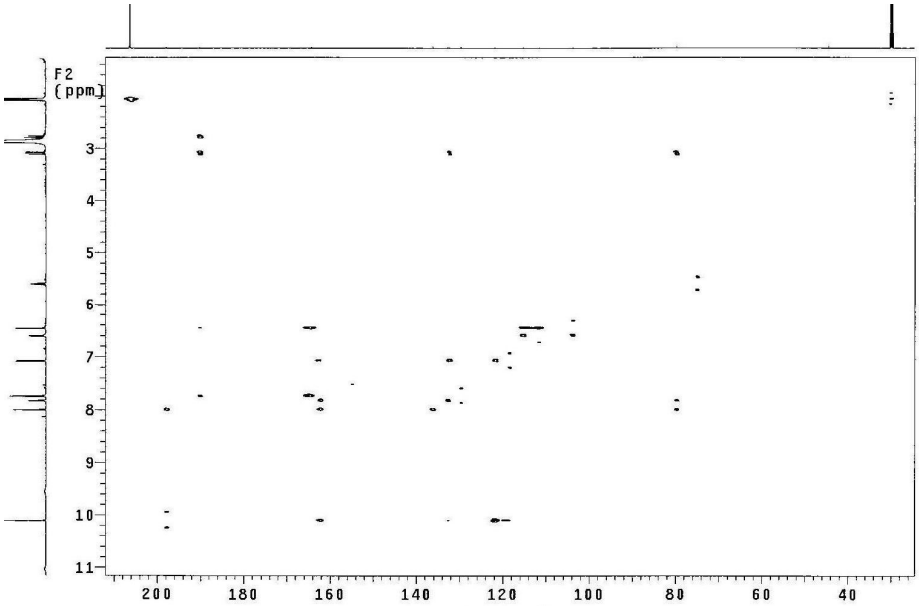

Fig. 35. HMBC spectrum of compound **11** (500 MHz, acetone-d_6)

Table 13. ^{1}H and ^{13}C NMR spectral data of compound **11** (600 MHz, acetone-d_6)

position	δ_H mult. (J in Hz)	δ_C	HMBC (H → C)
1			
2	5.60 (dd, J = 2.5, 13.0)	79.8	C-2′, C-6′,
3	3.09 (dd, J = 13.0, 17.0) 2.77 (dd, J = 3.0, 17.0)	44.5	C-4, C-1′
4		190.1	
5	7.75 (d, J = 8.5)	132.8	C-4, C-7, C-9
6	6.60 (*dd,* J = 2.0, 8.5)	111.5	C-7, C-8, C-10
7		165.4	
8	6.46 (d, J = 2.0)	103.8	C-7, C-9, C-10
9		164.3	
10		115.3	
1'		132.4	
2'	7.83 (dd, J = 2.0, 8.5)	136.2	C-4′, C-6′
3'	7.07 (d, J = 8.5)	118.4	C-1′, C-4′, C-5′
4'		162.1	
5'		121.8	
6'	8.00 (d, J = 1.5)	129.7	C-2, C-2′, C-4′, C-5′
5'-CHO	10.10 (s)	197.9	C-4′, C-5′

1.12 Structure determination of compound 12

Compound **12** was obtained as white amorphous powder with the molecular formula $C_{25}H_{28}O_5$, as determined by the HR-EI mass spectrum ($[M]^+$, *m/z* 408.1937). The IR spectrum of compound **12** suggested the presence of OH functional groups at 3425, 2973, 2926 (C–C), 1599, 1450 (aromatic ring) cm^{-1}. Its UV spectrum showed absorption maxima at 210, 214, 232, 286, 320, 370 nm. The ^{1}H-NMR spectrum of compound **13** showed four signals at δ_H 4.20 (1H, dd), 3.57 (1H, dd), and 3.54 (1H, m), and 5.45 (1H, d), which were reminiscent of a pterocarpan skeleton.[50, 52] In addition, the ^{1}H and ^{13}C NMR spectra of compound **12** also revealed the presence of a 2,2-(3-hydroxy)-dimethylpyrano ring and a prenyl group. The configuration at C-6a and C-11a was inferred to be *R,R* by a negative optical rotation value -54.97. All of these results suggested a structure similar to erysubin D for compound **12**.[58] The HMBC correlation from proton H-1′ (δ_H 3.00) to C-3 (δ_C 156.0), and H-1″ (δ_H 3.26) to C-9 (δ_C 159.8) and C-10 (δ_C 112.0) indicated that the prenyl group was attached to C-10, the 2,2-(3-hydroxy)-dimethylpyrano ring fused to C-2 and C-3. Therefore, compound **12** was determined to be a derivative of erysubin D, 9-hydroxy-10-prenyl-[2′,2′-(3′-hydroxy)-dimethylpyrano]-(6a*R*,11a*R*)pterocapan.

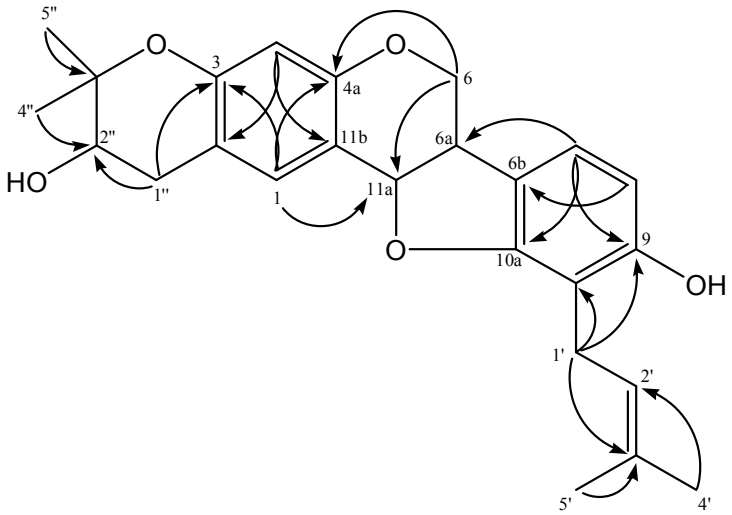

Key HMBC correlations of erythribyssin L (**12**) (H → C)

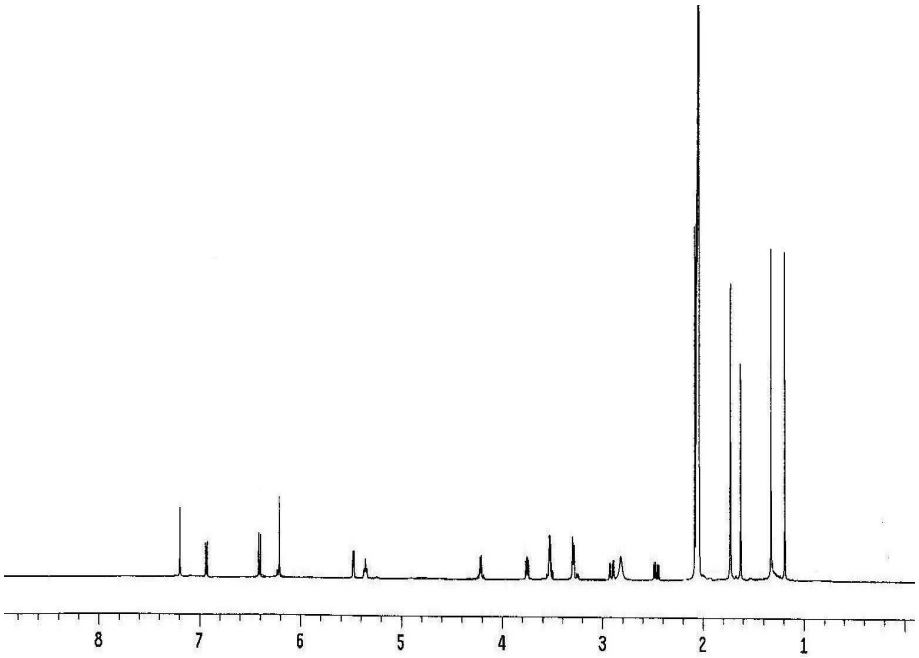

Fig. 36. ^{1}H-NMR spectrum of compound **12** (500 MHz, acetone-d_6)

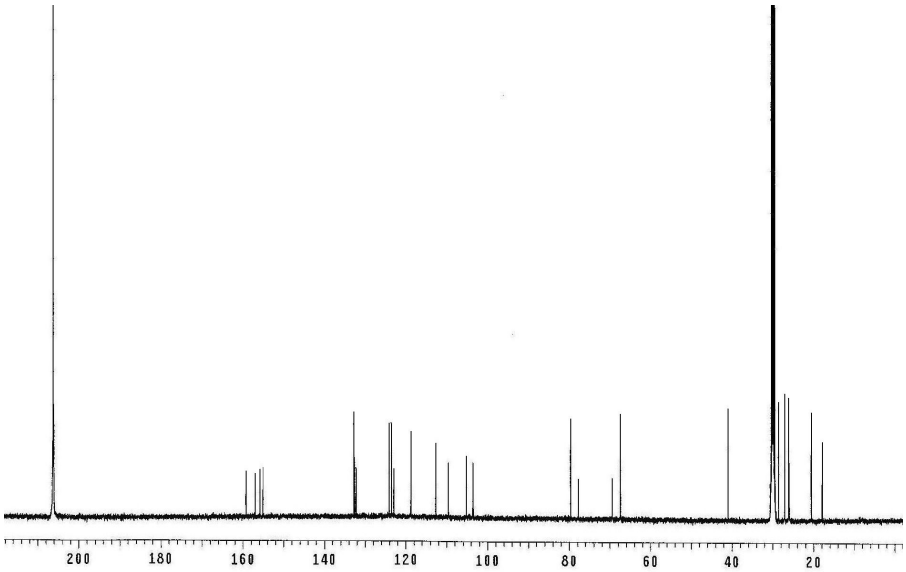

Fig. 37. ^{13}C-NMR spectrum of compound **12** (125 MHz, acetone-d_6)

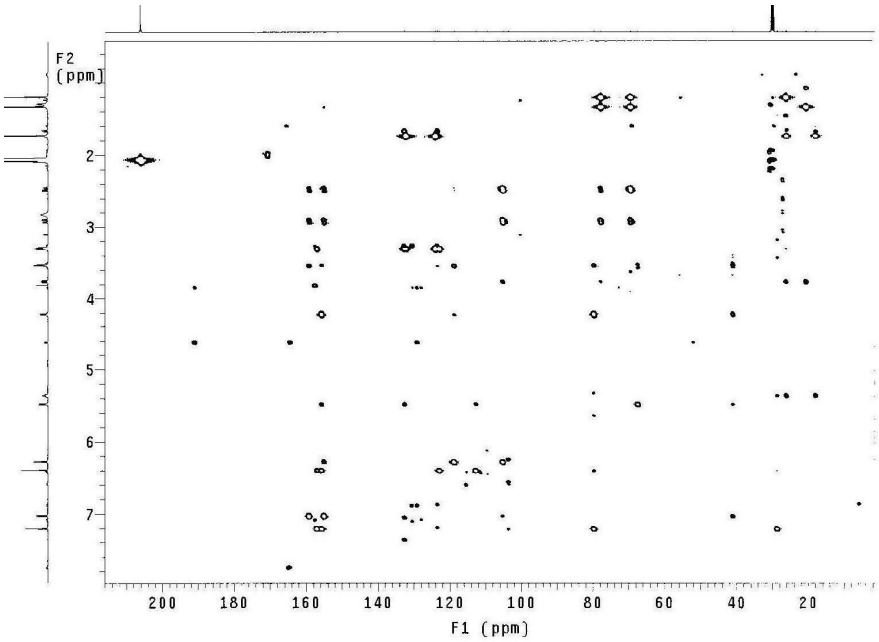

Fig. 38 HMBC spectrum of compound **12** (500 MHz, acetone-d_6)

Table 14. ^{1}H and ^{13}C NMR spectral data of compound **12** (600 MHz, acetone-d_6)

position	δ_H mult. (J in Hz)	δ_C	HMBC (H → C)
1	7.20 (s)	133.1	C-3, C-4a, C-11a
2		114.2	
3		156.0	
4	6.22 (s)	104.8	C-2, C-3, C-4a, C-11b
4a		155.3	
6	4.22 (dd, J = 4.2, 10.2) 3.57 (t, J = 10.2)	67.2	C-4a, C-11a, C-6b
6a	3.54 (m)	41.0	C-11b
6b		119.0	
7	6.95 (d, J = 7.8)	122.8	C-9, C-10a, C-6a
8	6.39 (d, J = 7.8)	108.1	C-6b, C-10
9		159.8	
10		112.0	
10a		156.8	
11a	5.45 (d, J = 7.2)	79.0	C-4a, C-10a
11b		115.3	
1'	3.00 (dd, J = 5.4, 15.6) 2.70 (dd, J = 8.4, 15.6)	31.6	C-2', C-3', C-3
2'	3.77 (dd, J = 4.8, 7.8)	70.0	C-2,
3'		78.2	
4'	1.23 (s)	20.7	C-2', C-3', C-5'
5'	1.34 (s)	26.3	C-2', C-3', C-4'
1'	3.26 (d, J = 6.6)	23.5	C-2", C-3", C-8, C-9, C-10
2'	5.25 (m)	123.7	
3'		131.3	
4'	1.61 (s)	25.9	C-2", C-3", C-5"
5'	1.73 (s)	18.0	C-2", C-3", C-4"

1.13 Structure determination of compound 13

Compound **13** was obtained as brown powder with the molecular formula $C_{22}H_{24}O_5$, as determined by the HR-EI mass spectrum ($[M]^+$, *m/z* 368.1624). The IR spectrum of compound **13** suggested the presence of OH functional groups at 3408 cm^{-1}, 2928 (C–C), 1657 and 1625, 1161–1033 cm^{-1}.Its UV spectrum showed absorption maxima at 208 nm (log ε = 4.80), 228 nm (log ε = 4.46), 277 nm (log ε = 4.32) and 363 nm (log ε = 3.71). The ^{1}H-NMR spectrum of compound **13** showed four signals at δ_H 4.27 (1H, dd), 3.57 (1H, t), and 3.51 (1H, m), and 5.41 (1H, d), which were reminiscent of a pterocarpan skeleton.[50, 52] A methoxyl group [δ_H 3.79 (3H, s), δ_C 57.5], one prenyl group [δ_H 5.29 (1H, m), 3.25 (1H, d, J = 7.2 Hz), 1.72 (6H, s), δ_C 132.3, 123.8, 28.5, 26.0 and 17.9], and four aromatic protons at δ_H 7.16, 7.01, 6.43, 6.34 (each 1H, s) were observed in the ^{1}H and ^{13}C NMR spectra of **13**. All of these data were resembled with those of eryvarin K, a pterocarpan isolated previously from the same source.[59] The major difference was that an additional methoxyl group [δ_H 3.81 (3H, s), δ_C 55.9] was found in **13**. HMBC correlations were observed between the first methoxyl protons (δ_H 3.79) to C-8 (δ_C 142.9), the second methoxyl protons (δ_H 3.81) to C-3 (δ_C 159.4) confirmed the arrangement of these two methoxyl groups. A negative optical rotation value was evidenced for the absolute stereochemistry of **13** to be (6a*R*:11a*R*).[52] Thus, compound **13** was established as 3,9-dimethoxy-2-prenyl-(6a*R*:11a*R*)pterocarpan, a new natural product named erythribyssin M.

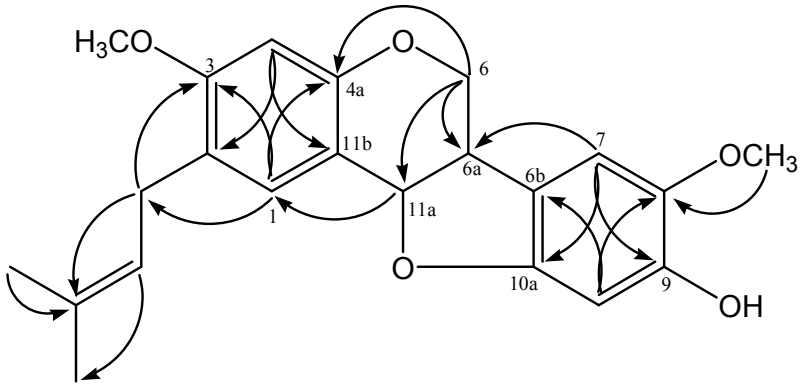

Key HMBC correlations of erythribyssin M (**13**) (H → C)

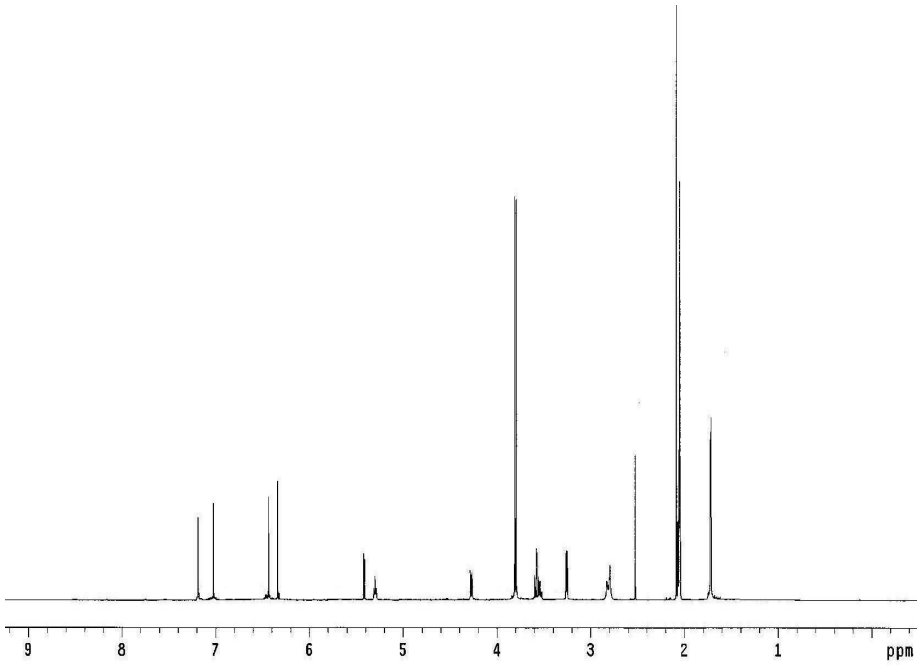

Fig. 39 ^{1}H-NMR spectrum of compound **13** (500 MHz, acetone-d_6)

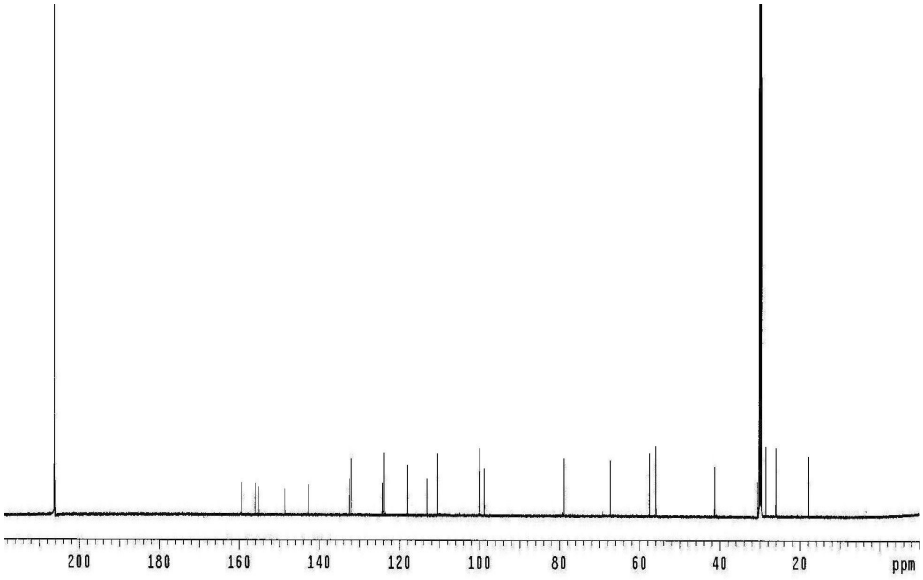

Fig. 40 ^{13}C-NMR spectrum of compound **13** (125 MHz, acetone-d_6)

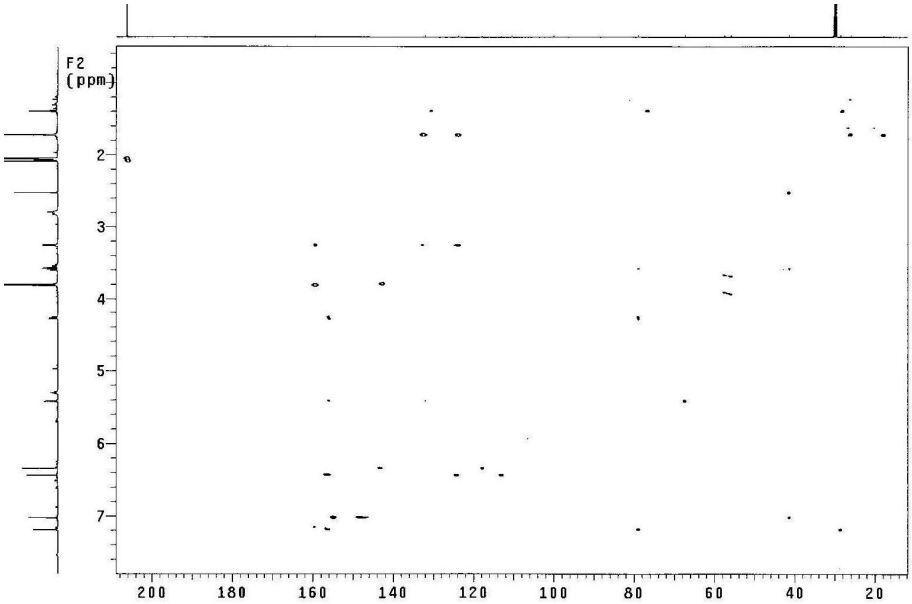

Fig. 41. HMBC spectrum of compound **13** (500 MHz, acetone-d_6)

Table 15. ^{1}H and ^{13}C NMR spectral data of compound **13** (600 MHz, acetone-d_6)

position	δ_H mult. (J in Hz)	δ_C	HMBC (H → C)
1	7.16 (s)	132.1	C-3, C-4a, C-1'
2		113.1	
3		159.4	
4	6.43 (s)	98.6	C-2, C-3, C-4a, C-11b
4a		156.0	
6	4.27 (dd, J = 4.2, 16.2) 3.57 (t, J = 16.2)	67.3	C-4a, C-6a
6a	3.51 (m)	41.3	C-11a
6b		117.9	
7	7.01 (s)	110.5	C-9, C-10a, C-6a
8		142.9	
9		148.6	
10	6.34 (s)	100.0	C-8, C-6b
10a		155.1	
11a	5.41 (d, J = 7.2)	78.9	C-1, C-11b, C-4a, C-6
11b		124.2	
1'	3.25 (d, J = 7.2)	28.5	C-2', C-3', C-3
2'	5.29 (m)	123.8	
3'		132.3	
4'	1.72 (s)	17.9	C-2', C-3', C-5'
5'	1.72 (s)	26.0	C-2', C-3', C-4'

1.14 Structure determination of compound 14

Compound **14** was isolated as brown prism with the molecular formula $C_{21}H_{18}O_5$, as determined by the HR-EI mass spectrum ($[M]^+$, *m/z* 350.1154). The IR spectrum of compound **14** suggested the presence of OH functional groups at 3447 cm^{-1}, 2923 (C–C), 1716 (C(=O)-O), 1628 (C=O), 1423 (aromatic absorption), 1264 (ether function), 1160-1036 cm^{-1}. Its UV spectrum showed absorption maxima at 210, 214, 242, 299, 336, 352 nm. The ^1H NMR spectrum showed characteristic signal for a prenyl group [δ_H 3.68 (2H, d), 5.36 (1H, m), 1.67 (3H, s) and 1.91 (3H, s)], an ABX type aromatic protons [δ_H 6.96 (1H, br, s), 7.02 (1H, br, d) and 7.91 (1H, d)], a pair of *ortho*-coupled aromatic protons [δ_H 7.17 (1H, d, J = 8.4 Hz) and 7.74 (1H, d, J = 8.4 Hz)]. The aromatic proton at the C-1 position (δ_H 7.91) in the AMX system displayed an HMBC correlation to the carbon at C-11a (δ_C 161.4) and the proton at the C-7 position (δ_H 7.74) exhibited correlation to the C-6a (δ_C 103.5). All of these data obtained resembled to isosojagol,[60] a previously isolated coumestan from the same source. Exception of an additional methoxyl group was found in **14** [δ_H 3.96 (3H, s), δ_C 57.1], this methoxyl moiety was assigned to the C-9 by an HMBC experiment (Table 16). The assignment of the prenyl group at the C-10 position was also confirmed from the HMBC experiment, revealing that the aliphatic protons at C-1′ (δ_H 3.55) correlated with carbons at C-9 (δ_C 157.3), C-10 (δ_C 115.1) and C-10a (δ_C 156.5). Thus, the structure of compound **14** was identified as 3-hydroxy-9-methoxy-10-prenyl-coumestan, and named erythribyssin N.

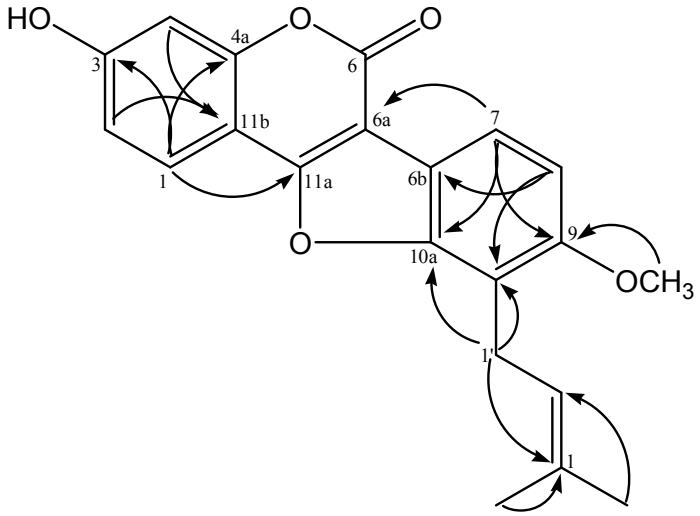

Key HMBC correlations of erythribyssin N (**14**) (H → C)

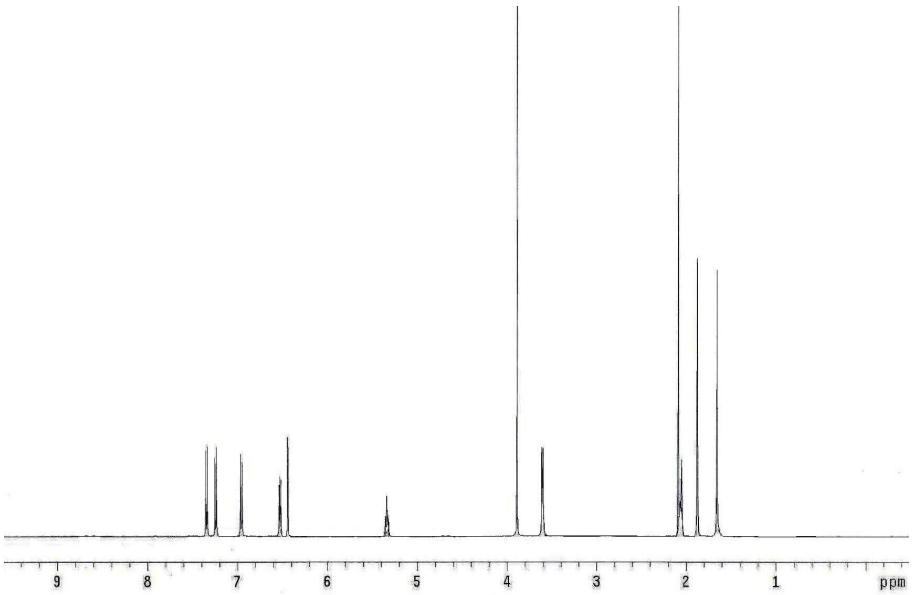

Fig. 42. ^{1}H-NMR spectrum of compound **14** (500 MHz, acetone-d_6)

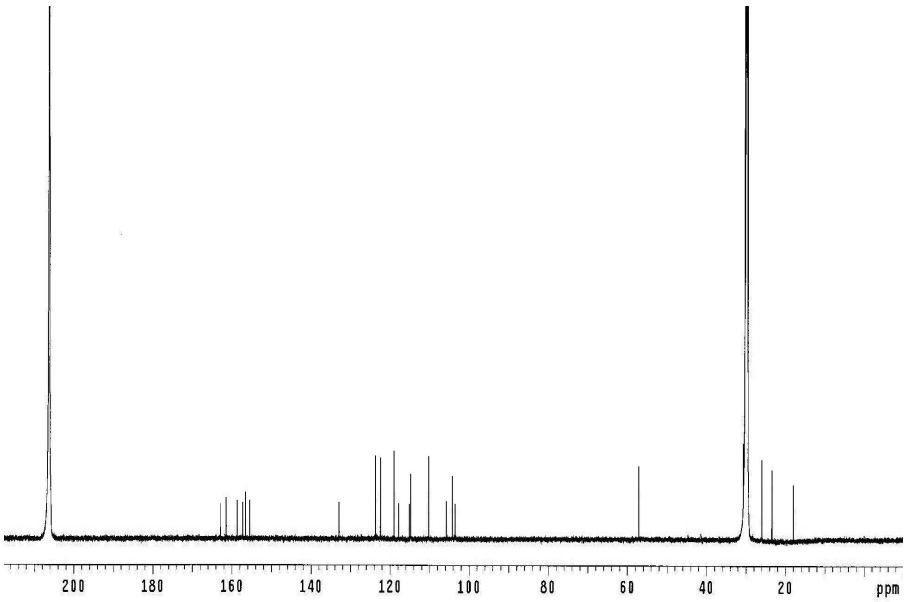

Fig. 43. ^{13}C-NMR spectrum of compound **14** (125 MHz, acetone-d_6)

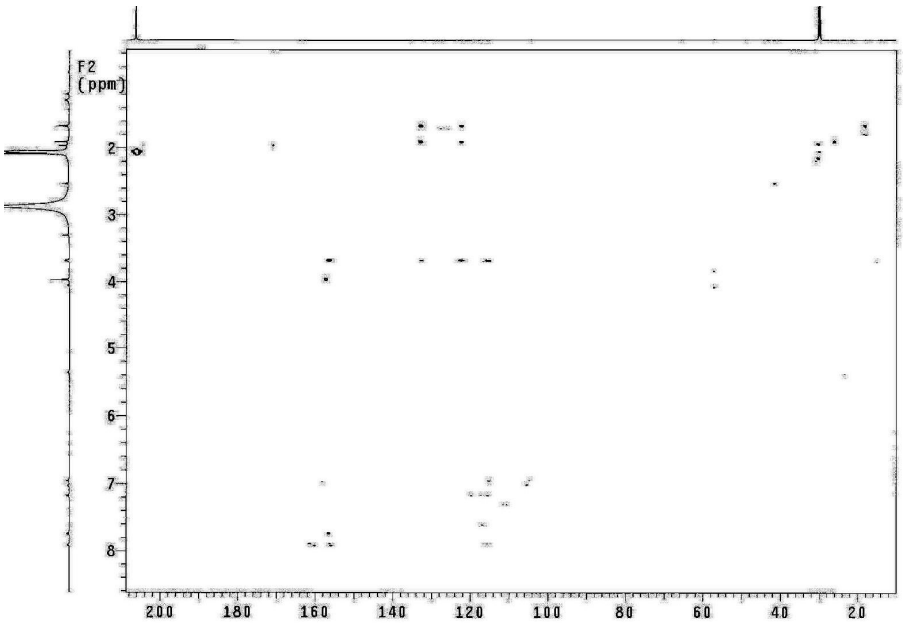

Fig. 44. HMBC spectrum of compound **14** (500 MHz, acetone-d_6)

Table 16. ^{1}H and ^{13}C-NMR spectral data of compound **14** (600 MHz, acetone-d_6)

position	δ_H mult. (J in Hz)	δ_C	HMBC (H → C)
1	7.91 (d, J = 8.5)	123.7	C-3, C-4a, C-11a
2	7.02 (br,d, J = 8.4)	110.2	C-4, C-11b
3		162.9	
4	6.96 (br, s)	104.3	C-6^{ss}
4a		155.5	
6		158.6	
6a		103.5	
6b		117.8	
7	7.74 (d, J = 8.4)	119.0	C-6a, C-9, C-10a,
8	7.17 (d, J = 8.4)	114.7	C-6b, C-9, C-10
9		157.3	
10		115.1	
10a		156.5	
11a		161.4	
11b		105.7	
1'	3.68 (d, J = 7.2)	23.4	C-2', C-3', C-10, C-10a
2'	5.36 (m)	122.4	C-1', C-3'
3'		132.9	
4'	1.67 (s)	18.0	C-2’, C-3’, C-5’
5’	1.91 (s)	25.9	C-2’, C-3’, C-4’
9-OMe	3.96 (3H, s)	57.1	C-9

1.15 Structure determination of compound 15

Compound **15** was isolated as yellow amorphous powder with the molecular formula $C_{21}H_{18}O_5$, as determined by the HR-EI mass spectrum ($[M]^+$, *m/z* 350.1154). The IR spectrum of compound **15** suggested the presence of OH functional groups at 3418 cm^{-1}, 2924 (C–C), 1708, 1622 (C=O), 1418 (aromatic absorption), 1265 (ether function), 1160-1032 cm^{-1}. Its UV spectrum showed absorption maxima at 210, 214, 242, 299, 336, 352 nm. The ^1H NMR spectrum showed a characteristic singlet signal at C-6 [δ_H 5.75 (2H, s)], which were reminiscent of a pterocarpan skeleton.[61] The carbon resonances at δ_C 67.7, 108.6 and 145.1 in the ^{13}C NMR spectrum supported this observation. In addition, the ^1H NMR spectrum displayed two singlet signals at δ_H 6.45 and 7.82, a pair of *ortho*-coupled aromatic protons δ_H 6.89 and 7.18 (each 1H, d, J = 8.5 Hz) and a prenyl group (δ_H 1.67, 1.88, 3.64 and 5.40), and one formyl moiety [δ_H 9.94 (1H, s), δ_C 196.1]. The assignment of the prenyl group at the C-10 position was also confirmed from the HMBC experiment, revealing that the aliphatic protons at C-1′ (δ_H 3.64) correlated with carbons at C-9 (δ_C 156.2), C-10 (δ_C 113.1) and C-10a (δ_C 154.0). These observations were reminiscent of erypoegin H.[61] The aldehyde group attached to the C-2 position was deduced by an HMBC experiment, correlations between the proton at δ_H 9.94 and C-2 (δ_C 116.6), C-3 (δ_C 164.9) established this attachment. Thus, compound **15** was identified as 3,9-dihydroxy-10-prenyl-2-formylcoumestan, and named erythribyssin O.

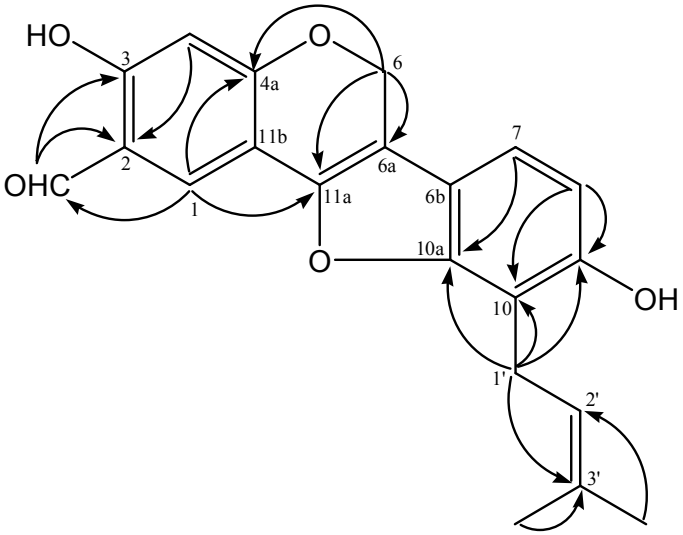

Key HMBC correlations of erythribyssin **O** (**15**) (H → C)

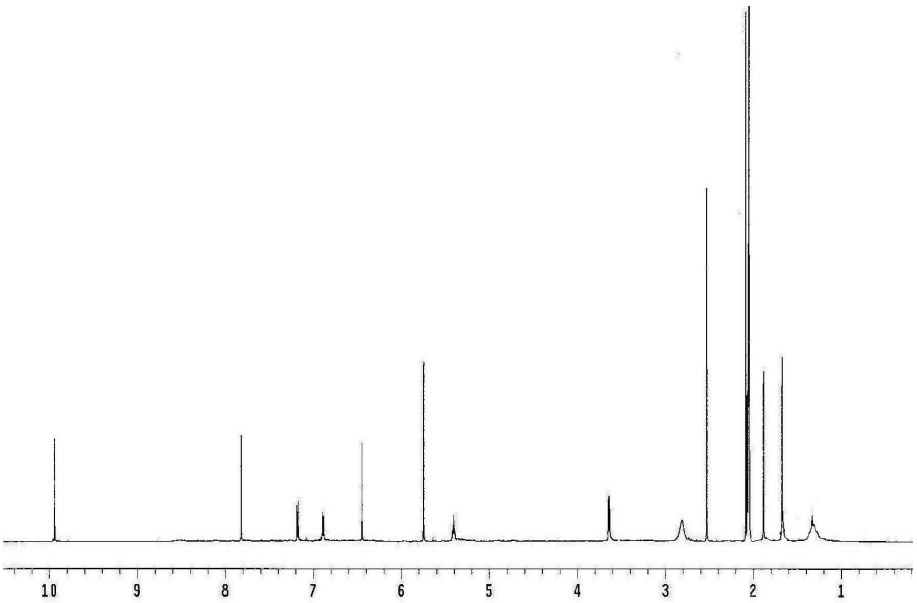

Fig. 45. ^{1}H-NMR spectrum of compound **15** (500 MHz, acetone-d_6)

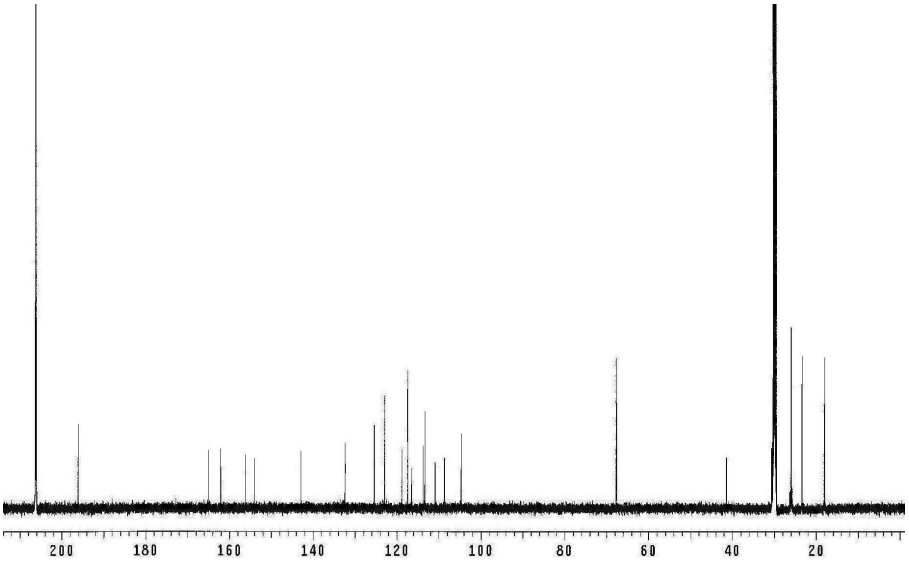

Fig. 46 ^{13}C-NMR spectrum of compound **15** (125 MHz, acetone-d_6)

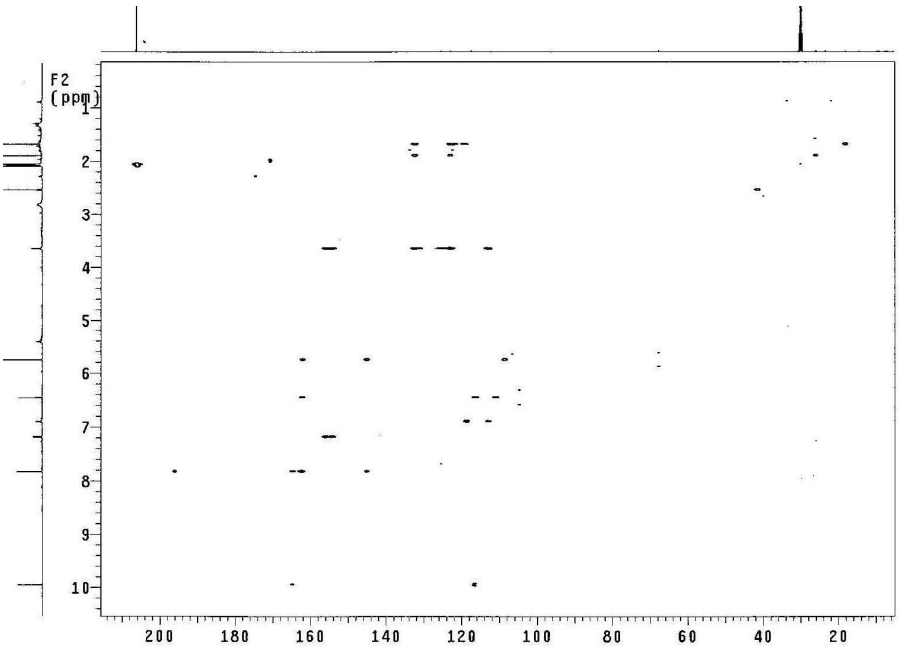

Fig. 47. HMBC spectrum of compound **15** (500 MHz, acetone-d_6)

Table 17. ^{1}H and ^{13}C-NMR spectral data of compound **15** (600 MHz, acetone-d_6)

position	δ_H mult. (J in Hz)	δ_C	HMBC (H → C)
1	7.82 (s)	123.7	C-3, C-4a, C-11a, 2-CHO
2		110.2	
3		162.9	
4	6.45 (s)	104.3	C-2, C-4a, C-11b
4a		155.5	
6	5.75 (2H, s)	158.6	C-4a, C-6a, C-11a
6a		103.5	
6b		117.8	
7	7.18 (d, J = 8.4)	119.0	C-6a, C-9, C-10a,
8	6.89 (d, J = 8.4)	114.7	C-6b, C-10
9		157.3	
10		115.1	
10a		156.5	
11a		161.4	
11b		105.7	
1'	3.64 (d, J = 7.2)	23.4	C-2', C-3', C-9, C-10, C-10a
2'	5.40 (m)	122.4	C-1', C-3'
3'		132.9	
4'	1.67 (s)	18.0	C-2’, C-3’, C-5’
5’	1.88 (s)	25.9	C-2’, C-3’, C-4’
2-CHO	9.94 (s)	196.1	C-2, C-3

2. Results of PTP1B inhibitory activity

Protein tyrosine phosphatase-1B (PTP1B) plays a major role in the negative regulation of insulin signaling, and thus had been considered as an attractive therapeutic target for diabetes. Bioassay-guided fractionation of the EtOAc-soluble extract of the stem bark of *E. abyssinica* afforded fifteen new compounds, named erythribyssin A–**O** (**1–15**).

The inhibitory effects on PTP1B of isolated compounds (**1–15**) were tested *in vitro* according to a reported method.[46] The result is presented in **Table 18** as compared with the known PTP1B inhibitors, ursolic acid (IC_{50} = 3.6 ± 0.2 μM), as the positive control. Many tested compounds, with the exception of **2–4**, **6**, **8, 9, 11**, inhibited PTP1B enzyme dose-dependently, yielding IC_{50} values ranging from 4.2 ± 0.4 to 26.7 ± 1.2 μM.

Among the isolates, compound **14**, which is a new natural courmestan derivative, showed the strongest compound. This courmestan has quietly identical structure to proralidin, one of the known PTP1B inhibitor derived from natural source, except only for an addition of a methoxyl group to the B ring of compound **14**. However, the inhibitory activity of compound **14** (IC_{50} = 4.2 μM) was twice stronger with compared to that of psoralidin (IC_{50} = 9.4 μM). This finding suggests that courmestan was the most active component compared with flavonoids, ptercarpans, and benzofurans in this species.

Even thought compounds **1**, **5**, **8**, **10** and **13** were different structural skeleton, they were all substituted by two methoxyl groups in their structures, and all of these compounds, except for compound **8** with a prenyl group, had similar activity with IC_{50} values ranging from 14.9 ± 1.6 to 19.3 ± 1.9 μM. Compounds **6** and **8**, which are new natural bezofuranoids, did not show any inhibitory effect on PTP1B enzyme (IC_{50} > 50 μM). Compound **6** which was substituted by two methoxy groups on the B ring of

flavonoids without prenyl group and compound **8** with carboxyl group, even bearing two prenyl groups, did not have any activity on this enzyme. This result could also be suggested that benzofuran-type compounds were the most inactive component in this plant.

Compound **3, 4** and **9**, which were fused as the 3-hydroxy-2,2-dimethylpyran moiety on the B ring, did not showed any inhibition at PTP1B enzyme activity over the final concentration of 50 μM with compared to those of compound **7** (22.6 ± 1.5 μM) and compound **12** (9.8 ± 1.1 μM) which the prenyl groups were present. However, other compounds **1, 5, 10, 12 - 15** which were attached by either methoxyl groups or prenyl groups showed a stronger activity with IC_{50} value ranging from 4.2 ± 0.4 to 26.7 ± 1.2 μM than compounds **6, 8, 9** and **11** (IC_{50} > 50 μM), which the prenyl groups are absent or compounds were substituted by CHO or COOH functional groups. These results indicated that the addition of a prenyl group or methoxyl substituent to functional group of compounds may be responsible for increasing PTP1B activity, whereas substitution into the CHO or COOH groups may be related with decrease in the inhibitory activity on this enzyme.

Although structure-activity relationships of all flavonoids bearing prenyl groups were not thoroughly investigated, the results indicated that substitution of prenyl groups on flavonoids may be important for *in vitro* PTP1B inhibitory activity. Flavonoids, isoflavonoids, pterocarpans and benzofurans, as well as courmestans with prenyl groups could be consider as promising classes of PTP1B inhibitors. Thus, *Erythrina abyssinica* and its constituents can be used beneficially in the treatment of diabetes as well as obesity.

Table. 18 Inhibitory activity of the compounds isolated from *Erythrina abyssinica* against PTP1B (**1**–**15**)

Compounds	**IC_{50} (μM)**[a]
erythribyssin A (**1**)	19.3 ± 1.9
erythribyssin B (**2**)	> 50
erythribyssin C (**3**)	> 50
erythribyssin D (**4**)	> 50
erythribyssin E (**5**)	15.2 ± 1.2
erythribyssin F (**6**)	> 50
erythribyssin G (**7**)	22.6 ± 1.5
erythribyssin H (**8**)	> 50
erythribyssin I (**9**)	> 50
erythribyssin J (**10**)	14.9 ± 1.6
erythribyssin K (**11**)	> 50
erythribyssin L (**12**)	9.78 ± 1.1
erythribyssin M (**13**)	17.9 ± 0.4
erythribyssin N (**14**)	4.2 ± 0.4
erythribyssin O (**15**)	26.7 ± 1.2
Ursolic acid[b]	3.6 ± 0.2

[a] IC_{50} values were determined by regression analyses and expressed a means ± SD of three replicates.

[b] Positive control.

IV. CONCLUSIONS

Insulin resistance is one of the characteristic pathogenic signs of type-2 diabetes, and several drugs that increase the insulin sensitivity are currently in clinical trial. However, these drugs have a number of limitations, which include adverse effects and high rates of secondary failure. Of the various potential drug targets for treatment of type-2 diabetes, protein tyrosine phosphathase-1B (PTP1B) has recently been considered as a major negative regulator in the insulin signaling pathway. It has been suggested that compounds reducing PTP1B activity or the genetic expression levels of PTP1B may be useful in the treatment of type-2 diabetes and possibly obesity as well.

Although there have been a number of reports on the development of PTP1B inhibitors, new types of PTP1B inhibitors having improved pharmacological properties remain to be discovered. Since plants are a promising source for the development of new PTP1B inhibitors, we have undertaken a screen of hundreds of plant extracts against PTP1B.

In the course of *in vitro* PTP1B inhibitory screening on various extracts from medicinal plants, a methanol-soluble extract of the stem bark of *Erythrina abyssinica* was found to inhibit PTP1B activity at a concentration 30 μg/ml. The MeOH solution was concentrated, suspended in H_2O, and sequentially partitioned with EtOAc. The EtOAc-soluble fraction exhibited moderate activity with inhibition values 80 % on PTP1B at final concentration 30 μg/ml.

Bioassay-guided fractionation of the MeOH extract of the stem bark of *Erythrina abyssinica* has resulted in the isolation of fifteen new compounds (**1-15**) using chromatography methods (silica gel, YMC, C_{18} and preparative HPLC). Their structures were elucidated on the basis of spectral (including 1D, 2D-NMR, IR, UV, CD, $[\alpha]_D$ and

MS) and physicochemical analyses. The inhibitory effects of the isolates on PTP1B enzyme were investigated.

Fifteen new isolated compounds (**1-15**) were elucidated and named erythribyssin A-O (**1-15**). Although structure-activity relationships were not thoroughly investigated, our results indicated that substitution of prenyl groups on flavonoids may be important for *in vitro* PTP1B inhibitory activity. In addition, PTP1B inhibitory effects by members of pterocarpans have not been previously reported.

Further confirmation of PTP1B inhibitory effects of these compounds in cells and evaluation of their potential *in vivo* efficacy in a diabetic mice model are in progress.

Finally, flavanones, isoflavanones, pterocarpans, and benzofurans as well as coumestans could be considered as promising classes of PTP1B inhibitors. Therefore, further investigation and optimization of prenylated flavonoid derivatives might enable the discovery of new PTP1B inhibitors that are potentially useful in the treatment of type-2 diabetes as well as obesity.

V. REFERENCES

1. Amos A. F.; McCarty D. J.; Zimmet P. The rising global burden of diabetes and its complications: estimates and projections by 2010. *Diabet. Med*. 1997, *14*, S5-S85.
2. UK prospective diabetes study (UKPDS) group 33. Intensive blood glucose control with sulphonylureas or insulin compared with conventional treatment and risk of complications with type-2 diabetes. *Lancet*, 1998. 352, 837-853.
3. Kumar S., Boulton AJ., Beck-Nielsen H., Berthezene F., Muggeo M., Persson B., Spinas G.A., Donoghue S., Lettis S., Stewart-Long P. Troglitazone, an insulin action enhancer, improves metabolic control in NIDDM patients. Troglitazone Study Group., *Diabetologia*, 1996. 39, 701-709.
4. Moller DE. New drug targets for type 2 diabetes and the metabolic syndrome. *Nature*, 2001. 414, 821-827.
5. Reaven GM., Banting lecture 1998, Role of insulin resistance in human disease. *Diabetes*, 1988. 37, 1595-1607.
6. Van Huijsduijnen RH., Bombrum A., Swinnen D., Selecting protein tyrosine phosphatase as drugs targets. *Drug. Discov. Today*, 2002. 7, 1013-1019.
7. Krebs EG., The enzymes (Boyer P. D., Krebs E. G., eds) XVII, Academic Press, 1986, New York.
8. Hunter T., A thousand and one protein kinases, *Cell*, 1987. 50, 823-829.
9. Knighton DR., Zheng JH., Ten Eyck LF., Ashford VA., Xuong NH., Taylor SS., Sowadski JM. Crystal structure of the catalytic subunit of cyclic adenosine monophosphate-dependent protein kinase. *Science*, 1991. 253, 407-414.
10. Stone RL., Dixon JE., Protein-tyrosine phosphatases, *J. Biol. Chem*, 1994. 269, 31323-31326.

11. Barford D., Das A.K., Egloff MP. The structure and mechanism of protein phosphatases: insights into catalysis and regulation. *Annu. Rev. Biophys. Biomol. Struct*, 1998. 27, 133-164.
12. Ishibashi T., Bottaro DP., Chan A., Miki T and Aaromson SA. Expression cloning of a human dual specificity phosphatase. *Prod. Natl. Acad. Sci. U. S. A.* 1992. 89, 12170-12174.
13. Guan KL., Broyles SS., Dxion JE. A Thr/Ser protein phosphatase encoded by vaccinia virus. *Nature*, 1991. 350, 359-362.
14. Fisher EH., Charbonneau H., Tonks NK. Protein tyrosine phosphatases: a diver's family of intracellular and transmembrane enzymes. *Science*, 1991. 253, 401-406.
15. Hunter T., Protein kinases and phosphatases: the yin and yang of protein phosphorylation and signaling, *Cell*, 1995. 80, 225-236.
16. Espanel X., Walchli S., Gobet RP., EI Alama M., Curchod ML., Gullu-Isler N., van Huijsduijnen RH. Pulling strings below the surface: hormone receptor signaling through inhibition of protein tyrosine phosphatases. *Endocrine*, 2001. 15, 19-28.
17. Asante-Appiah E., Kenneby BP. Protein tyrosine phosphatases: the quest for negative regulators of insulin action. *Am. J. Physiol. Endocrinol. Metab*, 2003. 284, E663-E670.
18. Goldstein BJ. Protein-tyrosine phosphatases and the regulation of insulin action. *J. Cell. Biochem*, 1992. 48, 33-42.
19. Johnson TO., Ermolieff J., Jirousek MR. Protein tyrosine phosphatase 1B inhibitors for diabetes. *Nat. Rev. Discov*, 2002. 1, 696-709.
20. Dadke S., Chernoff J., Protein-tyrosine phosphatase 1B as a potential drug target for obesity. *Current Drug Targets – Immune, Endocrine & Metabolic Disorders*, 2003. 3, 299-304.

21. Saltiel AR., Kahn CR., Insulin signaling and the regulation of glucose and lipid metabolism. *Nature*, 2001. 414, 799-806.

22. Miller DE., Flier JS. Insulin resistance-Mechanism, syndromes, and implications. *N Engl J Med*, 1991. 325, 938-948.

23. Ukkola O., Santaniemi M. Protein tyrosine phosphatase 1B: a new target for the treatment of obesity and associated co-morbidities. *Journal of Internal Medicine* 2002. 251: 467-475.

24. Bevan P. Insulin signalling. *J Cell Sci*, 2001. 114, 1429-30.

25. Frame S., Cohen P. GSK3 takes centre stage more than 20 years after its discovery. *Biochem. J*, 2001. 359, 1-16.

26. Zhang ZY. Protein tyrosine phosphatases: prospects for therapeutics. *Curr. Opin. Chem. Biol*, 2001. 5, 416-423.

27. Kenner K., Anyanwu E., Olefsky J and Kusari J. Protrin-tyrosine phosphatase 1B is a negative regulator of insulin and insulin-like growth factor-I-stimulated signaling. *J. Biol. Chem*, 1996. 271, 19810-19816.

28. Seely B., Staubs P., Reichart D., Berhanu P., Milarski K., Saltiel A., Kusan J and Olefsky J. protein tyrosine phosphatase 1B interacts with the activated insulin receptor. *Diabetes*, 1996. 45, 1379-1385.

29. Elchebly M., Payette P., Michaliszyn E et al. Increased insulin sensitivity and obesity resistance in mice lacking the protein tyrosine phosphatase-1B gene. *Science*, 1999. 283, 1544-1548.

30. Klaman LD., Boss O., Peroni OD et al. Increased energy expenditure, decreased adiposity, and tissue-specific insulin sensitivity in protein-tyrosine phosphatase 1B-deficient mice. *Mol Cell Biol*, 2000. 20, 5479–5489.

31. Fantus IG., Ahmad F., Deragon G. Vanadate augments insulin-stimulated insulin

receptor kinase activity and prolongs insulin action in rat adipocytes. Evidence for transduction of amplitude of signaling into duration of response. *Diabetes*, 1994. 43, 375-383.

32. Huyer G., Liu S., Kelly J., Moffat J., Payette P., Kennedy B., Tsaprailis G., Gresser MJ., Ramachandran C. Mechanism of inhibition of protein-tyrosine phosphatases by vanadate and pervanadate. *J. Biol. Chem*, 1997. 272, 843-851.
33. Goldwaser I., Gefel D., Gershonov E., Fridkin M., Shechter Y. Insulin-like effscts of vanadium: basic and clinical implications. *J. Inorg. Biochem*, 2000. 80, 21-25.
34. Hamaguchi T., Sudo T., and Osada H. RK-682, a potent inhibitor of tyrosine phosphatase, arrested the mammalian cell cycle progression at G1 phase. *FEBS. Lett*, 1995. 372, 54-58.
35. Huyer G., Liu S., Kelly J., Moffat J., Payette P., Kennedy B., Tsaprailis G., Gresser M. J., Ramachandran C., Mechanism of inhibition of protein-tyrosine phosphatases by vanadate and pervanadate. *J. Biol. Chem*, 1997. 272, 843-851.
36. Oh H., Kim BS., Bae EY., Kim MS., Kim BY., Lee HB., Kim CJ., Ahn JS. Inhibition of PTP1B by metabolites from *Micromucor ramannianus var. angulisporus* CRM000232. *J. Antibiot*, 2004. 57, 528-531.
37. Kim YC., Oh H., Kim BS., Kang TH., Ko EK., Han YM., Kim BY and Ahn JS. *In vitro* protein tyrosine phosphatase 1B inhibitory phenol from the seeds of *Psoralea corylifolia*. *Planta Med*, 2005. 71, 87-89.
38. Imparl-Radosevich J., Deas S., Polansky MM., Baedke DA., Ingebritsen TS., Anderson RA., Graves DJ. Regulation of PTP1B and insulin receptor kinase by fractions from cinnamon: implications for cinnamon regulation of insulin signaling. *Horm. Res*, 1998. 50, 177-182.
39. Suzuki T., Hiroki A., Watanabe T., Yamashita T., Takei I., Umezawa K., Potentiation

of insulin-related signal transduction by a novel protein-tyrosine phosphatase inhibitor, Et-3,4-dephostatin, on cultured 3T3-L1 adipocytes. *J. Biol. Chem*, 2001. 276, 27511-27518.

40. McKee TC., Bokesch HR., McCormick JL., Rashid MA., Spielvogel D., Gustafson KR., Alavanja MM., Cardellina II JH., Boyd MR. Isolation and Characterization of New Anti-HIV and Cytotoxic Leads from Plants, Marine, and Microbial Organisms. *J. Nat.Prod*, 1997. 60, 431-438.
41. (a) Chawla AS., Jackson AH**.** *Erythrina* and related alkaloids. *Nat. Prod. Rep*, 1989, *6*, 55-66. (b) Chawla AS., Jackson AH. *Erythrina* and related alkaloids. *Nat. Prod. Rep*, 1990. 7, 565-575. (c) Juma BF., Majinda RR. T. Erythrinaline alkaloids from the flowers and pods of *Erythrina lysistemon* and their DPPH radical scavenging properties. *Phytochemistry*, 2004. 65, 1397-1404.
42. (a) Njamen D., Mbafor JT., Fomum ZT., Kamanyi A., Mbanya JC., Recio MC., Giner RM., Máñez S., Ríos JL. Anti-Inflammatory Activities of Two Flavanones, Sigmoidin A and Sigmoidin B, from *Erythrina sigmoidea*. *Planta Med*, 2004. 70, 104-107. (b) Chacha M., Bojase-Moleta G., Majinda RR. T. Antimicrobial and radical scavenging flavonoids from the stem wood of *Erythrina latissima*. *Phytochemistry*, 2005. 66, 99-104.
43. (a) Mitscher LA., Okwute SK., Gollapudi SR., Keshavarz-Shokri A. *Heterocycles*, 1988. 27, 2517-2522. (b) Mitscher LA., Okwute SK., Gollapudi SR., Drake S., Avona E. Antimicrobial pterocarpans of nigerian *Erythrina mildbraedii*. *Phytochemistry*, 1988. 27, 3449-3452. (c) Njamen D., Talla E., Mbafor JT., Fomum ZT., Kamanyi A., Mbanya JC., Cerdá-Nicolás M., Giner RM., Recio MC., Ríos JL. Anti-inflammatory activity of erycristagallin, a pterocarpene from *Erythrina mildbraedii*. *Eur. J. Pharmacol*, 2003. 468, 67-74.

44. Kokwaro JO, Medicinal Plants of East Africa, 2nd edu, Kenya Literature Bureau, Nairobi. 1993. 158.

45. Kamat V. S.; Chuo F. Y.; Kubo I.; Nakanishi K. Aatimicrobial agents from an East Afican medicinal Plant *Erythrina abyssinica*. *Heterocycles*. 1981, *15*, 1163-1170.

46. (a) Cui L.; Na M.; Oh H.; Bae E. Y.; Jeong D. G.; Rhu S. E.; Kim S.; Kim B. Y.; Oh W. K.; Ahn J. S. Protein tyrosine phosphatase 1B inhibitors from *Morus* root bark. *Bioorg. Med. Chem. Lett*. 2006, *16*, 1426-1429. (b) Na M.; Yang S.; He L.; Oh H.; Kim B. S.; Oh W. K.; Kim B. Y.; Ahn J. S. Inhibition of Protein Tyrosine Phosphatase 1B by Ursane-Type Triterpenes Isolated from *Symplocos paniculata*. *Planta Med*. 2006, *72*, 261-263.

47. (a) Kamat, V. S.; Chuo, F. Y.; Isao Kubo, I.; Nakanishi, K. *Heterocycles* **1981**, *15*(2), 1163–1170. (b) Agne, E.; Gunatilakad, A. L.; Kingston, A. V. *J. Nat. Prod.* **1993,** *56*(10), 1831–1834.

48. Tanaka, H.; Tanaka, T.; Etoh, H. *Phytochemistry.* **1997**, *45*(4), 835–838.

49. (a) P. M. Dewick, "The Flavonoids: Advances in Research Since 1980," ed. By J. B. Harborne, Chapman and Hall, London, 1988, p. 166; (b) P. M. Dewick, "The Flavonoids: Advances in Research Since 1980," ed. By J. B. Harborne, T. J. Mabry, Chapman and Hall, London, 1988, p. 581.

50. Kitagawa, I.; Chen, W. Z.; Hori, K.; Uchida, E. H.; Yasuda, N.; Yoshikawa, M.; Ren, J. *Chem. Pharm. Bull* **1994**, *42*(5), 1056–1062.

51. Matsuda, H.; Morikawa, T.; Xu, F.; Ninomiya, K.; Yoshikawa, M. *Planta Med*. **2004**, *70*, 1201–1209.

52. Sakurai, Y.; Sakurai, N.; Taniguchi, M.; Nakanishi, Y.; Bastow, K. F.; Wang, X.; Cragg, G. M.; Lee, K. H. *J. Nat. Prod.* **2006,** *69,* 397–399.

53. Rukachaisirikul, T.; Innok, P. s.; Suksamrarn, A. *J. Nat. Prod.* **2008,** *71*(1)*,* 156–158.

54. (a) Nkengfack, A. E.; Vouffo, T. W.; Fomum Z. T.; Meyer, M.; Bergendorff, O. and Sterner, O. *Phytochemistry*. **1994**, *36*(4), 1047–1051. (b) Inuma, M.; Ohyama, M. and Tanaka, T. *Phytochemistry*. **1994**, *37*(6), 1713–1716.

55. Tanaka, H.; Hirata, M.; Etoh, H.; Sako, M.; Sato, M.; Murata, J.; Murata, H.; Darnaedi, D. and Fukai, T. *Chemistry & Biodiversity*. **2004**, *Vol . 1*, 1101–1108.

56. Cui, L.; Thuong, P. T.; Lee, H. S.; Ndinteh, D. T.; Mbafor, J. T.; Fomum, Z. T.; Oh, W. K. *Bioorganic & Medicinal Chemistry*. **2008**, *16*, 10356–10362.

57. Vila, J.; Balderrama, L.; Bravo, J. L.; Almanza, C. C.; Bastida, J. and Connolly, J. *Phytochemistry*. **1998**, *49*(8), 2525–2528.

58. Tanaka, H.; Etoh, H.; Wantanabe, N.; Shimizu, H.; Ahmad, M.; Rizwani, G. H. *Phytochemistry* **2001**, *56*, 769–773.

59. Tanaka, H.; Sudo, M.; Hirata, M.; Sako, M.; Sato, M.; Chen, I. S.; Fukai, T. *Heterocycles*. **2005**, *65*(4), 871–877.

60. O'Neill, J. M.; Adesanya, S. A. and Roberts. F. M. *Phytochemistry* **1984**, *32*(11), 2704–2705.

61. (a) Tanaka, H.; Uchi, T. O.; Etoh, H.; Shimizu, H.; Tateishi, Y. *Phytochemistry* **2002**, *60*, 789–794. (b) Tanaka, H.; Uchi, T. O.; Etoh, H.; Sako, M.; Sato, M.; Fukai, T.; Tateishi, Y. *Phytochemistry* **2003**, *63*, 597–602.

저작물 이용 허락서

학 과	약학과	학 번	20077774	과 정	석사
성 명	한글: 응구엔피훙 영문: NGUYEN PHI HUNG				
주 소	501-759 광주광역시 동구 서석동 375 조선대학교 약학과 생약학실험실				
연락처	E-mail: hungcbt1980@yahoo.com				
논문제목	한글: *Erythrina abyssinica*의 줄기 껍질로부터 protein tyrosine phosphatase 1B (PTP1B) 저해제의 분리 영문: Protein tyrosine phosphatase 1B (PTP1B) inhibitors from the stem bark of *Erythrina abyssinica*				

본인이 저작한 위의 저작물에 대하여 다음과 같은 조건 아래 -조선대학교가 저작물을 이용할 수 있도록 허락하고 동의합니다.

- 다 음 -

1. 저작물의 DB구축 및 인터넷을 포함한 정보통신망에의 공개를 위한 저작물의 복제, 기억장치에의 저장, 전송 등을 허락함
2. 위의 목적을 위하여 필요한 범위 내에서의 편집・형식상의 변경을 허락함.
다만, 저작물의 내용변경은 금지함.
3. 배포・전송된 저작물의 영리적 목적을 위한 복제, 저장, 전송 등은 금지함.
4. 저작물에 대한 이용기간은 5년으로 하고, 기간종료 3개월 이내에 별도의 의사표시가 없을 경우에는 저작물의 이용기간을 계속 연장함.
5. 해당 저작물의 저작권을 타인에게 양도하거나 또는 출판을 허락을 하였을 경우에는 1개월 이내에 대학에 이를 통보함.
6. 조선대학교는 저작물의 이용허락 이후 해당 저작물로 인하여 발생하는 타인에 의한 권리 침해에 대하여 일체의 법적 책임을 지지 않음
7. 소속대학의 협정기관에 저작물의 제공 및 인터넷 등 정보통신망을 이용한 저작물의 전송・출력을 허락함.

2009 년 8월

동의 여부: 동의 (0) 조건부 동의 ( ) 반대 ( )

저작자: NGUYEN PHI HUNG (서명 또는 인)

조선대학교 총장 귀하